

ASYMMETRIC AMPHIPHILIC TRIBLOCK COPOLYMERS
SYNTHESIS, CHARACTERIZATION AND SELF-ASSEMBLY

[Roxana Stoenescu](#)

Thesis submitted to Basel University in partial fulfillment of the requirements for the

Ph. D. Degree
in
Physical Chemistry

Prof. Dr. Wolfgang Meier, Referee
Prof. Dr. Helma Wennemers, Co-referee
Prof. Dr. Markus Meuwly, Committee President

July 2004,
Basel, Switzerland

Keywords: Amphiphilic block copolymers, Nanovesicles, Asymmetric membranes

Copyright©2004, Roxana Stoenescu, Basel

Genehmigt von der Philosophisch-Naturwissenschaftlichen Fakultät auf Antrag von Prof. Dr.
Wolfgang Meier, Prof. Dr. Helma Wennemers and Prof. Dr. Marcus Meuwly

Basel, den 6 July 2004-07-26

Dekan: Prof. Dr. Marcel Tanner

ASYMMETRIC AMPHIPHILIC TRIBLOCK COPOLYMERS

SYNTHESIS, CHARACTERIZATION AND SELF-ASSEMBLY

Abstract

We synthesized a new series of ABC triblock copolymers, with two chemically different, hydrophilic A and C blocks and a hydrophobic block B and investigated their unique ability to self-assemble to asymmetric superstructures. Our model ABC triblock copolymers are composed of poly(ethylene oxide), poly(dimethyl) siloxane and poly(2-methyl oxazoline) blocks (in short PEO-*b*-PDMS-*b*-PMOXA). The AB diblock copolymers were synthesized via ring-opening anionic polymerization of cyclosiloxanes. The third block of the ABC triblock copolymers was introduced using a subsequent cationic polymerization of cyclic imino-ethers. The resulting triblock copolymers could be selectively modified with fluorescent dyes at one of the outer blocks carrying a free hydroxy group. With the help of quenching experiments we could clearly show that these polymers form vesicles with asymmetric membranes in aqueous media. This asymmetry is a direct result of a molecular incompatibility of the two different water-soluble blocks that tend to segregate to two different sides of the membranes. Interestingly, the asymmetry of the membranes influences significantly the insertion process of integral membrane proteins. Here we could clearly show that there exists a direct relation between the orientation of the membrane and the preferential direction of inserted membrane proteins.

This thesis consists of 10 chapters, which describe the concept of supramolecular assemblies (Chapter 1), amphiphilic block copolymers (Chapter 2), polysiloxane synthesis and poly imino-ether synthesis (Chapters 3 and 4), synthesis of amphiphilic ABC (poly(ethylene)oxide-*b*-poly(dimethyl)siloxane-*b*-poly(methyl)oxazoline) and other comparable systems (i.e. ABA (poly(methyl)oxazoline-*b*-poly(dimethyl)siloxane-*b*-poly(methyl)oxazoline) triblock copolymers) (Chapter 5), characterization of triblock copolymers obtained (Chapter 6), applications of triblock copolymers for the transmembrane protein incorporation in asymmetric matrixes (Chapters 7 and 8), conclusions (Chapter 9) and outlooks for future research (Chapter 10).

TABLE OF CONTENTS

CHAPTER 0 Abstract

CHAPTER 1	Principles of self-assembly.....	1
1.1.	Thermodynamics of self-assembly.....	1
1.2.	Self-assembly systems. Lyotropic mesophases.....	4
1.3.	Biological membranes from amphiphiles.....	6
1.4.	Self-assemblies from ABC triblock copolymers.....	7
CHAPTER 2	Amphiphilic block copolymers: synthesis of amphiphilic or functional block and graft copolymers.....	10
2.1.	Block copolymers of polyethers, polydimethyl siloxanes and poly imino ethers: synthesis, properties and applications	
	2.1.1. Copolymers of poly(ethylene) oxides.....	10
	2.1.2. Copolymers of poly(dimethyl) siloxanes.....	13
	2.1.3. Copolymers of poly(methyl) oxazolines.....	15
2.2.	Synthetic methods to prepare block copolymers.....	16
CHAPTER 3	Introduction to polysiloxane polymers	20
3.1.	Overview of polysiloxane synthesis.....	20
3.2.	Ring-chain equilibrium: thermodynamic considerations.....	20
3.3.	Ring-opening polymerization: kinetic considerations.....	21
	3.3.1. Cationic polymerization.....	22
	3.3.2. Anionic polymerization.....	23
	3.3.2.1. General principles.....	23
	3.3.2.2. Kinetically controlled polymerization.....	25
3.4.	Preparation of triblock copolymers.....	27
CHAPTER 4	Introduction to poly-imino-ethers.....	30
4.1.	Cyclic imino-ethers.....	30
4.2.	Experimental procedure for the polymerization of 2-oxazolines.....	32

CHAPTER 5	Synthesis of poly(ethylene oxide)-b-poly(dimethyl)siloxane-b-poly(methyl)oxazoline triblock copolymers.....	33
5.1.	The synthetic approach.....	33
5.2.	Results and Discussions.....	35
	5.2.1. Polyethyleneoxide macroinitiator	37
	5.2.2. PEO-PDMS diblock copolymers.....	39
	5.2.3. POE-PDMS-PMOXA triblock copolymers	40
	5.2.4. Thermal analysis.....	41
5.3	Labelled triblock copolymers.....	46
5.4	ABA triblock copolymer.....	49
5.5	Conclusions.....	50
CHAPTER 6	Self-assemblies from asymmetric triblock copolymers in aqueous solution.....	51
	Results and discussions.....	51
CHAPTER 7	Asymmetric membranes from ABC triblock copolymers.....	64
7.1.	Labelling of asymmetric triblock copolymers.....	64
7.2.	Validation of the asymmetry via fluorescence measurements of labelled copolymers.....	64
CHAPTER 8	Biological Applications from asymmetric membranes.....	70
8.1.	Introduction.....	70
8.2	Results and discussions.....	74
CHAPTER 9	General conclusions and remarks.....	87
CHAPTER 10	Future work.....	89
CHAPTER 11	Experimental section.....	90

Summary

Vitae

Acknowledgments

I would like to express my sincere gratitude to my supervisor, Prof. Dr. Wolfgang Meier, for the opportunity he gave me, his patience, and trust. Without his encouragements and suggestions, I would not write today about “asymmetric copolymers”, but fight with anionic polymerizations in the lab. For the huge freedom and confidence he gave me I am deeply grateful.

I would also like to thank the other members of my committee, include Prof. Dr. H. Wennemers and Prof. Dr. M. Meuwly for their precious time and assistance.

Despite the fact that they are really busy, new members of Prof. Meier group, Dr. Andreas Taubert and Dr. Katarzyna Kita-Tokarczyk took time for me, advising me concerning this thesis. It was a pleasure to know them, to work with and to receive their advices concerning the preparation of this manuscript.

I would like to thank my colleagues, Daniel Streich, for German lessons early morning in chemistry lab, Samantha Benito, for her English advices at the very beginning of my thesis, Julie Grumeland, Caroline Fraysse, for her spiritual presence, Michael Strobel for all instructive discussions, Sven Kasper for his sense of humour, good mood and availability, Sandrine Poux and to all my new colleagues: Christian, Diana, Alex, Chantal, Olivier, Per, Ekaterina, Nicolas and Alessandro. It was a real pleasure to work with them in an enjoyable environment. Special thanks to Thomas Haefele for his friendship, help and availability always, Alexandra Graff for the discussions and ideas about biological aspects of this study and her good sense of humour, and Dr. Corinne Vebert for her help with light scattering, valuable advices and caffeine support.

It was a pleasure to meet and work with Dr. Klaus Kulike (Organic Chemistry Department).

I appreciate the help of Holger Hammerich, the work of the people from the workshop for chemistry laboratory and the availability of our secretaries, Esther Stalder and Daniela Tischhauser.

A number of people made my stay in Basel pleasant and sparkling. I want thank all my friends here and in Switzerland: Maria Praining, Michaela Chiru, Stephan Reinmann, Yavor

Kamdzhilov, Pawel Cias, Petre Bîrza, Nicola Solca, Thomas Galliker, Monique André-Barres, Christian Kobovski, Jerémy Jorda, Mateo Benedetto.

Special thanks to Dr. Dorinel Verdes for his friendship and his `online` support and advice. My special gratitude (hartehijk dank) for his friendship, patience, understanding and support to Sake Timmermans. Dank u veel.

Special and kind thanks to my family and friends from home, to my mother, sister and brother in Bucharest and Ploiesti, Mari, Georgiana and Paul, who always supported me in the decisions I have made. To my special friends, Radu Belu, Vlad, Rodica and Octavian Girigan, and to my father, for their help and care. Mulțumesc.

Roxana

ABBREVIATIONS

AN	acrylonitrile
AQP0	aquaporin 0
BAM	Brewster angle microscope
BSA	bovine serum albumine
γ Bz-Lg	benzylglutamat
b.p.	boiling point
BO	butylenes oxide
BisPT	bisphenol terephthalate
cmc (cac)	critical micelle (aggregation) concentration
D ₃	1,1,3,3,5,5-hexamethylcyclotrisiloxane or hexamethylcyclotrisiloxane
D ₄	1,1,3,3,5,5,7,7-octamethyltetracyclosiloxane or Octamethyltetracyclosiloxane
DIC	differential interference contrast
DSC	differential scanning calorimetry
DMAEM	dimethylaminoethylmethacrylate
DMS	dimethylsiloxane
DMSO	dimethylsulfoxide
DLS	dynamic light scattering
DPS	diphenylsiloxane
EO	ethylene oxide
EtOH	ethanol
F.W.	molecular weight
FeCyDMS	ferrocenyldimethylsilane

F.p.	fusion point
GTP	group transfer polymerisation
GPC	gel permeation chromatography
HRC	horseradish peroxidase
iPAA	isopropylacrylamide
IR	infrared spectroscopy
MMA	methylmethacrylate
MALDI TOF	matrix assisted laser desorption/ionisation time-of-flight
MeOH	methanol
m.p.	melting point
MW	molecular weight (polymers)
NMR	nuclear magnetic resonance
PBS	phosphate buffer
PBS-IF	sodium phosphate buffer
PC	phase contrast
PDI	polydispersity index
PEO	poly(ethylene oxide)
PEG	poly(ethylene glycol)
PMOXA	poly(methyl) oxazoline
PPO	propylene oxide
Ppho	polyphenylene oxide
PDMS	polydimethylsiloxane
RAFT	reversible addition-fragmentation chain transfer polymerization
ROMP	ring opening polymerization
α mSt	α -methylstyrene
SDS	sodium dodecyl sulfate

Sty	styrene
SEC	size exclusion chromatography
SLS	static light scattering
THF	tetrahydrofuran
TLC	thin layer chromatography
TMB	tetramethylbenzidine
UF	ultrafiltration
UV	ultraviolet
VPyO	vinylpyridine oxide

CONTENT OF FIGURES

FIGURE 1.1 The scheme of the association in aggregates.....	2
FIGURE 1.2 Two- and three-dimensional structures of aggregates.....	4
FIGURE 1.3. Schematic illustration of a membrane possible state.....	7
FIGURE 5.1 IR spectra of polyethylene oxide aniolalate.....	31
FIGURE 5.2 ^1H NMR spectra of PEO in DMSO- d_6	32
FIGURE 5.3 MALDI TOF spectra of PEO, $M_n = 2000$ g/mol.....	33
FIGURE 5.4 MALDI TOF spectra of PEO, $M_n = 1100$ g/mol.....	34
FIGURE 5.5 ^{29}Si NMR spectra of polydimethyl siloxane alkyl terminated.....	36
FIGURE 5.6 ^{29}Si NMR spectra for different analysed systems.....	38
FIGURE 5.7 ^{29}Si NMR of polymerized hexamethyl tricyclosiloxane.....	38
FIGURE 5.8 ^{29}Si NMR spectra of different analysed systems.....	39
FIGURE 5.9 ^1H NMR spectra of AB ester terminated diblock copolymer.....	40
FIGURE 5.10 ^1H NMR spectra of the AB hydroxy terminated diblock copolymer	41
FIGURE 5.11 ^1H NMR spectra of ABC triblock copolymers.....	43
FIGURE 5.12 DSC analysis of asymmetric triblock copolymers.....	45
FIGURE 5.13 ^1H NMR spectra of ABC-7-methoxy coumarin labelled copolymer.....	48
FIGURE 5.14 ^1H NMR spectra of ABC-tetramethy rhodamine labelled copolymer.....	48
FIGURE 5.15 2D NMR (COSY) and ^1H NMR spectra of ABA triblock copolymer	50
FIGURE 6.1 Distribution function of the radii of POE $_{25}$ PDMS $_{19}$ PMOXA $_{110}$ copolymer vesicles.....	52
FIGURE 6.2. Hydrodynamic radius for POE $_{25}$ PDMS $_{19}$ PMOXA $_{110}$ copolymers.....	53
FIGURE 6.3 Concentration profile of the static light scattering intensity (Kc)/R(0) by nanovesicles formed from POE $_{25}$ PDMS $_{19}$ PMOXA $_{110}$ triblock copolymer.....	54
FIGURE 6.4 Surface tension measurements for triblock copolymer	55
FIGURE 6.5 TEM of vesicular structures from ABC copolymers.....	56

FIGURE 6.6 Phase contrast of giant vesicles formed by ABC copolymers.....	57
FIGURE 6.7 Differential interference contrast of giant vesicles formed by copolymers.....	57
FIGURE 6.8 Light micrograph images of giant vesicles containing encapsulated chromophore Cy5.....	58
FIGURE 6.9 Compression isotherms of amphiphilic copolymers	59
FIGURE 6.10 Compression isotherms for POE ₄₅ PDMS ₆₅ PMOXA ₃₄₆ and POE ₂₅ PDMS ₁₉ PMOXA ₁₀₀ copolymers.....	60
FIGURE 6.11 Influence of temperature on the monolayers.....	61
FIGURE 6.12 Compression isotherm and Brewster angle microscopy for symmetric ABA triblock copolymer.....	62
FIGURE 6.13 Influence of LamB protein on a triblock copolymer bilayer.....	63
FIGURE 7.1 Fluorescence spectra of labelled and non labelled triblock copolymers	64
FIGURE 7.2 Fluorescence spectra for the PEO ₄₅ PDMS ₆₇ PMOXA ₃₄₆ –coumarin labelled copolymer.....	66
FIGURE 7.3 Fluorescence spectra for the PEO ₄₅ PDMS ₄₀ PMOXA ₆₇ –coumarin labelled copolymer	66
FIGURE 7.4 The variation of steady state fluorescence.....	67
FIGURE 7.5 Fluorescence microscopy of giant vesicles from ABC-fluorescein labelled copolymers.....	68
FIGURE 7.6 Fluorescence microscopy of giant vesicles from ABC-rhodamine labelled copolymers.....	68
FIGURE 8.1 Chemical constitution of the ABC triblock	71
FIGURE 8.2 Representation of Aquaporin 1, similar to Aquaporine 0.....	72
FIGURE 8.3 Schematic representation of proteovesicles reconstituted with Aquaporin. His-Tag head.....	73
FIGURE 8.4 Schematic representation of the orientation of His-Tag labeled Aquaporin 0 in ABA and ABC copolymer vesicles.....	74
FIGURE 8.5 Compression isotherms: polymer-Aquaporin 0 interaction.....	75
FIGURE 8.6 Influence of AQP0 on triblock copolymer monolayer.....	76
FIGURE 8.7 SDS-Page of purified proteovesicles.....	77

FIGURE 8.8 TEM of ABA triblock copolymer vesicles in immunogold labelling experiments.....	78
FIGURE 8.9 Transmission electron microscopy images of ABC triblock copolymer vesicles in immunogold labelling experiments.....	79
FIGURE 8.10 SEC HRC antibody –proteovesicles complexes.....	80
FIGURE 8.11 UV-Vis spectra of the Aquaporin-labelled antibodies for calibration standard.....	81
FIGURE 8.12 Calibration standard for binding of the horseradish peroxidase labelled antibody	82
FIGURE 8.13 Fluorescence spectra of Aquaporin 0 contained in ABA, ABC, CBA and lipid vesicles	85
FIGURE 8.14 Fraction of His-tag labeled Aquaporin 0 in non-physiological orientation	85

LIST OF TABLES

TABLE 2.1 Poly(ethylene oxide) in AB diblock copolymers	11
TABLE 2.2 Poly (ethylene oxide) in ABA triblock copolymers.....	12
TABLE 2.3 Polyethylene oxide in multiblock copolymers.....	12
TABLE 2.4 Polyethylene oxide in ABC triblock copolymers.....	13
TABLE 2.5 Polydimethylsiloxane in AB diblock copolymers.....	14
TABLE 2.6 Polydimethyl siloxanes in ABA triblock copolymers.....	14
TABLE 2.7 Polydimethyl siloxane in multiblock copolymers.....	15
TABLE 2.8 Polymethyl oxazoline in block copolymers.....	16
TABLE 5.1 Molecular weight of poly(ethylene oxides) by ¹ H NMR and MALDI TOF	34
TABLE 5.2 Determination of poly(ethylene glycol) in PEO.....	34
TABLE 5.3. Composition of AB diblock copolymers.....	41
TABLE 5.4. Compositions of ABC triblock copolymers.....	42
TABLE 5.5. Molecular weight estimation by ¹ H NMR and MALDI-TOF	44
TABLE 5.6 Transition temperatures for homopolymers in triblock copolymers.....	45
TABLE 6.1 DLS of triblock copolymers.....	53
TABLE 6.2 ABC triblock copolymers in monolayers experiments.....	60
TABLE 7.1 Relative fluorescence intensities.....	65
TABLE 8.1 Amount of His-tag labeled Aquaporin 0 in lipid, ABA, ABC and CBA triblock copolymer vesicles.....	83

LIST OF SCHEMES

SCHEME 3.1 Mechanism for Brønsted acid initiated polymerization of cyclosiloxanes.....	23
SCHEME 3.2 Mechanism for anionic polymerization of cyclic siloxanes.....	24
SCHEME 3.3 Mechanism for specific redistribution.....	24
SCHEME 3.4 Kinetics of anionic polymerization of cyclosiloxanes.....	25
SCHEME 3.5 Polymerization of D ₃ /D ₄ monomers.....	26
SCHEME 3.6 Preparation of PPS-b-PDMS-b-PPS copolymers.....	27
SCHEME 3.7 Preparation of PDMS-b-PMOXA copolymers.....	28
SCHEME 4.1. Izomerisation of iminoether group to amide group.....	30
SCHEME 4.2. Polymerization of 2-methyl-oxazoline.....	30
SCHEME 4.3 The mechanism of cationic polymerization.....	31
SCHEME 4.4 Cationic ring opening polymerization of methyl oxazoline	32
SCHEME 5.1 Flow chart for preparing POE-b-PDMS-b-PMOXA triblock copolymers.....	34
SCHEME 5.2. Terminal stage of ring anionic polymerization.	51
SCHEME 5.3 Flow chart for preparing PMOXA-PDMS-PMOXA block copolymers.....	49

CHAPTER 0

PREFACE

Molecular self-assembly is a process by which molecules spontaneously organize into ordered assemblies via non-covalent intermolecular forces, such as hydrogen bonds, electrostatic interactions, ion-ion interactions, ion-dipole interactions, hydrophobic interactions, etc.¹. As a result of the self-assembly process, small molecules as well as macromolecules organize in a library of complex structures, such as nano-objects or synthetic membranes. Self-assembly is one of the most universal strategies used in biology for the development of complex and functional structures: fascinating examples are biomembranes, viruses, multimeric proteins and nucleic acid multiplexes.

Inspired by these biological architectures, the design and synthesis of various molecules that are able to self-assemble spontaneously has become an active field of chemistry². In nature, most often the superstructures are formed from amphiphilic molecules, due to their structural specificity. Namely, such molecules possess in their structure at least two parts, which have different (opposite) affinity to water. Hydrophobic parts have a tendency to group together away from aqueous medium, while hydrophilic groups are exposed towards polar medium (water). One example of such aggregation of amphiphilic molecules is formation of biological membranes, which are in fact lipid bilayers. Such systems have been extensively studied over years, to allow for a better understanding of the membrane structure and functions.

Lipid molecules aggregate in dilute aqueous solutions into different morphologies, depending on many factors such as the molecular shape of the lipid, concentration and temperature. One possible morphology is lipid vesicles (liposomes): spherical, closed lipid bilayers³. Liposomes are frequently employed in both theoretical and experimental studies mainly because they are an ideal model system for investigation of biological structures.

Since Bangham first isolated lipids and reconstituted them into liposomes⁴, various applications of such vesicles were introduced. For example, biomolecules such as proteins were integrated into liposome membranes and functional biomolecules encapsulated in their hollow cavities. Similarly, liposomes could be used for encapsulation of therapeutic or cosmetically active agents, for which they serve as transporting vehicles, and the encapsulated species are delivered to a body. However, the main disadvantage of liposomes is their chemical and

mechanical instability to environmental changes⁵, which are considerable limitations in applied science.

In order to overcome this problem, one strategy is to polymerize the lipids in the membrane, thus producing robust entities. However, stabilizing the structure usually decreases membrane permeability, which is a crucial parameter for drug delivery⁶. Another possibility to produce more stable self-assembled superstructures is offered by polymer chemistry, by applying amphiphilic block copolymers.

Block copolymers are structures formed by at least two chemically different polymer chains linked together by a covalent bond. This way, many structural possibilities emerge, such as linear (alternating, statistic or block copolymers) and graft copolymers (reference). It is possible to obtain block copolymers differing with respect to chemical composition, block length and block ratio⁷. If we combine, within one block copolymer macromolecule, both hydrophilic and hydrophobic chains, the resulting species will have amphiphilic characteristics. Such amphiphilic block copolymers also self-assemble in solution⁸, producing a variety of morphologies, in which the insoluble blocks are shielded as far as possible by the soluble ones from the surrounding medium. Depending on block length ratio, the hydrophilic-to-hydrophobic balance (HLB), concentration, temperature, preparation method, etc., different morphologies can be observed in solution⁹, one of them being vesicles (polymersomes), a possible alternative for liposomes.

In practical aspects, structures from block copolymers are superior to liposomes, due to increased toughness, elasticity and mechanical stability¹⁰. Such properties result from block copolymer membranes being considerably thicker (i.e., around 10 nm compared to 3-5 nm in lipids) and more cohesive than conventional lipid bilayers¹². Moreover, almost unlimited possibilities exist for producing amphiphilic block copolymer vesicles: first of all, many chemically different monomers can be used, and additionally, after varying the block length and ratios, it is possible to tailor the structure for particular applications. Contrary to lipids, polymers can be easily modified with reactive groups, and therefore the resulting structures can be further stabilized by crosslinking polymerisation¹¹.

Owing to those properties polymer membranes can be obviously regarded as a mimetic of biological membranes. The contribution of polymer science to the mimetic membrane chemistry is becoming increasingly high¹³. As model systems, vesicular membrane of polymersomes and polymeric free-standing giant films as alternative for black lipid membranes could be studied. Recently, it has been shown that despite the enormous thickness and stability of polymer membranes, integral membrane proteins can be inserted and remain fully functional in such artificial environment^{14,15}. In such a way, completely new types of polymer-protein hybrid

systems can be achieved. Nature provides a wide variety of different membrane proteins that could allow additional control of interactions, transport and ‘communication’ between these synthetic polymer membranes and biological structures.

On the other hand, it has to be emphasized, that in biological systems, lipids and proteins are asymmetrically distributed across biological membranes^{16,17}. This plays a crucial role for many membrane-related processes like carrier-mediated transport or insertion and orientation of integral membrane proteins. Most artificial membranes, such as in AB and ABA block copolymer systems, are, however, symmetric with respect to their midplane and membrane proteins are incorporated with random orientation. To allow for directed insertion, it is necessary to engineer a membrane system in which protein asymmetry will be taken account of¹⁸.

Such an alternative for preparation of asymmetric membranes could be offered by amphiphilic ABC triblock copolymers. With two hydrophilic chains (A and C), separated by a hydrophobic middle block (B), these copolymers may self-assemble in aqueous solutions in vesicular structures. A special feature of the walls of such vesicles arises from molecular incompatibility between hydrophilic chains A and C. Thus we expected in such systems a segregation of A and C chains on different sides of the hydrophobic block B leading to intrinsically asymmetric membranes.

The motivation for this thesis was therefore to engineer novel amphiphilic ABC block copolymers able to self-assemble in water into asymmetric “Janus”-membranes¹⁹. In such a system, it should be possible to insert transmembrane proteins in a controlled manner, similarly to natural cells, where, in lipid membranes, such proteins assume only the physiological orientation. On the other hand, in conventional lipid vesicles membrane proteins are mostly inserted randomly. Until now, to our best knowledge, there exist no studies concerning the induced orientation of biomolecules into asymmetric of amphiphilic systems, especially formed by block copolymers.

The scope of this thesis was to synthesize such asymmetric triblock copolymers. After further characterization of the obtained material, we planned to study self-assembly in aqueous solutions, with emphasis on the membrane properties. The next step was to prove membrane asymmetry in polymeric vesicles, and afterwards we planned to insert a transmembrane protein in such vesicles. Thus, the main objective for this study was to achieve directed orientation of the inserted protein.

The ABC triblock copolymers synthesized in this work were composed by poly(ethylene oxide) as hydrophilic block A, poly(dimethyl siloxane) as hydrophobic block B and poly(2-methyl oxazoline) as hydrophilic block C.

The use of polyethylene-oxide (PEO) was dictated by the well-known biocompatible properties of this hydrophilic polymer: high chain mobility, low interfacial energy with water, steric stabilization effects, lack of binding sites for reactive proteins, non-immunogenicity and non-antigenicity. The poly 2-methyl oxazoline (PMOXA) chain was recently found to be biocompatible and comparable to polyethylene-glycol (PEG) for vesicular drug delivery systems *in vivo*; its biocompatibility resembles the one for POE.

Polydimethyl-siloxane (PDMS) was chosen for its strong hydrophobicity (which improves thermodynamic stability of the aggregates), low glass transition temperature (146 K), high biocompatibility, low surface tension and low surface activity, high oxygen and nitrogen permeability, small temperature dependence of the viscosity.

Such properties of the constituent blocks allow obtaining ABC block copolymers, which should be fully compatible with living organisms, and therefore one could foresee their further application in biological sciences.

Although the synthesis of ABC triblock copolymers was reported previously²⁰, up to now there was no evidence for a membrane forming system. Therefore, our system could be the first example of asymmetric vesicle formation by an ABC triblock copolymer with different chemical compositions of both hydrophilic A and C chains.

It has to be emphasized that asymmetric block copolymer-protein hybrid material would open a whole new area, taking advantage of many possibilities that polymer chemistry offers. It opens the possibility to benefit from the enhanced stability and diversity of such block copolymer aggregates and to incorporate membrane proteins into such completely artificial polymer membranes. The significant advantage offered by the new asymmetric triblock copolymers could be directed insertion of membrane proteins. The resulting protein-polymer hybrid materials could be expected to possess a great potential for applications in the area of diagnostics, sensor technology, protein crystallization, and even drug delivery.

CHAPTER 1

PRINCIPLES OF SELF-ASSEMBLY

1.1. Thermodynamics of self-assembly

Self-assembly refers to a cooperative and reversible assembly of predefined components into an ordered structure²¹. Self-assembly in soft materials relies on the fact that the dissipated energy due to the fluctuations of the position or orientation of the molecules or particles is comparable with the thermal energy²².

The thermodynamic properties of amphiphiles in solution are controlled by the tendency of the hydrophobic region to avoid the contact with water. This phenomenon has been termed the hydrophobic effect². Also, the hydrophobic effect is believed to have its origin in the entropy associated with local hydrogen binding of water molecules²³. In solutions, hydrophobic molecules tend to attract each other stronger than they do in the gas phase. That is the fundamental interaction controlling the molecular assembly ranging from micelle formation to biological membrane structures and protein conformation.

In accordance with the thermodynamic laws, the specific value of the Gibbs function, with respect to the formation of supramolecular structures, tends to be minimum. The chemical potential permits the state of equilibrium in a complex chemical system to be defined precisely, for ideal phases¹: $\mu_i = \mu_i^\theta(T, P) + RT \ln X_i$, where μ_i is the chemical potential of a defined component in the system, μ_i^θ is the standard function, composition-independent for an isolated molecule of type i , R is the gas constant, T is the absolute temperature and X_i is the mole fraction (the X_i is in fact the activity of the system, $a_i = \gamma_i X_i$, for $\gamma_i = 1$, $a_i = X_i$).

The assembly of molecules into organized structures is under thermodynamic control. The organized structures result simply from the search of each molecule for its lowest chemical potential. Following the principles of equilibrium thermodynamics, for a system of molecules, which are forming ordered aggregated structures in solution; the chemical potential of all identical molecules is defined by means of equations*:

$$\text{(Eq. 1.1)} \quad \mu = \mu_1^\theta + kT \lg X_1 = ct. \quad (\text{for monomeric forms})$$

* theory adapted from reference 22

(Eq. 1.2.) $\mu = \mu_2^0 + \frac{1}{2}kT \lg \frac{1}{2}X_2 = ct.$ (for dimeric forms)

(Eq. 1.3.) $\mu = \mu_N = \mu_N^0 + \frac{kT}{n} \lg \left(\frac{X_N}{N} \right) = ct.$ (for N-meric forms, with N=1,2,3...)

Where N : the mean number of aggregates

μ_N : the chemical potential of a “N” molecule in a “N” aggregate

μ_N^0 : the standard chemical potential in a “N” aggregate

X_N : the concentration of molecules in N aggregates number

ct.: constant

At equilibrium, the chemical potential of all molecules of the same kind, whether free molecules or in aggregates, has to be the same, in agreement with the principles of thermodynamics.

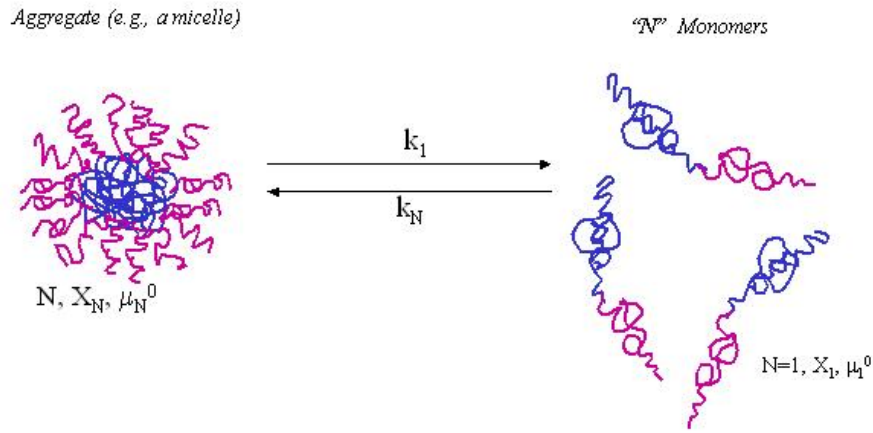


Figure 1.1 The scheme of the association of N monomers into an aggregate (e.g., micelles)

Referring to Figure 1.1., by using the law of mass action approach (eq. 1.4-1.5)²², the equation 1.3. could be written in the form:

$$k_{assoc.} = k_1 X_1^N \quad (Eq.1.4; Eq. 1.5.)$$

$$k_{dissoc.} = k_N \left(\frac{X_N}{N} \right)$$

$$K = \frac{X_N}{X_1^N} \quad (Eq. 1.6.)$$

$$K = \frac{k_1}{k_N} = e^{[-N(\mu_N^0 - \mu_1^0)/kT]}$$

with K: the equilibrium constant of the “aggregation reaction”. This equation is adapted for ideal mixing. For diluted systems, the same law could not describe the effect of the interactions between aggregates.

The last equation, Eq. 1.6, could be written in a more convenient form using the arbitrary reference of aggregates (M) with aggregation number of M.

$$X_N = N \left\{ \frac{X_M}{M} \cdot e^{[M(\mu_M^0 - \mu_N^0)/kT]} \right\}^{\frac{N}{M}} \quad (\text{Eq.1.7.})$$

For the aggregation number of 1, M=1, the previous expression becomes:

$$M=1 \Rightarrow X_N = N \left\{ X_1 e^{[(\mu_1^0 - \mu_N^0)/kT]} \right\}^N \quad (\text{Eq. 1.8.})$$

The total concentration of solute molecules is expressed by the form of the conservation relation for the solute:

$$C = X_1 + X_2 + X_3 + \dots = \sum_{N=1}^{\infty} X_N \quad (\text{Eq. 1.9.})$$

Equations 1.7, 1.8 and 1.9 completely define the ideal mixing system.

The necessary condition for the formation of aggregates relies on the existence of a difference in the cohesive energies between the molecules that participate in the formation of aggregates and dispersed molecules (monomers)²⁴.

If we assume that each of aggregated molecules has the same interaction with their close environments, the mean interaction free energy per molecule (μ_N^0) will be constant. Consequently, the equation 1.8 could be written as:

$$X_N = N \left\{ X_1 e^{[(\mu_1^0 - \mu_N^0)/kT]} \right\}^N$$

$$X_N = NX_1^N, \text{ with } \mu_1^0 = \mu_2^0 = \mu_3^0 = \dots = \mu_N^0 \quad (\text{Eq. 1.10})$$

In particular, C and X_N can never exceed unity.

Then, since $X_1 < 1$, that implies $X_N \ll X_1$, so that most of the molecules will be in monomeric dispersed state.

The necessary condition for the formation of aggregates is that $\mu_N^0 < \mu_1^0$ for all values of N. The relation between μ_N^0 and N determines the mean size and polydispersity of aggregates. Since the functional variation between both parameters may be complex, many structurally different populations may coexist in thermodynamic equilibrium with each other.

More than one functional form of μ_N^0 could be expressed for simple structures; in terms of monomer-monomer binding energy in the aggregates (with α the constant characteristic of intermolecular interactions), the total interaction free energy of an aggregate formed by N monomers is elaborated in Eq.1.11 a. This form of the equation contains the parameter μ_∞^0 , the “bulk” energy of molecules in an infinite aggregate.

$$N\mu_N^0 = -(N-1)\alpha kT \Rightarrow \quad \text{(Eq. 1.11a. 1.11.b)}^{22}$$

$$\mu_N^0 = -(1-1/N)\alpha kT = \mu_\infty^0 + \alpha kT / N^{1/2}$$

This relation is valid for two-dimensional aggregates (e.g., disc-like aggregates, Fig. 1.2.a).

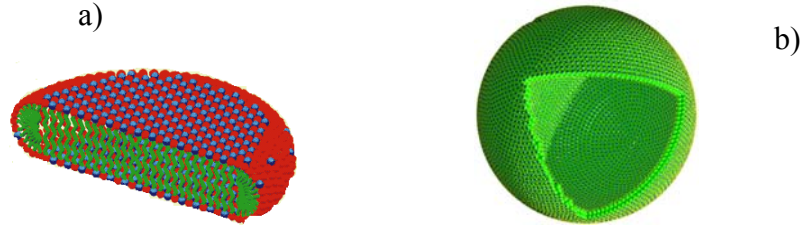


Figure 1.2 a) Two- and b) Three-dimensional structures formed by the association of identical monomers in solution.

For three-dimensional aggregates (e.g., spheres, Fig. 1.2.b), when N is proportional to the volume, the interaction free energy of the molecules can be expressed as:

$$\mu_N^0 = \mu_\infty^0 + \frac{\alpha kT}{N^{1/3}} \Rightarrow \mu_N^0 = \mu_\infty^0 + \frac{\alpha kT}{N^p} \quad \text{(Eq. 1.12a. and Eq.1.12.b.),}$$

with α : the constant dependent on the strength of the intermolecular interactions and p: the number dependent on the shape of the aggregates. This last equation applies to various micellar

structures and to spherical vesicles in which the bilayers bend elastically¹². The condition for aggregate formation is accomplished in this way, since μ_N^0 approaches μ_∞^0 .

Therefore, if the aggregates' shape is known, their physical properties are necessarily given by the thermodynamic equations.

1.2. Self-assembling systems. Lyotropic mesophases

At high concentrations or in bulk, amphiphiles tend to form lyotropic liquid crystal mesophases²⁵. These structures include for example cubically packed spherical micelles, hexagonally packed cylindrical micelles, lamellae, bicontinuous cubic phases²⁶.

Paragraph 1.1 discussed the formal analysis of the thermodynamics of self-assembly. To understand the structural aspects of the association of amphiphilic molecules in aqueous solutions, the type of interactions occurring between amphiphilic molecules in aggregates should be specifically considered. These forces induce the molecular packing, which implies the nature of the formed structure²⁷. The self-assembly of amphiphiles into well-defined structures such as micelles and bilayers is governed by the hydrophobic interactions at the hydrocarbon-water interface. One interaction tends to decrease since the other one increases the interfacial area (a) per molecule (or the surface area occupied per headgroup a) exposed to the aqueous phase. The expression of the attractive interfacial free energy contribution serves as first approximation, since μ_N^0 is expressed as function of two measurable parameters, γ and a_0 ²².

$$\mu_N^0 = 2\gamma a_0 + \frac{\gamma}{a}(a - a_0)^2 \quad (\text{Eq. 1.13.}),$$

where γ represents the interfacial free energy per unit area characteristic of the hydrocarbon-water interface, and a_0 the optimal surface area per molecule, defined at the same hydrocarbon-water interface.

The above equation implies that the interaction energy between lipids has a minimum at a certain headgroup area, a_0 .

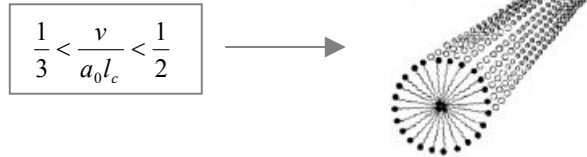
For the accurate description of the geometry of molecules within aggregates, some parameters have to be taken in account. For instance, a_0 (the area), v (the volume of the hydrocarbon or just hydrophobic chains) and l_c (the chain length), will influence the *shape factor* (or *packing parameter*), $v/a_0 l_c$. The packing parameter is responsible for the nature of the structure formed by

molecules. Each of these aggregates corresponds to the minimum sized aggregate in which all the lipids have minimum free energy. The possible structures are schematised below.

- *Spherical micelles* are formed for $a_0 \gg v$ and $v \ll l_c$, $l_c < R$ (the radius of a micelle)



- *Cylindrical (rod-like) micelles* are formed for $a > a_0$, $v/a_0 l > 1/3$



- *Bilayers* are formed by lipids with a small headgroup area a_0 and bulky hydrocarbon chains.



- *Inverted structures* (e.g., inverted micelles) are formed for:



- *Vesicles* are formed for:



All these structures described previously are sensitive to their environment and conditions. Transitions between them can for example be induced by temperature (when both a_0 and l_c can be altered), presence of ions, chain unsaturation or branching (with the diminution of l_c)²⁴.

1.3. Biological membranes from amphiphiles

A cell membrane is built from a bilayer of lipids, associated with membrane proteins and polysaccharides. The lipid bilayer (or, by extrapolation, the amphiphilic components of the membrane) is the structural foundation and the proteins and polysaccharides provide chemical and biological functionality. At physiological temperatures, the membranes are in fluid state. An important aspect of the chain fluidity is that lipids or different amphiphile types pack together. That means that they mutually accommodate to each other while remaining within a planar or curved bilayer configuration.

The membrane-associated proteins are usually amphiphilic, consisting of hydrophilic and hydrophobic regions, and can be incorporated into a bilayer where the hydrophobic region is incorporated into the hydrophobic core of the bilayer and the hydrophilic residues are exposed to the aqueous phase. Proteins are associated with cell membranes in a variety of ways. Those spanning the membrane are known as transmembrane proteins. These are obviously important in the transport of ions or molecules across the cell membrane²⁸.

When proteins are incorporated into an amphiphilic (lipid) bilayer, they usually induce a lateral stress on amphiphilic molecules or lipid and their vicinity (Fig.1.3). Lipids have only a very limited number of possible conformations. A slight mismatch in their dimensions causes a huge energy penalty, which usually provides protein inversion²⁹.

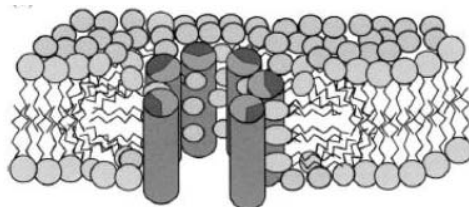


Figure 1.3. Schematic illustration of a possible state, which the membranes can adopt when, bound at the bilayer; strong distortions of the lipid chain packing are observed in the vicinity of the proteins.

Additional lipid-protein interaction includes specific electrostatic or hydrogen-bonding interactions between the hydrophilic headgroups and the exposed amino acid residues of the proteins. A crucial factor to the interaction between integral proteins and membrane amphiphiles is the extent to which each perturbs the dynamic movements of the other.

The functional mechanism can be linked to various molecular models and mechanisms. Thermodynamic models for describing phase diagrams of mixtures of lipid bilayers and amphiphilic proteins in aqueous solutions, using as basic geometrical variables the thickness of

the hydrophobic region of the lipid bilayer and the length of the hydrophobic regions of the proteins are well known today³⁰, however, most models still remain hypothetical. Apart from strong interactions, in particular due to hydrophobic matching and electrostatics, weak long-range interactions due to elasticity may also play an important role³¹. In terms of asymmetry of lipids and proteins in membranes, it is proven that, since the membranes serve to compartmentalize discrete regions within a cell and possess a vectorial nature, both lipids and proteins are asymmetrically distributed across the biological membranes.

1.4 Self-assemblies from asymmetric ABC and symmetric ABA triblock copolymers: vesicular structures

In solution, many different types of vesicles and vesicle-like structures can be prepared from amphiphilic block copolymers. In the case of block copolymer vesicles, each block can be tailored synthetically to modify its length and polydispersity, which, in turn, affects the vesicle size³². Structural features of vesicles, as well as properties including stability, fluidity, and intermembrane dynamics are influenced by the characteristics of the polymer³³. In terms of preparation of block copolymer vesicles, the composition, concentration, water content, and temperature can affect the size of vesicles produced. The three fundamental parameters that affect the block copolymer vesicles morphology³⁴ are core stretching, interfacial energy between the core and the outside solvent, and the corona-corona repulsion; these factors represent the key to the formation and modification of the block copolymer vesicles under equilibrium conditions.

Up to now, only a few publications described vesicle formation from ABC and ABA triblock copolymers. For example, vesicles from the ABC triblock copolymer, polystyrene-*b*-poly(methyl methacrylate)-*b*-poly(acrylic acid) (PS₁₈₀-*b*-PMMA₆₇-*b*-PAA₃₇), were prepared from a dioxane-water mixture by Yu et al.^{8c}. Both PS and PMMA blocks are forming the wall, because both are hydrophobic, and the hydrophilic PAA blocks form the corona. Another example of vesicles from an ABC triblock copolymer, poly(5-(*N,N*-dimethylamino) isoprene)-*b*-polystyrene-*b*-poly(methacrylic acid) was given by Müller's group³⁵. Two different types of vesicles from this polymer were prepared under different pH conditions, and it was shown that the vesicles have different structures. Under acid conditions, both the polyamino-isoprene blocks and the polymethacrylic acid blocks were soluble and formed the coronas of the vesicles, while the polystyrene blocks formed the wall due to their insolubility in water. Under basic conditions, however, both polyaminoisoprene and the polystyrene blocks were insoluble, and only

polymethacrylates blocks formed the corona. Recently, Eisenberg et al.³⁶ presented the vesicles from a new asymmetric ABC triblock copolymer: poly(acrylic acid)-b-polystyrene-poly(4-vinyl pyridine) and they report on pH inversion dependency of these structures in DMF/THF/H₂O mixtures.

Meier et al. studied ABA-type triblock copolymers formed by poly(methyl oxazoline)-b-poly(dimethyl siloxane)-b-poly(methyl oxazoline) triblock copolymer bearing polymerizable groups at the end of the A hydrophilic blocks^{8a, 8c}.

In order to be able to form vesicles in water, block copolymers should have a hydrophilic-hydrophobic volume ratio (“hydrophilic weight fraction”) similar to lipids. The hydrophobic block length largely affects the membrane thickness, which can be several times larger than the value typical for liposome. Concerning the thermodynamic stabilization mechanism of block copolymer vesicles, Eisenberg et al.³⁷ have shown that, since the size of the vesicle could be changed reversibly by changing the composition of the solvent mixture in which they have been prepared, the vesicles may be possibly the equilibrium structures. The hypothesis for the thermodynamic stabilization of the vesicles is based on the segregation of the hydrophilic chains of different length between the inside and outside of the vesicles. The stabilization of the curvature of the vesicles is accomplished by having the long hydrophilic chains segregated to the outside of the vesicles. The short hydrophilic chains are segregated to the inside of the vesicles. In this way, the repulsion among corona chains outside is stronger than that inside the vesicles and a curvature is thermodynamically maintained.

There is a growing interest in the synthesis and characterization of ABC triblock copolymers in the bulk, because of their complex morphologies in the solid state. The formation of these morphologies is due to the inherent incompatibility of most polymers above a certain molecular weight threshold, which, because of the covalent attachment of the segments, leads to micro phase separation³⁸. These morphologies include cylinders in cylinders³⁹, cylinders surrounded by rings⁴⁰, and cylinders surrounded by helices⁴¹. A comprehensive theoretical study on ABC triblock copolymers⁴² predicted that the block sequence should have a dramatic effect altering the solid-state morphology of an equimolar triblock from lamellae, to cylinders in lamellae.

CHAPTER 2

AMPHIPHILIC BLOCK COPOLYMERS: SYNTHESIS OF AMPHIPHILIC OR FUNCTIONAL BLOCK AND GRAFT COPOLYMERS. VESICULAR STRUCTURES.

2.1. Block copolymers of polyethers, polydimethyl siloxane and poly imino ethers

Block copolymers consist of linear arrangements of blocks of the same monomer composition. A diblock copolymer, for instance, is composed of two monomer species that are completely segregated and thus form two different blocks linked together by a covalent bond⁴³. These blocks generally exhibit the macroscopic properties, e.g. glass transition temperature (T_g), of the corresponding homopolymers⁴⁴.

The focus of this chapter, therefore, is the review of block copolymers consisting of combination of polyethylene oxide, polydimethyl siloxanes and poly2-methyl oxazolines. All these three components are found in the composition of the ABC triblock copolymers described further in the thesis.

2.1.1. Copolymers of polyethylene oxide

Polyalkylene oxide polymers, (i.e. PEO) appear in many ways to be unique. No other polymer has as wide a range of biological applications as polyethylene oxide⁴⁵. One of the prime properties of PEO is its “exclusion effect”, determined by the strong hydration, good conformational flexibility and high chain mobility. The number of copolymer combinations for a specific application formed by this polymer is impressive. The tables below are an overview of the polyethylene oxide copolymers.

Table 2.1 Poly(ethylene oxide) in AB diblock copolymers

	Block A	Block B	Initiator system or synthetic method	Reference
AB diblock copolymers	Propylene oxide	Ethylene oxide	RONa	46,47
	Butylene oxide	Ethylene oxide	RONa	47
	Formaldehyde	Ethylene oxide	BF ₃ ·O(C ₄ H ₉) ₂	48
	Ethylene oxide	Styrene	C ₉ H ₁₁ K	49,50
	Ethylene oxide	Ethylene	Peroxide initiation; oxygen-containing telomers	51
	Methyl-ε-caprolactone	Ethylene oxide	(C ₄ H ₉) ₂ Zn	52,53
	Ethylene sulfide	Ethylene oxide	K carbazyl	54
	Ethylene oxide	Methacrylate	Sequent. ionic polym.	55
	Ethylene oxide	L-amino acid	Anionic polymerization	56
	Ethylene oxide	Butadiene	Two steps anionic polym.	57
	Ethylene oxide	Propylene-fumarate	Transesterification	58
	Ethylene oxide	Vinyl chloride	Coupling reaction	59
	Ethylene oxide	Carbosilane	Hydrosilylation	60
	Ethylene oxide	MMA	GTP polymerization	61

Table 2.2 Polyethylene oxide in ABA triblock copolymers

	Block A	Block B*	Initiator system	Conditions	Reference
ABA triblock copolymers	EO	PPO	NaOCH ₂ C(CH ₃)HONa	120°C	46,62,63
		BO	NaORONa	135°C	64,65
	Styrene	EO	Living anionic polym.,	-78°C	66
	ε-Caprolactone	EO	tol.	THF	67
	Lactide	EO	ROP of cyclic monomers	-	68
	Isobutylene	EO	Coupling reaction	-	69
	EO	PDMS/iPA	Hydrosilylation	-	70
		A	AROP / coupling reaction	-	71
		Styrene	PEO peroxy carbamate	-78°C	72
	Acrylonitrile	α-mSty	dianion of α-MS tetramer	-20±10°C	73, 74
	caprolactone		⁺ M ⁻ O(CH ₂ CH ₂ O) _b ⁻ M ⁺	60°C	75, 76
	EO	disodium salt EO			
	EO				

*: EO: ethylene oxide; PPO: propylene oxide; BO: butylenes oxide; PDMS: polydimethylsiloxane ;iPAA: isopropyl acrylamide; α-mSty: methyl styrene.

Table 2.3 Polyethylene oxide in multiblock copolymers

	Block A	Block B	Synthetic method	References
-(AB)_n block copolymers	Ethylene terephthalate	EO	Melt condensation of dialkyl terephthalate	77, 78
	Bisphenol A terephthalate	EO	Coupling of ClCOO-polyether +HO-polyester	79, 80
	Ethylene adipate	EO	Oligomer condensation	81

ABC triblock copolymers	Block A	Block B*	Block C	Synthetic method	Reference
	Styrene	N-iPAA	EO	RAFT technique	82
	Styrene	EO	MMA	Anionic & charge transfert polymerization	83
	EO	MMA	Styrene	Living anionic & photo-induced charge transfert polymerization	84

Table 2.4 Polyethylene oxide in ABC triblock copolymers

*: N-iPAA: N-isopropyl acrylamide; EO: ethylene oxide; MMA: methyl methacrylate

In this thesis, for the preparation of ABC amphiphilic triblock copolymers, polyethylene oxide has been chosen mainly because of the potential applications of nanovesicles formed by ABC triblock copolymers. Since the “soft” PEO homopolymer is well known for being electrically neutral, its solubility in both water and organic solvents and chemical inertness, it is appropriate to consider this polymer for the synthesis of asymmetric triblock copolymers.

2.1.2. Copolymers of polydimethylsiloxane

Due to their unique combination of properties, such as surface activity, physiological inertness (biocompatibility), high oxygen permeability, hydrophobicity, low glass transition temperature and atomic oxygen resistance, organofunctional siloxan oligomers and siloxane containing copolymers offer a wide range of specialty applications in many diverse fields. These applications range from surfactants to photoresistant protective coatings to contact lenses and gas separation membranes. A variety of block and segmented copolymers containing PDMS as the soft segment have been synthesized and characterized. The tables below present the advances in copolymers containing siloxane segments.

Table 2.5 Polydimethyl siloxane in AB diblock copolymers

AB diblock copolymers	Block A*	Block B*	Initiator system or synthetic method	Conditions	Ref.
	DMS	DPS	(CH ₃) ₃ SiOK	-40°C	85
	VPyO	anionic polymerization		86	
	FeCyDMS	anionic polymerization		87	
	Sty	C ₄ H ₉ Li	+100°C	88,89	
	Sty	AIBN + cond.	80°C	90	
	MMA	C ₄ H ₉ Li	-	91	
	MMA	Li ⁺ (C ₆ H ₅) ₂ C ⁻ O ⁻ Li ⁺	-	92	
	AN	C ₄ H ₉ Li	-	93	
	EO-PPO	Condensation	150°C	94	

- DMS : dimethylsiloxane; DPS: diphenylsiloxane ; Sty: styrene; MMA: methyl methacrylate; AN: acrylonitrile; EO-PO: ethylene oxide-propylene oxide; FeCyDMS: Ferrocenyldimethylsilane; VPyO: Vinyl-pyridine oxide

Table 2.6 Polydimethyl siloxanes in ABA triblock copolymers

ABA triblock copolymers	Block A	Block B	Initiator system	Conditions	Ref.
	2-DMAEM	DMS	Radical polym./Cu	-	95
Caprolactone	DMS	AROP cyclics	-	96	
Ethylene oxide	DMS	Hydrosilylation	-	95	
DPS	DMS	C ₆ H ₅ -Si(OLi) ₂ -C ₆ H ₅	25° to 125°C	96	
DMS	Sty	Na, K, Li naphthalene	-80°C to 0°C	97	
DMS	α-Msty	α-Msty tetramer dianion	25 to 50°C	98	
	Isoprene	K naphthalene/ K metal	-80°C	99	
	MMA	Na naphthalene	0°C	88	
	AN	Na naphthalene	0°C	100	
2-Vinylpyridine	DMS	K naphthalene	-	100	
Caprolactam	DMS	Lactam terminated siloxane oligomer + LiAlH ₄	110°C	101	
Lauryllactam	DMS	Lactam terminated siloxane oligomer + LiAlH ₄	110°C	102	

Table 2.7 Polydimethyl siloxane in multiblock copolymers

	Block A*	Block B	Initiator system	Conditions	Ref.
-(AB)_n- triblock copolymers	DPS	DMS	[Li ⁺ O ⁻ Si(C ₆ H ₅) ₂] ₂ -O, HMPA complex+coupling	25-150°C	103,104
	PhO	DMS	Oligomer condensation via silylamine-hydroxy reaction	200°C	104
	Sty	DMS	Dehydrocondensation of SiOH- terminated A-B-A	-	105
	α-MeSty	DMS	Oligomer condensation via silylamine-hydroxy	120-180°C	106,107 108
	BisPT	DMS	Oligomer condensation via silylamine-hydroxy reaction	180°C	109
	γ-Bz-L-g	DMS	Oligomer condensation	120°C	110
	Urethane	DMS	Oligomer condensation	50°C	111
	Imide	DMS	Oligomer condensation Oligomer condensation	-	

- *PhO*: poly(phenylene) oxide; *BisPT*: bisphenol-terephthalate; *γ-Bz-L-g*: benzyl-L-glutamate;
DMAEM: dimethyl aminoethyl methacrylate;

ABC triblock copolymers possessing the polysiloxane hydrophobic segment have not been thoroughly studied. Therefore, there are not many examples of ABC triblock copolymers containing siloxanes.

1.4.1. Copolymers of polymethyl oxazolines

The attractive features of oxazoline polymerizations include the ease with which alternating blocks, graft and random copolymers can be produced.

The range of applications of this polymer is impressive. This polyimino-ether could be used for recycling, hybrid organic/inorganic composites, composite resins, surfactant, chelators and hydrogels. The table below contains information about multiple possibilities in block-copolymers formed of methyl oxazolines.

Table 2.8 Poly(methyl) oxazoline in block copolymers.

Copolymerization	Monomers	References
Alternating/Zwitterionic	Acrylic monomers, propiolactones	112,113,114
Block (AB, ABA block copolymers)	Styrene, 2-vinylnaphtalene, butadiene, polyethylene glycol, siloxanes, caprolactone, styrene oxide	115,116,117,118,119,120, 121
Graft	Acrylates, styrenic compounds, polyvinylalcohol derivatives, alkyl chloro polyethers	122, 123,124
Linear Polyamines	Poly(oxazolines), poly(oxazines)	125,126

1.5. Synthetic methods for preparation of block copolymer

Classical routes to block copolymers consist of living polymerization methods, active center transformation of sites of polymers and polymer-analogous reactions.

Living Polymerization methods are employed for the production of polymers with predetermined degree of polymerization and low polydispersities. Briefly, from these category one could cite: anionic polymerization, ring opening polymerizations, group-transfert polymerization, ring opening methathesis polymerization, cationic polymerization, living radical polymerization, atom transfer radical polymerization.

In this thesis, we used a combination of both anionic and cationic polymerization for the preparation of triblock copolymers.

- *Anionic polymerization* generally involves an active site where there is a negative charge; the reactive group is an anion. This technique is specific for a series of monomers as: styrene, vinylpyridines, methacrylates, butadiene, and isoprene
- *Cationic polymerization* requires a positive charge in the molecule to be polymerized. This polymerization is initiated by acids. Monomers as isobutylene and vinyl ethers are polymerizable by this method.

CHAPTER 3

INTRODUCTION TO POLYSILOXANES POLYMERS

1.6. Overview of polysiloxanes synthesis

Polysiloxanes can be regarded as derivative of inorganic silicates by partial substitution with organic groups. Polysiloxanes offer a wide spectrum of properties that cannot be offered by common organic polymers. This is a result of the polar Si-O backbone, combined with the contribution from the organic substituents. Some of the outstanding properties of polysiloxanes are high stability, high flexibility and excellent dielectric properties. Therefore, they found increasingly applications during the last years. Today, polydimethylsiloxanes (PDMSs) are used as rubbers, resins, dielectric multimedia, hydraulic or heat transfer fluids, lubricants, medical materials and as surfactants.

The synthesis of polysiloxanes usually starts with dichlorosilanes. Hydrolysis and condensation of silanes, including dichlorosilanes give linear and cyclic siloxanes. The preparation of polysiloxanes from hydrolysis and condensation of chlorosilanes results in poor molecular weight control. Therefore, the synthesis of polysiloxanes was gradually replaced by ring opening polymerization of cyclic siloxanes.

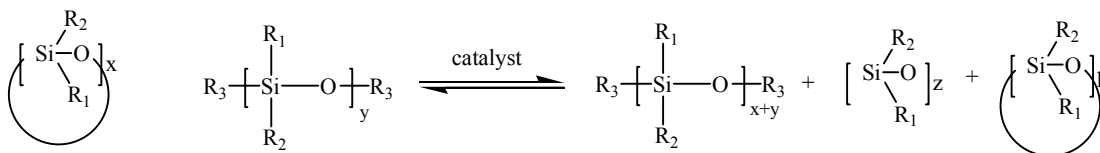
Kinetically controlled polymerization of cyclosiloxanes is based on anionic polymerization of ring strained cyclotrisiloxanes and is quite similar to living polymerization. Therefore, it allows preparation of nearly monodisperse polysiloxanes and novel polysiloxanes with tailored structures. The limitation of kinetically controlled polymerization is that cyclotrisiloxanes are more difficult to synthesize than unstrained cycles. Modification of existing polysiloxanes is an indispensable method for preparing novel polysiloxanes, which cannot be prepared by equilibrium polymerization. For example, liquid crystalline polysiloxanes, which have various bulky substituents, are difficult to prepare from their cyclic precursors. However, these polymers can be obtained by hydrosilylation of polyhydrogen-methylsiloxanes with olefin containing mesogenic groups.

This chapter only reviews the knowledge relevant to this thesis, which includes preparation of polysiloxane chains, ring-chain equilibrium, ring-opening polymerization and preparation of amphiphilic polysiloxane ABC tribloc copolymers. For more information on polysiloxanes, references 127-130 are recommended.

1.7.

Ring-chain equilibrium: thermodynamic considerations

Siloxanes are thermally very stable. In the presence of strong base or strong acid, cyclic polysiloxanes will give a mixture of cyclic and linear polysiloxanes:



with x , y and $x+y$ indicating the number of siloxane units; $z > x$, $p < x$.

The equilibrium concentration of the cycles depends on polymerization enthalpy change and polymerization entropy change. For most cycles, the polymerization enthalpy change is close to zero since the reaction does not involve net changes in chemical bonding except rearrangements of siloxane bonding. An exception is the cyclotrisiloxane, whose polymerization is accompanied by release of ring strain energy (for D_3 , it is 15 kJ/mol). Thus cyclotrisiloxanes have low concentrations in polysiloxanes equilibrates. The equilibrium concentration of cycles is not related to the catalyst and the degree of polymerization. Therefore, if the concentration of the total of siloxanes (including cyclic and linear polysiloxanes) in a solution is below a critical concentration, no linear polymer should coexist with the cycles in equilibrates. This conclusion was confirmed experimentally for many polysiloxanes. The equilibrium concentration of cyclosiloxanes depends mainly on the substituents. The general trend is that long or bulky substituents lead to high equilibrium concentrations of cycles¹³¹. Equilibrium concentrations of unstrained cycles are nearly independent of temperature since the enthalpy changes of polymerization are negligible. Equilibrium concentrations of cyclotrisiloxanes, however, increase considerably with temperature because of the negative polymerization enthalpy¹³².

1.8.

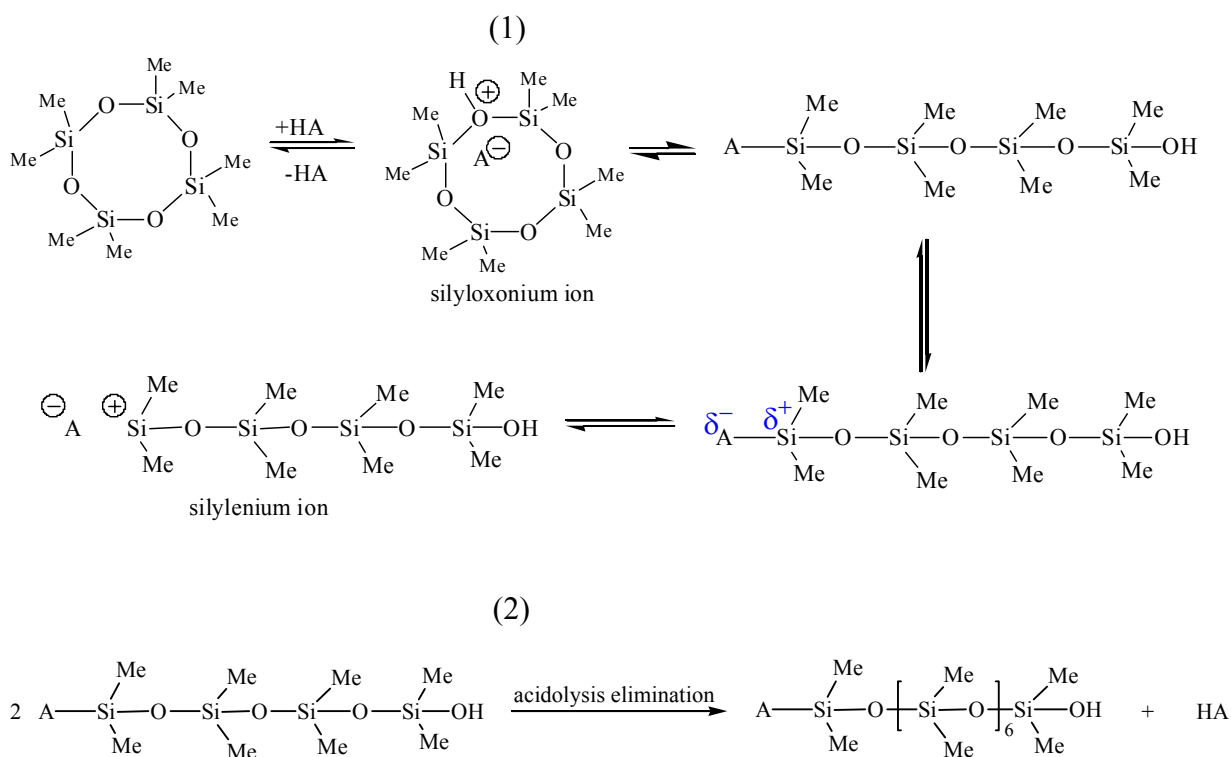
Ring-opening polymerization: kinetic considerations

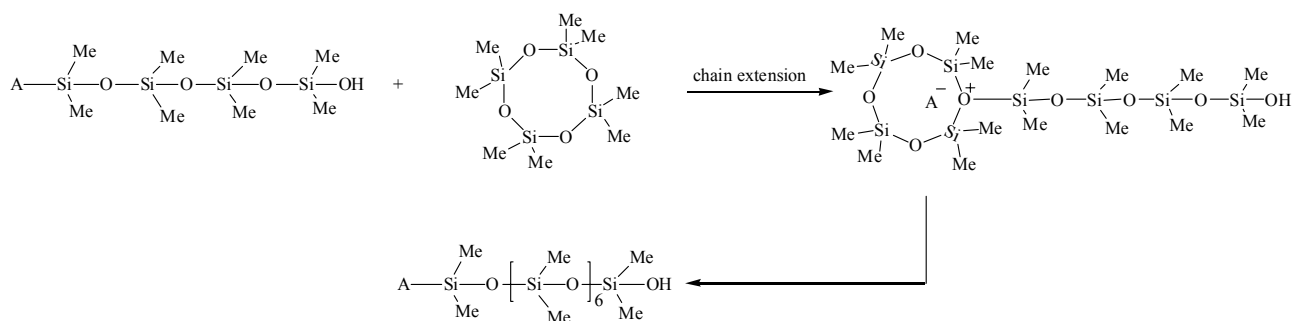
A wide variety of catalysts have been reported for ring opening polymerization of cyclic siloxanes, including strong organic and inorganic acids or bases¹³³, dispersed metals and metal oxides¹³⁴, and ion-exchange resins¹³⁵. According to the type of catalyst, ring-opening polymerization can be generally divided into cationic and anionic polymerization. This section will first briefly describe mechanisms of cationic polymerization, and then focus on anionic polymerization.

1.8.1. Cationic polymerization

Catalysts for cationic polymerization can be strong Brønsted acids like sulfuric acid, or combination of Lewis acids with Brønsted acids ($\text{SnCl}_4/\text{H}_2\text{O}$), or irradiation. The mechanism of polymerization is poorly understood. The active species depend strongly on the nature of catalyst. Briefly, for the proton-initiated polymerization, the acid first protonates the cyclosiloxane to form a cyclic silyloxonium salt, which subsequently opens to an oligosiloxane chain with one silanol and one silyl ester end. The linear polysiloxane chains can condense bimolecularly with elimination of acid and give longer chains. The regenerated acid then reacts with cyclic siloxane to additional oligosiloxane chains. This polymerization path is generally called „acidolysis-condensation mechanism“¹³⁶ (1). Alternatively, cyclic siloxanes can also react with a silyl ester group to form a cyclic silyloxonium ion, which immediately opens to regenerate the silyl ester group and form longer polysiloxane chains. This process is called „chain extension mechanism“¹³⁷ (2), because according to this mechanism chains can continuously react with monomer (Scheme 3.1).

Acid catalyzed polymerization can be carried out by using ring strained cyclotrisiloxanes. However, the reaction yields mixtures of macrocycles and linear polysiloxanes because of the competing unimolecular acidolysis condensation¹³⁸. Thus this method has only very limited applicability.



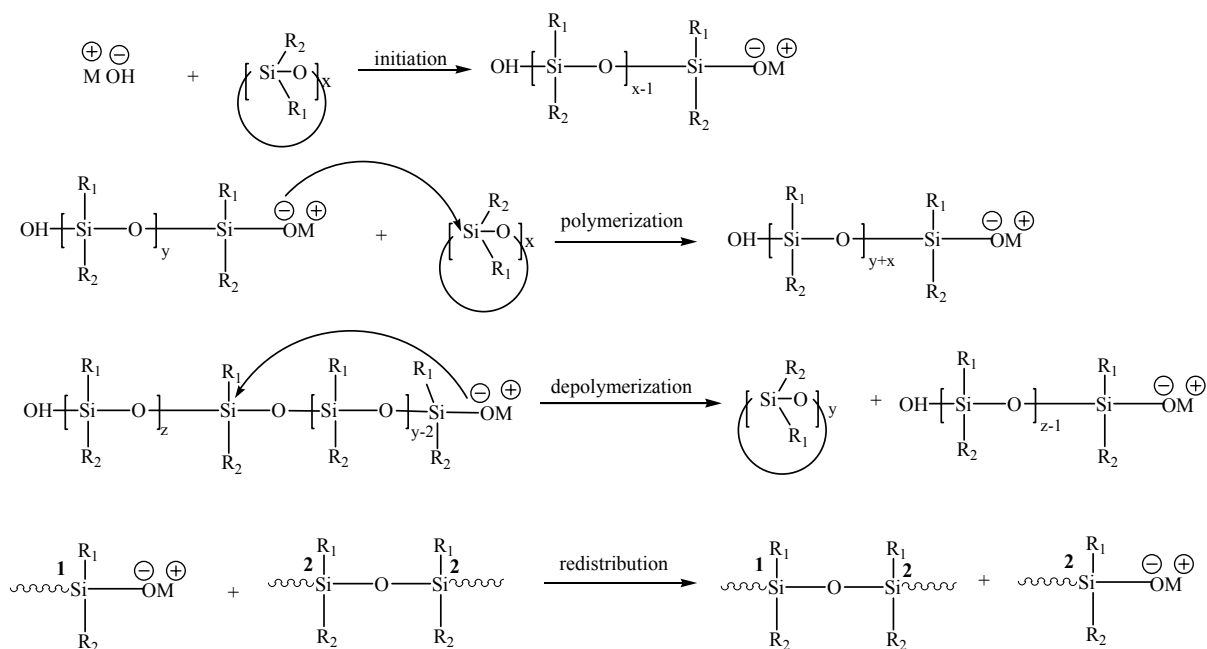


Scheme 3.1 Mechanism for Brønsted acid initiated polymerization of cyclosiloxanes

1.8.2. Anionic Polymerization

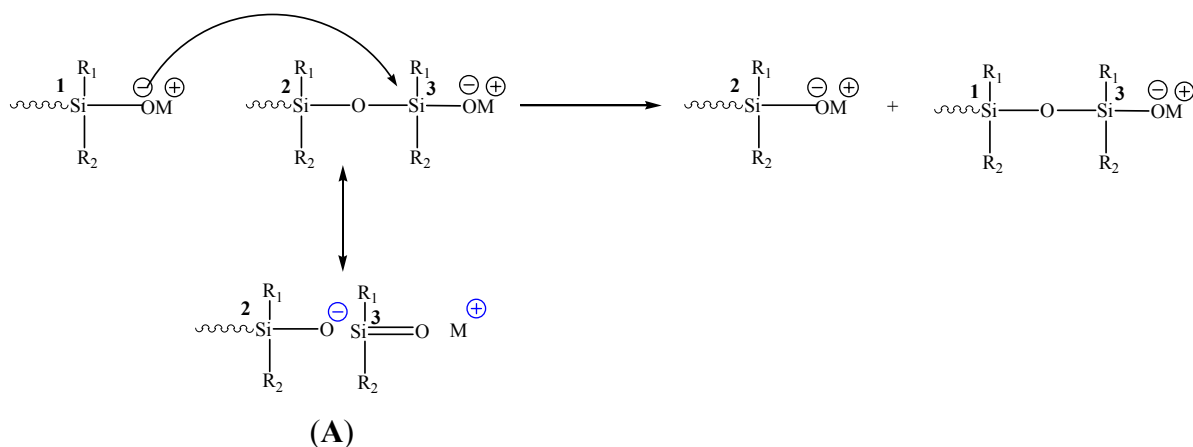
1.8.2.1. General Principles

Anionic polymerization provides a controlled reaction mode, which can be used for preparing polysiloxanes with broader molecular weight distributions⁴⁴. Catalysts for anionic polymerization include alkaline metal hydroxides or silanolates, alkyllithium, quaternary ammonium hydroxides and quaternary phosphonium hydroxides. The anionic polymerization of cyclosiloxanes is a chain extension reaction. Any catalyst used, reacts with cyclic monomer to yield short silanolate-ended chains (chain initiation). The silanolate ions then attack the cyclic monomer to form cyclic five-coordinated silicon complexes, which subsequently open to form longer silanolate-ended chains. By repetitious reaction of silanolate ions (end groups) with the cyclic monomer and repetitious regeneration of longer silanolate ended chains, high molecular weight polysiloxanes are formed (chain propagation). Silanolate ions are reactive to both cyclic monomers and linear polymers. When reacting with their host chain (backbiting), they cause depolymerization and yield cycles of various sizes; reactions with other chains lead to redistribution or reshuffling of polymer chains (Scheme 3.2).



Scheme 3.2 Mechanism for anionic polymerization of cyclic siloxanes; *M*: alkaline metal of initiator

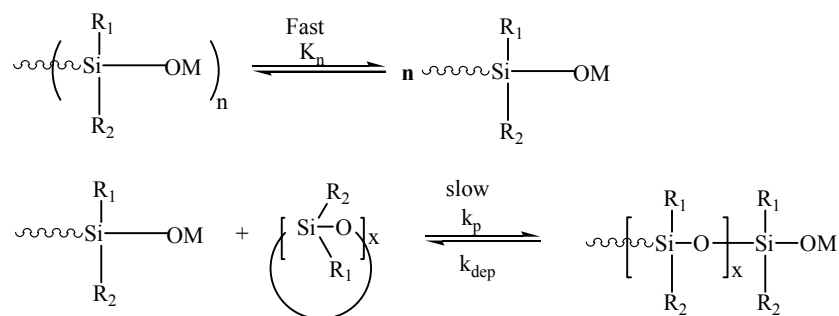
The reaction between two silanolate ions (specific distribution) is much faster than the one between a silanolate and a siloxane unit in linear polysiloxanes (normal reshuffling reactions)¹³⁹. The unusual reactivity in a specific redistribution reaction is due to resonance structure (A), which stabilizes the transition state (Scheme 3.3).



Scheme 3.3 Mechanism for specific redistribution

Generally, during the early stages of polymerization, the polymerization is predominant since most siloxanes exist as cyclic monomers. As the concentration of linear polysiloxanes increases, depolymerization and redistribution become more important. Similar to cationic polymerization,

anionic polymerization leads to a dynamic equilibrium between cycles and linear polysiloxanes. Stable polysiloxanes can be obtained after destroying the silanolate ions by adding chlorosilanes. The silanolates exist more or less as ionic aggregates rather than as free ions¹³¹. The polymerization and depolymerization reactions are the rate determining steps (Scheme 3.4). The rate of anionic polymerization of cyclosiloxanes depends on counterions.



Scheme 3.4 Kinetics of anionic polymerization of cyclosiloxanes; K_n = the equilibrium constant of the reaction between silanolate and the silanolate aggregates; k_p = the rate constant of polymerization; k_{dp} = the rate constant of depolymerization

The catalytic activity for alkali metal or onium hydroxides was reported as: $\text{Li}^+ < \text{Na}^+ < \text{K}^+ < \text{Rb}^+ < \text{Cs}^+ \sim (\text{C}_2\text{H}_5)_4\text{N}^+ \sim (\text{C}_2\text{H}_5)_4\text{P}^+$ ⁽¹²⁷⁾. Such a sequence reflects an increasing volume of counterions, therefore a corresponding increase in dissociation constant. Electron donating molecules, even in trace amounts, can greatly accelerate the rate of polymerization since they can solvate the cations and increase the concentration of free silanolate ions. These molecules are usually called co-catalysts or promoters (example: poly(ethylene glycol), crown ethers, macrotricyclics)¹⁴⁰.

1.8.2.2. Kinetically controlled polymerization

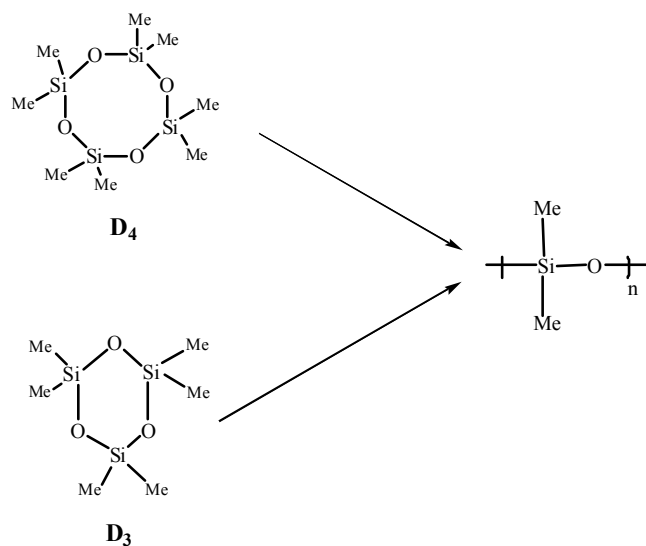
In anionic polymerization of cyclosiloxanes, depolymerization and redistribution are generally considered as bothersome side reactions because they only result in lower conversion of the monomers and large polydispersity of molecular weight. To minimize or eliminate these two reactions, it is necessary to use cyclic monomers that have much higher reactivities than linear polysiloxanes or to use catalysts that react very selectively with cyclic monomers. Therefore, polymerization can be terminated before any substantial depolymerization and redistribution occur (kinetically controlled mode). Unfortunately, no selective catalysts have been found for unstrained cyclosiloxanes. All kinetically controlled polymerizations are based on ring strained cyclotrisiloxanes, which have higher reactivities than unstrained cycles and polymers.

Monodisperse PDMS was prepared in nonpolar solvents like hexane or xylene with 1-4% tetrahydrofuran (THF) or dimethylsulfoxide (DMSO) as promoters and butyllithium or lithium trimethylsilanolate as initiators¹⁴¹. Promoters are mainly used to increase the reactivity of the silanolate, but they also suppress silanolate counterion-siloxane interaction, thus hindering depolymerization and redistributions. Less electrophilic cations such as quaternary ammonium or quaternary phosphonium can also decrease silanolate-siloxane interactions and increase the selectivity of silanolates¹⁴².

Unlike carbanionic polymerization, siloxane polymerizations are not particularly moisture sensitive although moisture does affect the molecular weight of polymers. The reason for this is that the silanol generated by hydrolysis is in rapid equilibrium with silanolates¹⁴³. In the presence of water, a system initiated with a monofunctional initiator forms two different groups of chains, one group is initiated directly by the initiator, and the other is initiated by hydroxide ions from hydrolysis of silanolate. The former chain is monofunctional, while the latter is difunctional. When the concentration of water is much higher than that of initiator, contribution from chains can be neglected, and the polymer shows a narrow molecular weight distribution. However, if the concentration of water and initiator are close, the contributions from either group cannot be neglected, with formation of polysiloxanes with broad molecular weight distributions.

n-Butyllithium and secondary butyllithium are commonly used monobasic initiators for hexamethyltricyclosiloxane (D_3) polymerizations. It was reported that n-butyllithium reacts with an equivalent amount of hexamethylcyclotrisiloxane in nonpolar solvent like cyclohexane giving exclusively $BuMe_2SiOLi$, while 2/3 of D_3 remain unreacted¹⁴⁴. Dilithium diphenylsilanolate (DLDPDS) was used as a dianionic initiator by Bostick¹⁴⁵ to make polydiphenylsiloxane-*b*-PDMS-*b*-polydiphenylsiloxane, yielding PDMS with broad molecular weight distributions.

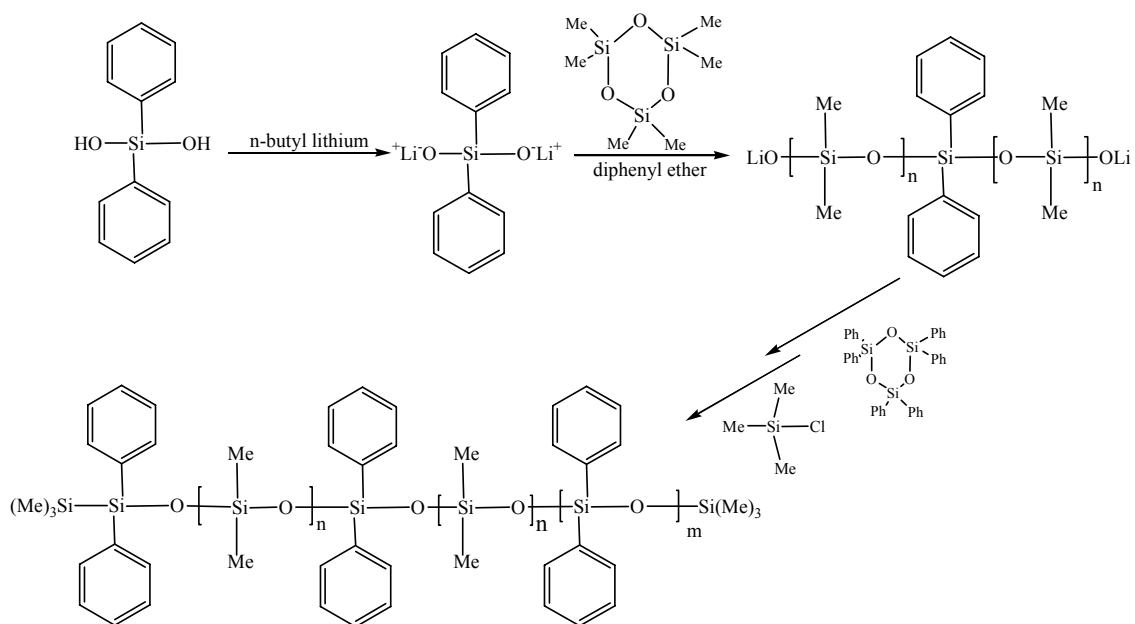
Octamethyl tetracyclosiloxane (D_4) (Scheme 3.5), compared to D_3 has a reduced reactivity^{146,147}. For instance, in polymerization of D_4 (initiated in bulk by potassium hydroxide at high temperatures), the highest polymer yield obtained is ca. 85%. In the case of polymerization of D_3 , the synthesis of the polymer is well controlled for conversions, up to 95%.



Scheme 3.5 Polymerization of D_3/D_4 leads to linear polysiloxanes polymers

1.9. Preparation of triblock copolymers

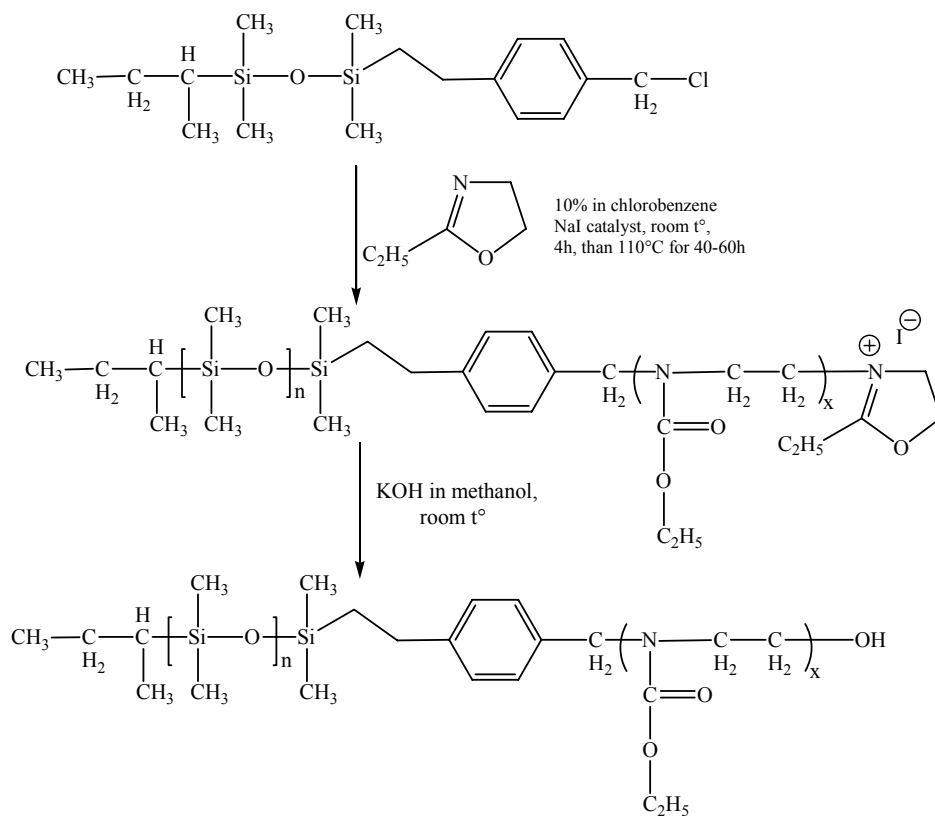
Block copolymers can be prepared by sequential addition of monomers through living polymerization. Polydiphenylsiloxane-b PDMS-b-polydiphenylsiloxane was introduced¹⁶⁰ using kinetically controlled polymerization of hexamethyltricyclosiloxane initiated by dilithium diphenylsilanediolate (DLDPs), followed by adding hexaphenylcyclotrisiloxane (Scheme 3.6). The appropriate solvent for this reaction is diphenylether, which is a good solvent for both hexaphenylcyclotrisiloxane and polydiphenylsiloxane¹⁴⁸.



Scheme 3.6 Preparation of polydiphenylsiloxane-*b*-PDMS-*b*-polydiphenylsiloxane

Multiblock copolymers of polystyrene and PDMS were prepared by condensation of PDMS-*b*-polystyrene-*b*-PDMS oligomers¹⁴⁹. The triblock oligomers were prepared by sodium naphthalene promoted polymerization of styrene, followed by addition of hexamethylcyclotrisiloxane.

Poly(oxazoline)-*b*-PDMS copolymer, a good surfactant, was prepared by transformation of anionic polymerization to cationic polymerization¹⁵⁰. Oxazoline monomers can be polymerized by cationic living polymerization using alkyl chloride catalyst in conjunction with sodium iodide. In the presence of sodium iodide, the alkyl chloride endgroup in PDMS can initiate the polymerization of oxazolines (Scheme 3.7).



Scheme 3.7 Preparation of PDMS-*b*-poly(ethyl oxazoline) by cationic polymerization

Similarly, PMOXA-*b*-PDMS-*b*-PMOXA triblock copolymers were prepared using cationic ring opening polymerization of methyl oxazoline, initiated with triflic acid^{8a}.

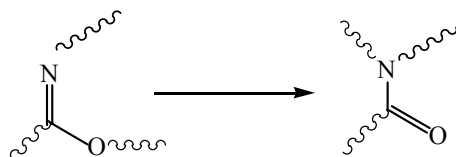
It has to be emphasized that block copolymers, which have two or more organic polymer blocks, separated by one or more polysiloxane blocks are difficult to prepare using non-continuous polymerization processes.

CHAPTER 4

INTRODUCTION TO POLY IMINO ETHERS

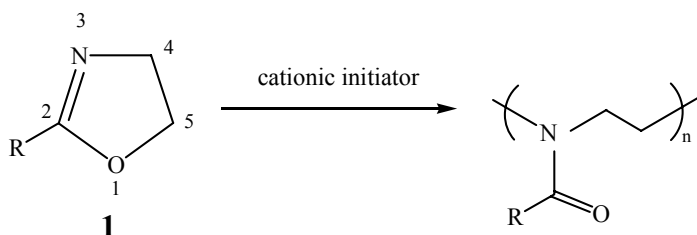
4.1. Cyclic iminoethers

Cyclic iminoethers are heterocyclic compounds with an iminoether linkage. Polymerization of cyclic imino ethers generally proceeds via thermodynamically favorable isomerization of the iminoether group to the amide (Scheme 4.1).



Scheme 4.1. Isomerisation of an iminoether group to amide group

2-Oxazolines (4,5-dihydrooxazoles) are commonly synthesized from the corresponding nitriles or carboxylic acids with modest to good yields. 2-Oxazolines are polymerized with various kinds of cationic initiators as Lewis acids, strong protic acids and their esters, and alkyl halides, to produce derivatives of poly(N-acylimino)ethylene via ring-opening isomerization^{151,152,153}.

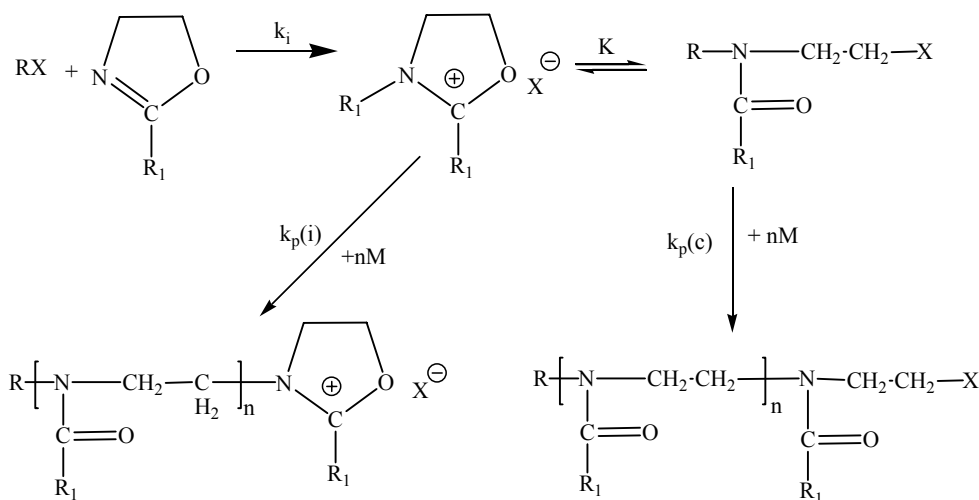


Scheme 4.2.: Polymerization of 2-methyl-oxazoline

Scheme 4.2 gives the general initiation and propagation mechanism of the structure 1.

The reaction proceeds via two different species, that is, ionic and covalent types, depending on the initiator. In conventional cationic polymerization, the nucleophilic attack of nitrogen atom of the cycle onto the carbon atom at the 5-position of the propagating species results in the O(1)-C(5) bond cleavage, as well as isomerization of the ionic complex to yield the structure with N-acylethylenimine units. Chain transfer and termination under the appropriate condition do not disturb the polymerization reaction of 2-oxazolines¹⁵³. The ionic propagating species of a 2-oxazolinium salt is not fragile. Thus, it is conveniently used in the synthesis of end-reactive polymers and block copolymers.

Since its discovery, the mechanism of this cationic (or electrophilic) polymerization has been studied in great detail. It is probably one of the best-understood mechanisms in polymer chemistry (Scheme 4.3).

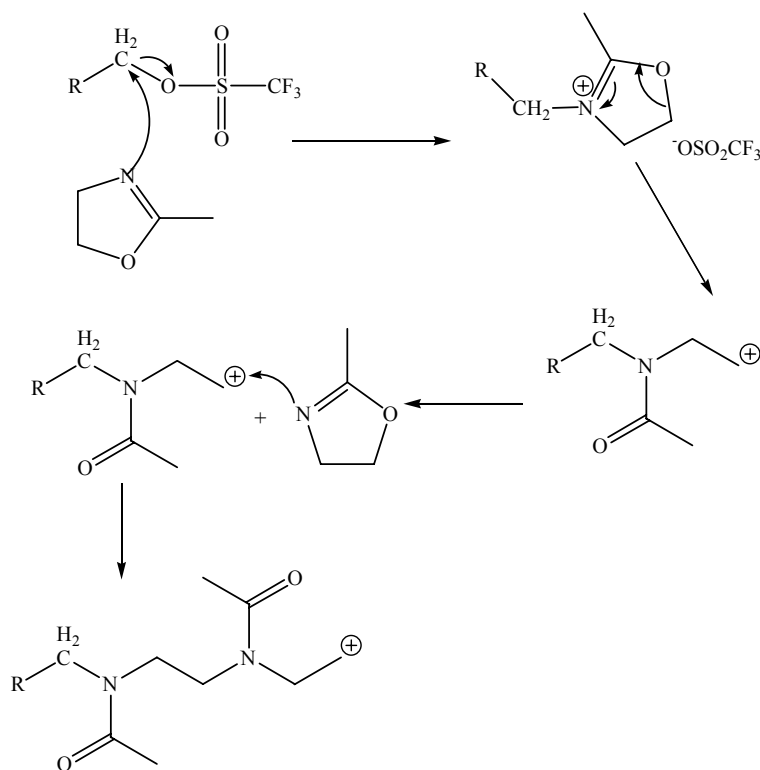


Scheme 4.3 The mechanism of cationic polymerization; k_i : the rate constant of the protonation reaction; $k_p(i)$: the rate constant of the propagation reaction by ionic type mechanism; $k_p(c)$: the rate constant of the propagation reaction by covalent type mechanism; K : the equilibrium constant; M : methyl oxazoline monomer; n : number of monomers for the polymerization, corresponding to the number of units in the polymer composition

The nature of active centers, proven by NMR spectroscopy, depends on the nucleophilicity of the oxazoline (the nature and position of ring substituents), the nucleophilicity of the counterion, the solvent, and temperature. The reactivity of the monomer depends very strongly upon the kind and position of a substituent.

NMR studies confirm the linear structure of polyoxazolines, which follows from the reaction mechanism. These studies also reveal that the rotation about the amide N-C bond is restricted, which leads to distinguishable syn-anti isomers in the chain. Circular dichroism spectra measured on a number of optically active polyoxazolines suggest that the prevailing conformation is a 14/3 helix¹⁵⁴.

For the preparation of triblock copolymers, I employed the cationic ring-opening polymerization of methyl oxazoline initiated with triflic anhydride (Scheme 4.4).



Scheme 4.4 Cationic ring opening polymerization of methyl oxazoline monomer

1.10. Experimental requirements for the polymerization of 2-oxazolines

The cationic polymerization of 2-oxazolines proceeds under anhydrous conditions. High vacuum experiments are necessary. The reagents and solvents used for polymerization should be absolutely dried and the contact with water avoided. For the synthesis of block copolymers and ω -end functional polymers, a test tube or a flask with three-way stopcock is convenient as a reaction vessel. Second monomer or terminating agents are easily added through the cock. In the experimental setup and methodology employed, all impurities capable of deactivating the initiator and the terminating the propagating chain (moisture, oxygen, etc) must be excluded from the polymerization mixture as much as possible. Moisture influences the polymerization degree considerably.

CHAPTER 5

SYNTHESIS OF POLY (ETHYLENE OXIDE)-b-POLY(DIMETHYL) SILOXANE-b-POLY(MEHL) OXAZOLINE TRIBLOCK COPOLYMERS

Amphiphilic block copolymers are generally prepared via ionic polymerization under anhydrous conditions. The synthetic conditions make this method difficult and only a limited number of functional groups can be used.

This chapter describes the synthesis concept, purification of chemicals, preparation of macroinitiators, AB diblock copolymers, ABC triblock copolymers and characterization of homopolymer initiators and polymers. Additionally this chapter contains a detailed scheme of the preparation of the symmetric ABA triblock copolymer used further (chapter 8) in this thesis.

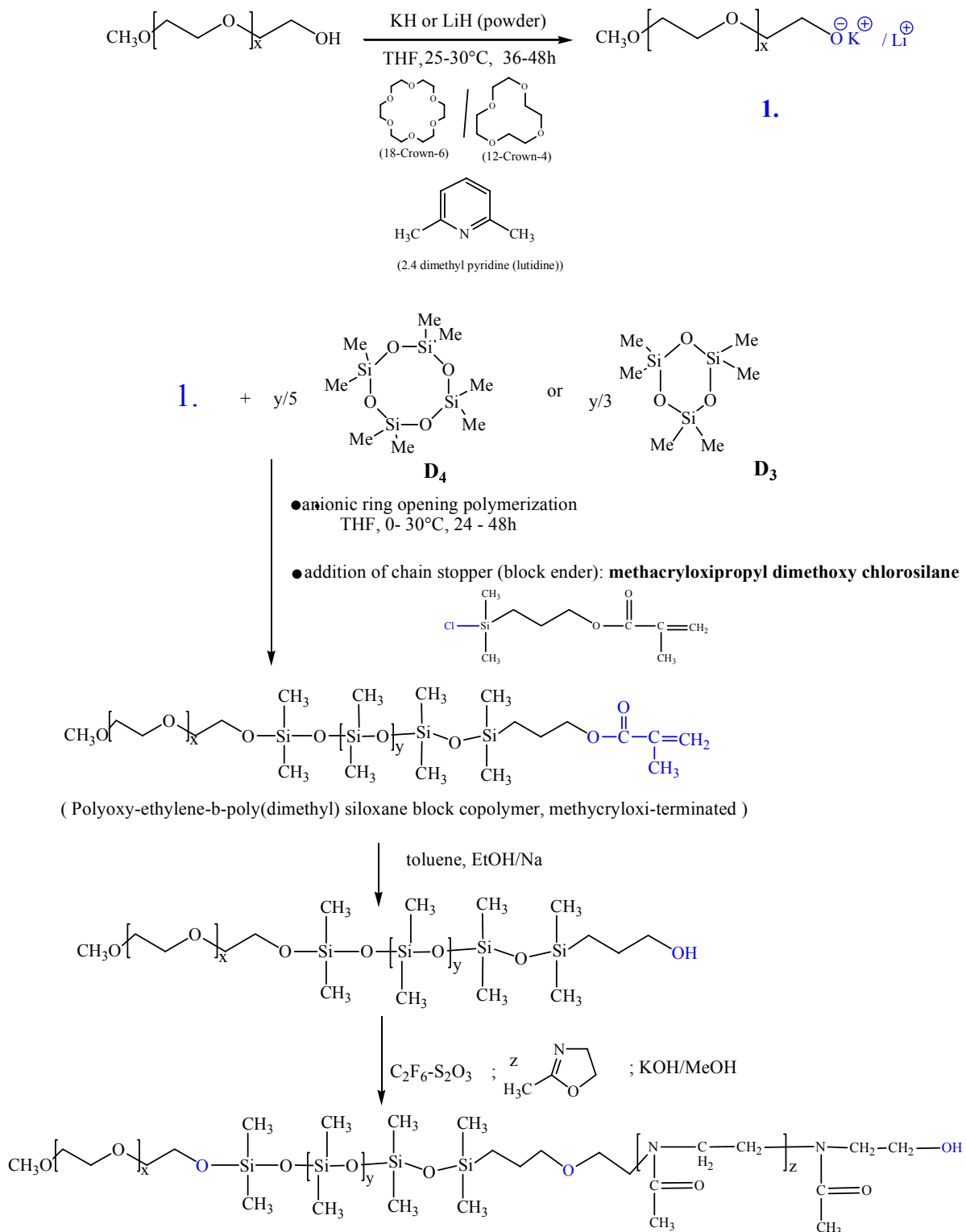
5.1. The Approach

The approach for preparing PEO-*b*-PDMS-*b*-PMOXAs is illustrated in Scheme 5.1. The synthesis starts with poly (ethylene oxide) – potassium alcoholate in THF at room temperature. This PEO macroinitiator can start a ring opening polymerization of octamethyltetracyclosiloxane or hexamethyltricyclosiloxane thus leading to poly(ethylene oxide)-*b*-poly(dimethyl) siloxane diblock copolymers.

The anionic polymerization of cyclosiloxanes is stopped by the addition of, methacryloxypropyldimethoxychlorosilane. Subsequently, the insaturated ester is reduced to a terminal alcohol function. After activation with triflic anhydride, the AB-diblock copolymer itself is used as a macroinitiator for cationic ring opening polymerization of 2-methyl oxazoline.

An alternative for the triblock copolymer synthesis could be a hydrosilylation reaction between an α,ω -difunctional telechelic polydimethylsiloxane (hydrogen terminated one end) obtained by anionic polymerization of hexamethyltricyclosiloxane (D₃) and an allyl-terminated methoxy-poly ethylene glycol. This synthesis was successfully performed four years ago¹³⁵. In our case, the major obstacle for the last method concerns the time optimization and the purity of copolymers as compared to the first approach.

In this thesis, the copolymers were prepared using the first approach, the polymerization of D₄ or D₃ using strong bases (potassium and lithium hydride) and the cationic polymerization of methyl oxazoline initiated by triflic anhydride.



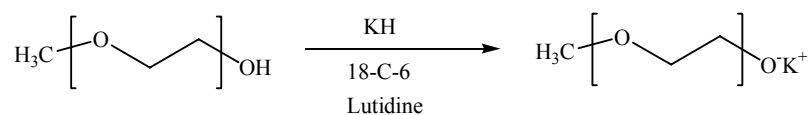
Scheme 5.1 Flow chart for preparing POE-b-PDMS-b-PMOXA triblock copolymers

5.2. Results and Discussions

5.2.1. Poly(ethylene oxide) macroinitiators

There are several ways to convert the terminal hydroxyl group of polyethylene oxide to a potassium alcoholate. One of them is to react PEO with potassium in the presence of naphthalene in THF solution¹⁵⁵. Another method is to react PEO with metal hydrides in THF under nitrogen or argon¹⁵⁶. In this work, the latter method was used.

The synthetic scheme for the preparation of potassium alcoholate has been explored by the direct substitution with potassium hydride.



Here, the presence of small amounts of 18-crown-6 ether enhanced drastically the rate of polymerization¹⁵⁷, since the ethers can solvate the cations and increase the concentration of the free silanolate ions. 2,6-dimethylpyridine (lutidine) was used as a proton scavenger¹⁵⁸ in the activation of the macroinitiator.

For the low molecular weight (1100 g/mol; 2000 g/mol) poly(ethylene oxides) this conversion is relatively fast and only 20 % of the remained hydroxyl groups (i.e., 80%) are detectable by FTIR (Fig. 5.1) when the reaction is carried for 120 minutes, at 30°C. The use of LiH decreases the conversion (60%) with respect to KH. However, in the case of PEO with 113 units (5000 g mol⁻¹) it took 240 minutes to convert only 18% of the hydroxyl groups.

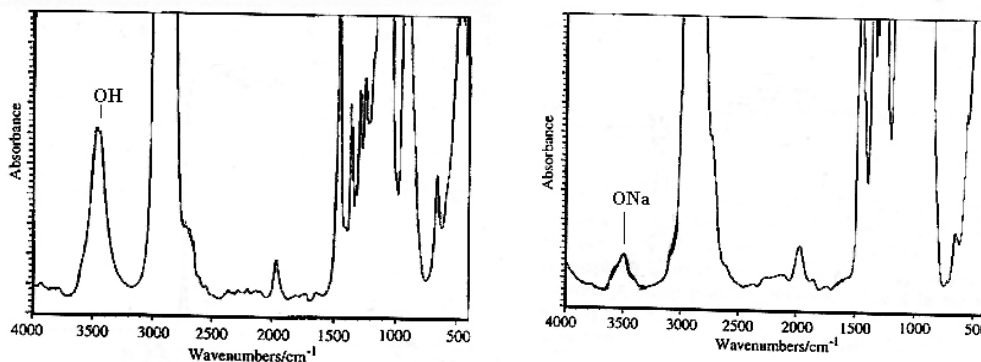


Figure 5.1 IR spectra of polyethylene oxide copolymer and macro-aniolate

Preparation of polyethylene oxide macroinitiators requires highly pure starting materials. Commercially available mono-methyl polyethylene oxide contains also polyethylene glycol and traces of dimethylated-polyethylene oxides¹⁵⁹. It is of primary importance that (1) the polymers are pure semi-telechelics and do not contain any bifunctional (telechelic) PEG because this might lead to poly(blocks) and/or polymer networks and (2) the polymers to have a high ionization degree.

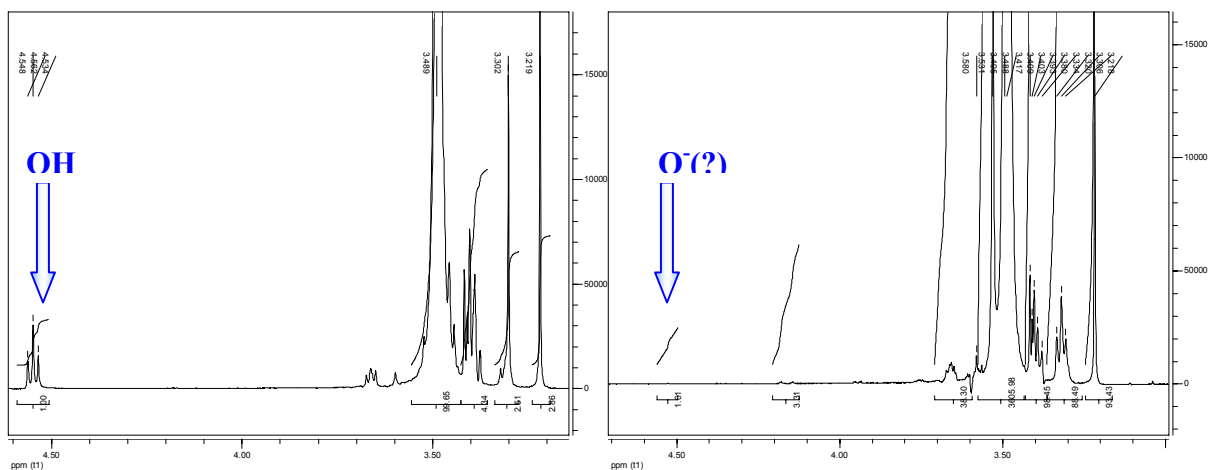


Figure 5.2 ^1H NMR spectra of PEO in DMSO-d_6 at 3.33 ppm, the central peak of the PEO backbone is augmented in area by overlap with the peak for water from DMSO-d_6 solution

We found that the direct determination of the number of hydroxyl termini by proton NMR is complicated due to the small size of the peak and a concentration dependent shift and broadening of the peak through interactions and impurities (including water). This is the reason for using DMSO-d_6 for ^1H NMR studies here. Unlike in CDCl_3 , in DMSO-d_6 , the hydroxyl protons at the polymer terminus appear as a triplet (at 4.54 ppm, see Figure 5.2), which is separated from the large backbone peak (OCH_2CH_2 ; 3.45 ppm). The area of this hydroxy peak can be compared to the areas of other peaks in the spectrum to provide a simple, direct method for determining the degree of conversion of hydroxyls to other groups. The same approach could be also useful for estimating the relatively low-molecular weight PEGs in which the ratio of backbone protons to hydroxyl protons is small to moderate (<200:1).

To assess the purity, i.e. the number of bifunctional telechelics, the following study was performed.

a) Determination of molecular weight: the samples were prepared as above and the spectra acquired as described before. The integral for the OH triplet (4.56 ppm) was normalized to a

single proton and compared to the average of the integrals for the polymer backbone (3.51 ppm). This ratio was equal to the number of protons in the backbone. The molecular weight was then calculated from the following equation:

$$M_n = [(\text{integral backbone})/(\text{integral OH}/2)]/4 \times 44 + 18$$

The results obtained fit well to the values given by the supplier (Table 5.1) and the values obtained with MALDI TOF spectrometry (Figures 5.3 and 5.4).

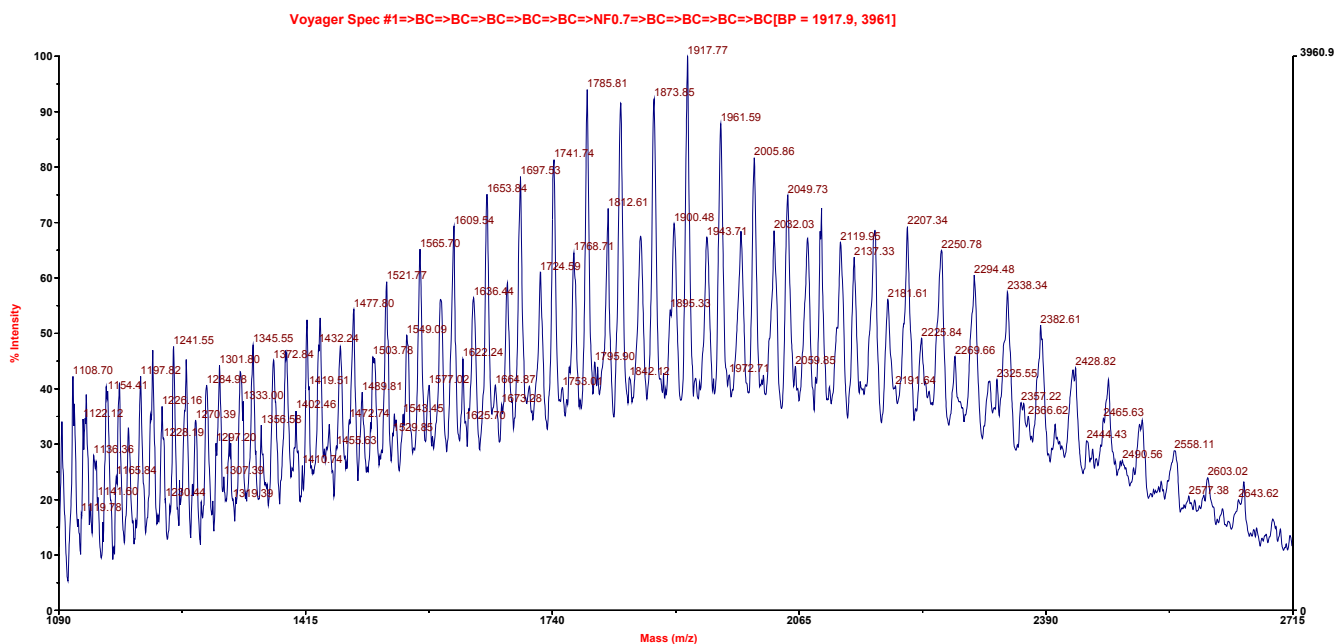


Figure 5.3 MALDI TOF of polyethylene glycol monomethyl ether, (Fluka, $M_n = 2000$ g/mol); the spectra indicates a molecular weight of 1920 g/mol. The difference between the two values (one give by supplier and the other measured by MALDI TOF) is not significant and does not affect our further studies.

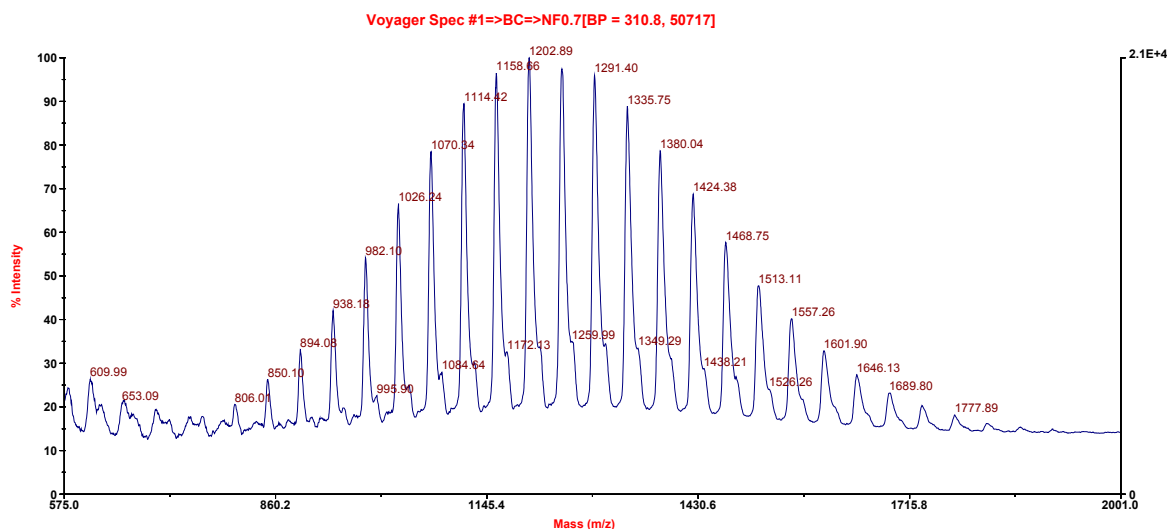


Figure 5.4 MALDI TOF of polyethylene glycol monomethyl ether, Fluka, $M_n = 1100$ g/mol

Table 5.1 Molecular weight of polyethylene oxides obtained by ^1H NMR and MALDI TOF spectrometry

Polyethylene oxide (Fluka)	M_n (MALDI)	M_n (supplier)	M_n (^1H NMR)
25 units	1202	1100	1224
45 units	1920	2000	2232

b) The identification of PEG contaminant in monomethyl ether of polyethylene glycol from NMR spectra¹⁵⁹ allow an estimation of the purity degree.

The ratio of the OH integral to the integral of the normalized (i.e., divided by 3) methoxy singlet (at 3.26 ppm) should be 1 for pure monomethyl ether of PEG. If are taken into account polyethylene oxide with two hydroxyl groups, allows the calculation of the percentage of PEG in the commercial ether samples (Table 5.2).

$$\% \text{ PEG} = \{[(\text{OH integral})/(\text{methoxy integral}/3)-1]\}/2 \times 100$$

Table 5.2 Determination of poly(ethylene glycol) contaminant in monomethyl ether of poly(ethylene glycol)

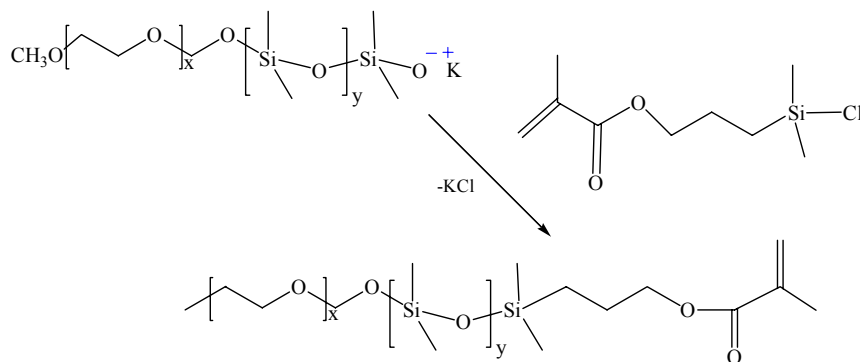
Polyethylene oxide	M_n (MALDI)	M_n (supplier)	Normalized OH/MeO ratio	%PEG
25 units	1202	1100	1.004	1.2
45 units	1920	2000	1.029	1.48

Although the present determination of molecular weight ^1H NMR is limited to lower molecular weight PEO's, it appears suitable for many applications. It is a direct method, dependent only on PEO not on outside standards. It is relatively rapid and easy to apply.

As a result, the starting product of the synthesis of the triblock copolymer is slightly contaminated with polyethylene glycol. This free polyethylene glycol will not influence the formation of the telechelic symmetric polymers in a considerable amount.

5.2.2. AB diblock copolymers

The polymerization of cyclic siloxane monomers with polyethylene oxide macroinitiator prepared is an anionic ring opening polymerization. The cyclic monomer (D_4 and/or D_3) was added and polymerized in the THF solution of polyethylene oxide alcoholate. Finally the polymerization was terminated by the introduction of an end-capping agent (i.e., unsaturated ester of chlorosilane, Scheme 5.2).



Scheme 5.2 Terminal stage of ring anionic polymerization. The chlorosilane has a role of end blocker for the growing anionic species

This end-capping ester allows controlling the growth of the molecular weight of the preformed polysiloxane polymer. Without the addition of an end blocker for the silanolate end chain, the product would hydrolyze.

The purification and optimization of AB diblock copolymers is briefly summarized below. The control of hydrophobic chain was achieved by using lutidine. The unreacted polyethylene oxide is successfully removed from the polymerization mixture by repeated precipitations with cold hexan and additional ultrafiltration. However, an additional step for purification of diblock copolymers by column chromatography is necessary.

Issue	Practical solutions developed in this thesis
Control of the hydrophobic chain	Lutidine as proton scavenger
Unreacted polyethylene oxide	Increase of the temperature, control of the amount of solvent (THF, for assuring good solubility and low viscosity of the polyethylene oxide chains)
Salt formation with trapping of polymers	Rapid filtration under reduced pressure and addition of a mixture of hexane/THF (2/1, v%)
Removal of unreacted polyethylene oxide	Repeated precipitations in cold hexane, followed by ultrafiltration

The optimization of AB diblock copolymer synthesis would require kinetic studies that are beyond the scope of this work. As presented in Chapter 3, anionic polymerization has a number of difficulties. Most important in this context are the number possible of back biting reactions.

^{29}Si NMR was used for the identification of the polysiloxane backbones of copolymers, detection of end-stopper residue as impurity in the copolymer matrix and choice of monomers. Because no standards are available for ^{29}Si NMR studies, we have used commercial alkyl terminated polydimethyl siloxane to identify corresponding peak of the polysiloxane (Figure 5.5)

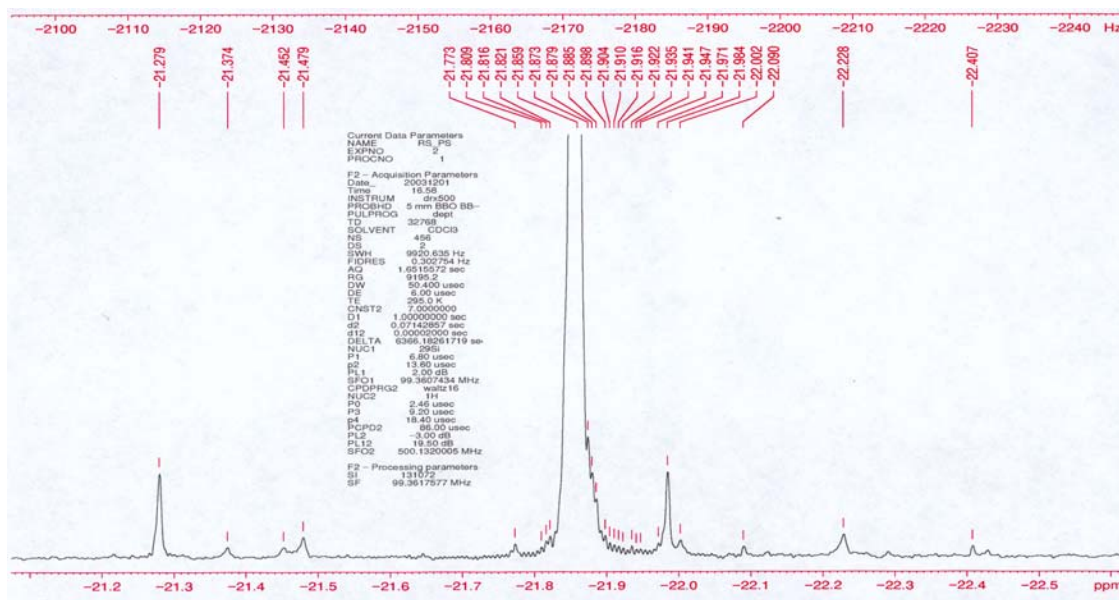


Figure 5.5 ^{29}Si NMR of alkyl terminated polydimethyl siloxane; the corresponding Si atom in the polysiloxane chain shows a signal at $-21,859$ ppm

Since the yield of the anionic polymerization of cyclosiloxanes can be low, the choice of the right monomer is important.

A study performed with different systems indicates low conversion in the case of octamethyltetracyclosiloxane monomer (D₄). For this reason, we decided to use hexamethyltricyclosiloxane (D₃) as monomer. For this study, the polyethylene oxide macroinitiator was replaced with diethylene-glycol monomethyl ether in order to reduce the polymerization time and to allow an accurate ²⁹Si NMR characterization.

The different systems employed were:

1. octamethyltetracyclosiloxane initiated by KH in THF
2. hexamethyltricyclosiloxane initiated by LiH in THF
3. octamethyltetracyclosiloxane initiated by diethylene-glycol monomethyl ether potassium alcoholate in THF
4. hexamethyltricyclosiloxane initiated by diethylene-glycol monomethyl ether lithium alcoholate in THF

Conclusions concerning the analyzed systems:

1. In 24 hours, octamethyltetracyclosiloxane (D₄) does not show a significant conversion (Figure 5.6). A peak corresponding to the silicon atom in polysiloxanes chains appears, but there is no indication that this oligosiloxane has more than 2-3 units. The corresponding peak of the monomer (D₄) shows a singlet at -19.0075 ppm. Moreover, there are few peaks very difficult to be assigned, which probably correspond to oligo – and cyclic siloxanes. The polymerization of D₄ needs a three fold higher reaction time than the polymerization of D₃.
2. In 24 hours, hexamethyltricyclosiloxane (D₃) does polymerize with 80% conversion of the monomer to the polymer as major product. Secondary reactions lead to the formation of cycles and low molecular weight homopolymers (Figure 5.7).

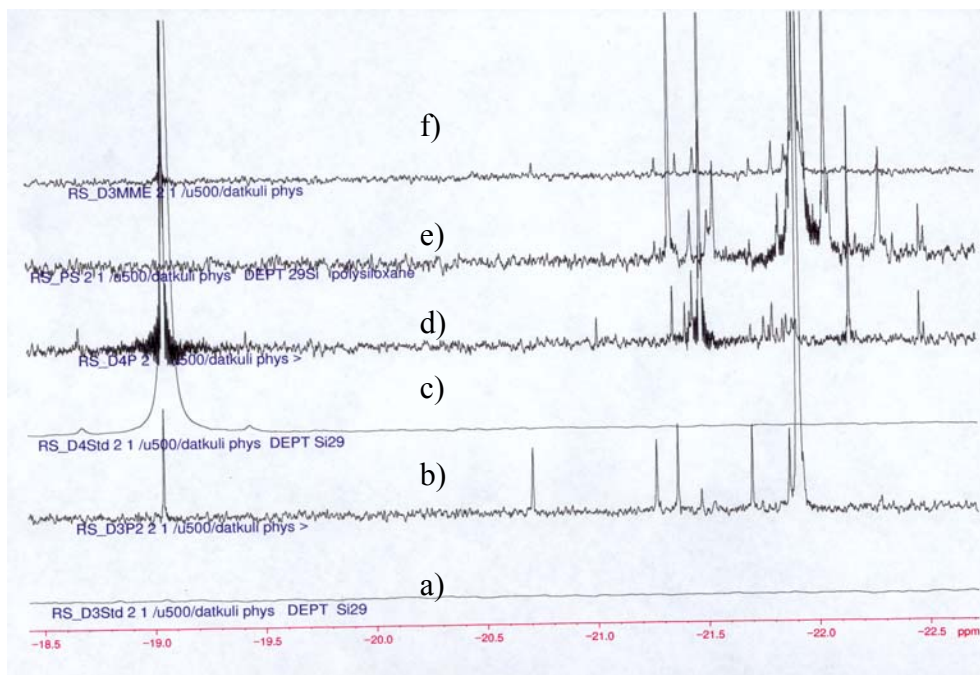


Figure 5.6 ^{29}Si NMR spectra for analyzed systems; a) D_3 monomer standard – no signal in the range of -18 – -22.5 ppm, the only singlet is showed at -8.2 ppm; b) D_3 polymerized by initiation with lithium hydride in THF – polysiloxane chain formation and side cycle in 4 members; c) D_4 monomer standard – one corresponding singlet at -19 ppm; d) D_4 polymerized by initiation with potassium hydride in THF – slow rate polymerization of monomer, the polymerization leads to a mixture of homopolymers and side cycles; e) commercial (Aldrich) polysiloxane alkyl terminated – one corresponding peak for polysiloxane backbone at -21.9 ppm; f) D_3 polymerized by initiation with diethylene-glycol monomethyl ether lithium alcoholate in THF – the system behave similarly with the polymerization of D_3 in the presence of lithium salts.

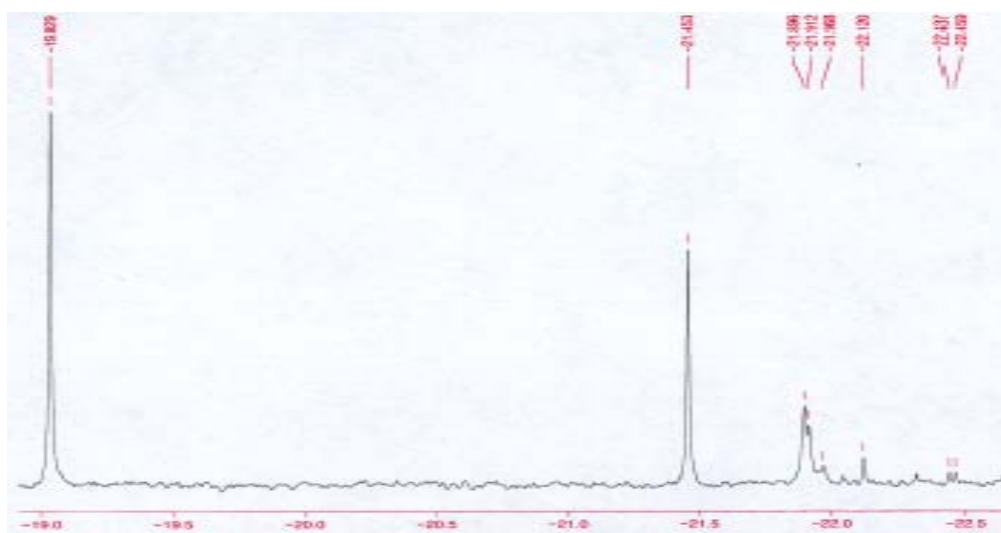


Figure 5.7 ^{29}Si NMR of hexamethyl tricyclosiloxane initiated with lithium hydride in THF; in 24 hours, the monomer is converted 30% to the polysiloxane (singlet at -21.493 ppm) and to the side-products:

octamethyltetracyclosiloxane (D_4) (singlet at -19.0075 ppm, corresponding for D_4) and cycles in 6 or 7 members (-22 ppm)

Interestingly, the polymerization of D_3 leads in both cases to the formation of 4-members cycles, D_4 . The conversion of D_3 to unstrained cycles is not important and we believed that the polysiloxane chain, formed during the first hours of polymerization is in equilibrium with unstrained cycles, including D_4 . Thus could explain the impurities in the final product of polymerization. D_4 has a slow rate polymerization: after 24 hours, the monomer is unreacted (Figure 5.8). The formation of main polysiloxane chains imply a longer reaction time.

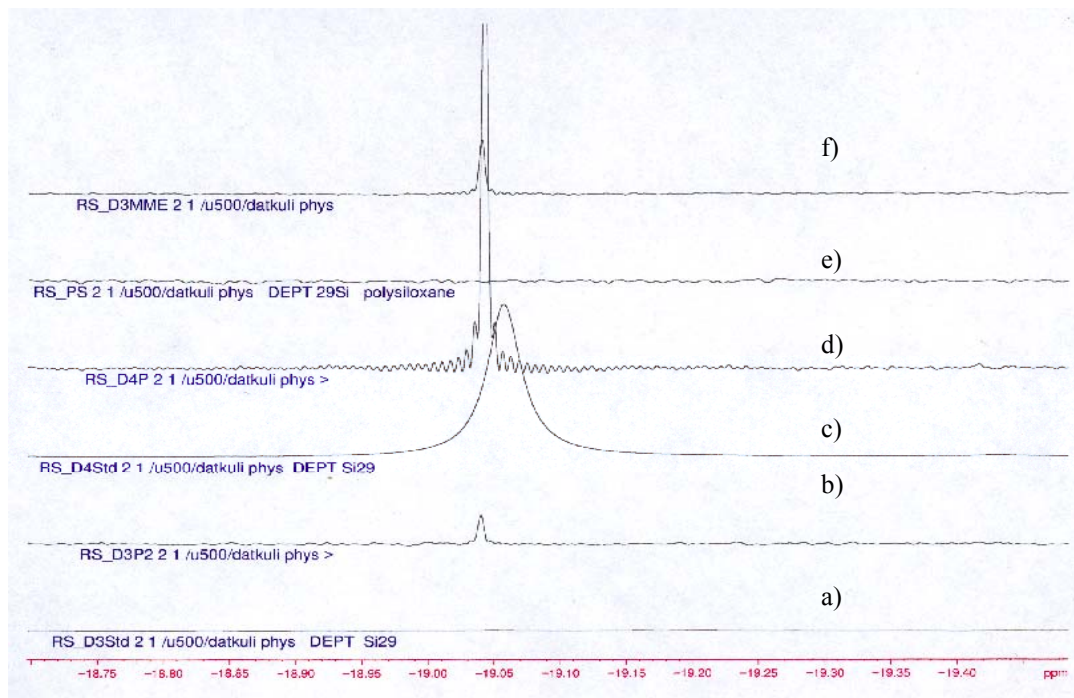


Figure 5.8 ^{29}Si NMR spectra for analyzed systems; a) D_3 monomer standard; b) D_3 polymerized by initiation with lithium hydride in THF; c) D_4 monomer standard; d) D_4 polymerized by initiation with potassium hydride in THF; e) commercial (Aldrich) polysiloxane alkyl terminated; f) D_3 polymerized by initiation with diethylene-glycol monomethyl ether lithium alcoholate in THF. In 24 hours, the polymerization of D_3 leads to the formation of 4-members cycles (D_4). In 24 hours, the D_4 is converted ca. 5% to the polysiloxane.

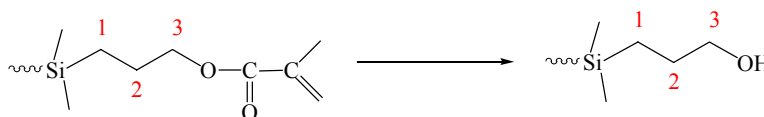
The ^{29}Si study supported my choice in using D_3 instead of D_4 . The polymerization of hexamethyltricyclosiloxane is faster and leads the desired polysiloxanes. The purity of reaction mixture after polymerization is considerably improved compared to the polymerization of octamethyltetracyclosiloxanes.

Purification

The mixture of diblock copolymers, cycles, unreacted polyethylene oxide, and unreacted block ender was purified by column chromatography on silica gel. This method proved to be efficient for the purification of AB diblock copolymers.

Reduction

Reduction of the diblock copolymer carrying an unsaturated end to the corresponding hydroxyl group is the next step of the synthesis (see the scheme below).



Activation of the hydroxy groups with triflic acid is only possible for primary hydroxy groups. Moreover, activation is only possible if between the terminal silicon atoms of the polysiloxane chain and the OH terminal groups are at least 3 methylene units¹⁶⁰.

The reduction of the unsaturated ester has been performed following a modified procedure described by Bouveault et al.¹⁶¹. The conversion was monitored via the decrease of olefinic peaks at 6.1 and 5.5 ppm in ¹H-NMR (Figure 5.9 and Figure 5.10).

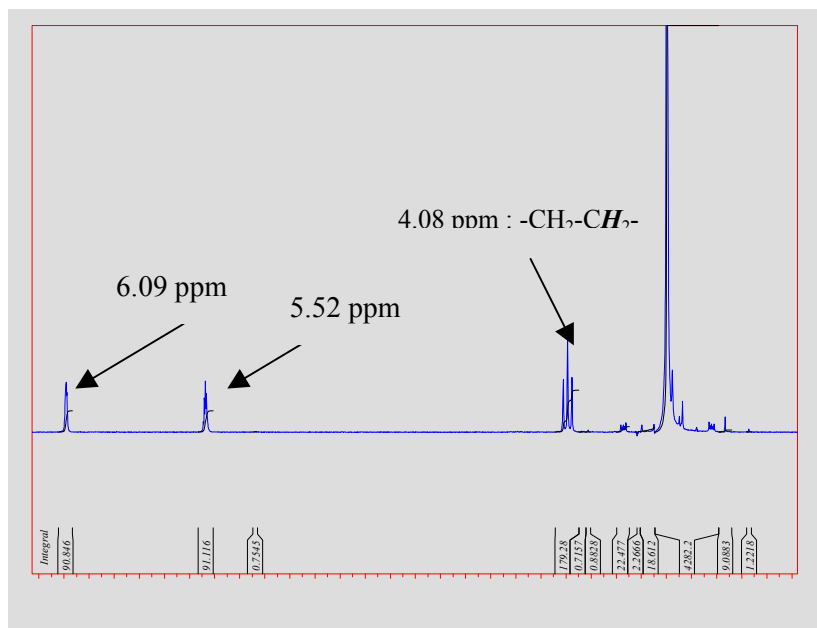


Figure 5.9 ¹H NMR spectra of the AB diblock copolymer after purification, before reduction with sodium/ethanol; peaks at 6.09 and 5.52 ppm, corresponding to olefine indicates the presence of unsaturated group at the end of POE-PDMS diblock copolymers

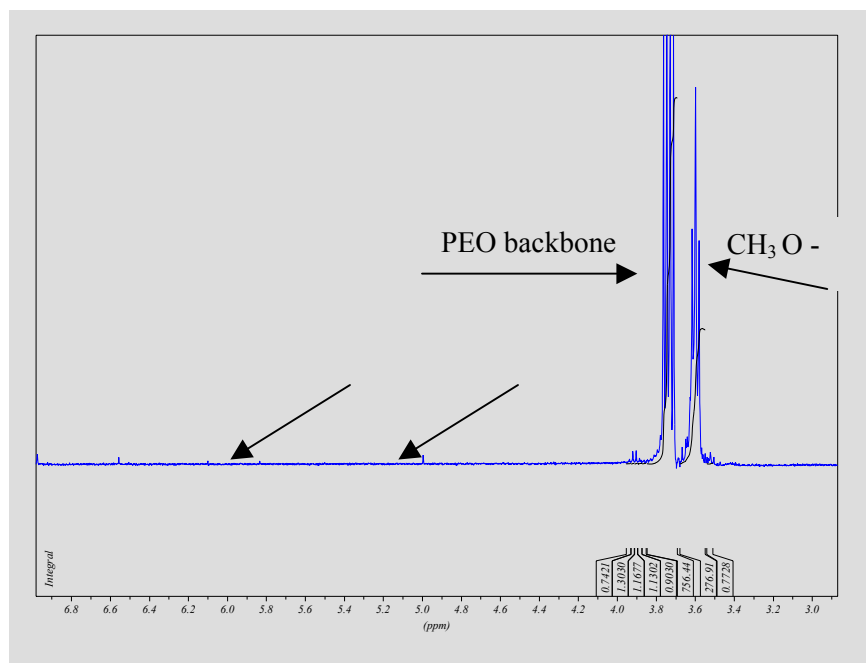


Figure 5.10 ^1H NMR spectra of the POE-*b*-PDMS diblock copolymer after reduction. The disappearance of the olefinic signals indicates complete reduction.

The molecular weight of resulting AB diblock copolymer (polyethylene oxide-*b*-polydimethyl siloxane) was calculated by ^1H NMR. The conversion of monomeric cycles was reported relative to the initial quantity of monomer. Table 5.3 gives more details concerning the diblock copolymers prepared.

Table 5.3 Composition of AB diblock copolymers, with A: monomethyl ether polyethylene glycol; B: polydimethylsiloxane, D₄: octamethyltetramethylsiloxane and D₃: hexamethyltrimethylsiloxane, POE: polyethylene oxide and PDMS: polydimethyl siloxane.

Units number	M _n , g/mol		Conversion (%)		Reduction yield (%)	Composition (mass %)	
	POE	PDMS	D ₄	D ₃		PEO	PDMS
A ₂₅ B ₁₂₃	1202	9100	10	-	45	12	88
A ₂₅ B ₁₁₃	1202	8360	6	-	67	13	87
A ₄₅ B ₆₇	1920	4810	22	-	31	31	69
A ₄₅ B ₄₀	1920	2960	23	-	43	42	58
A ₂₅ B ₈₀	1202	5624	42	-	16	18	82
A ₂₅ B ₁₉	1202	1406	-	52	32	46	54

The conversion of D₄ monomer is generally lower than the conversion of D₃. The unstrained cycle has a lower polymerization rate or the polymerization leads to oligosiloxanes and long siloxanes chains, which are eliminated by chromatography, before reduction step. Thus, since the conversions are calculated after purification, one can assume that these are the principal reasons for low conversions.

The reduction yields vary between 16 and 67%. The amount of sodium and the temperature of water that the reduction implies are believed to be the main factor affecting the reduction yield.

5.2.3. Polyethylene oxide-*b*-polydimethyl siloxane-*b*-polymethyloxazoline triblock copolymers

The ABC triblock copolymers were prepared using the AB diblock copolymer macroinitiator, by activating the hydroxy terminus of the diblock with triflic anhydride.

The table below indicates the composition of the ABC triblock copolymers obtained by a) anionic ring opening polymerization of D₄ and b) by anionic ring opening polymerization of D₃.

Table 5.4. Compositions of ABC triblock copolymers

a) ring-opening polymerization of octamethyltetracyclosiloxane (D₄)

Units number	M _n , g/mol (¹ H NMR)			Conversion (%) PMOXA	Composition, %		
	POE	PDMS	PMOXA		PEO	PDMS	PMOXA
A ₂₅ B ₁₂₃ C ₂₄	1202	9100	2040	60	10	73	17
A ₂₅ B ₁₁₃ C ₄	1202	8360	340	6	12	84	4
A ₄₅ B ₆₇ C ₃₄₆	1920	4810	29410	60	6	13	81
A ₄₅ B ₄₀ C ₆₇	1920	2960	8250	53	16	22	62
A ₂₅ B ₈₀ C ₂₈₅	1202	5920	24225	34	4	18	78
A ₄₅ B ₁₀₀ C ₇₁₅	1920	7400	60775	64	3	10	87

b) ring-opening polymerization of hexamethyltricyclosiloxane (D₃)

Units number	M _n , g/mol (¹ H NMR)			Conversion (%) PMOXA	Composition, %		
	POE	PDMS	PMOXA		PEO	PDMS	PMOXA
A ₂₅ B ₁₉ C ₁₁₀	1202	1406	9350	32	10	12	78
A ₂₅ B ₈ C ₆₂	1202	592	5270	54	14	7	79
A ₄₅ B ₅₀ C ₄₇	1920	3700	3995	66	22	38	40

The values of PMOXA conversion are generally good. A lower conversion of the methyl oxazoline is usually the result of an insufficient conversion of ester end function to hydroxy function in a previous step of the synthesis. Moreover, during the polymerization of methyl oxazoline, conversion is drastically influenced by impurities.

Since GPC of amphiphilic copolymers is generally difficult because of the lack of suitable standard and adsorption phenomena on the chromatography column, NMR and MALDI TOF were used for determination of molecular weight.

The calculated number average degree of polymerization from ^1H NMR (Figure 5.11) is in agreement with the one found from MALDI TOF spectrometry (Table 5.5).

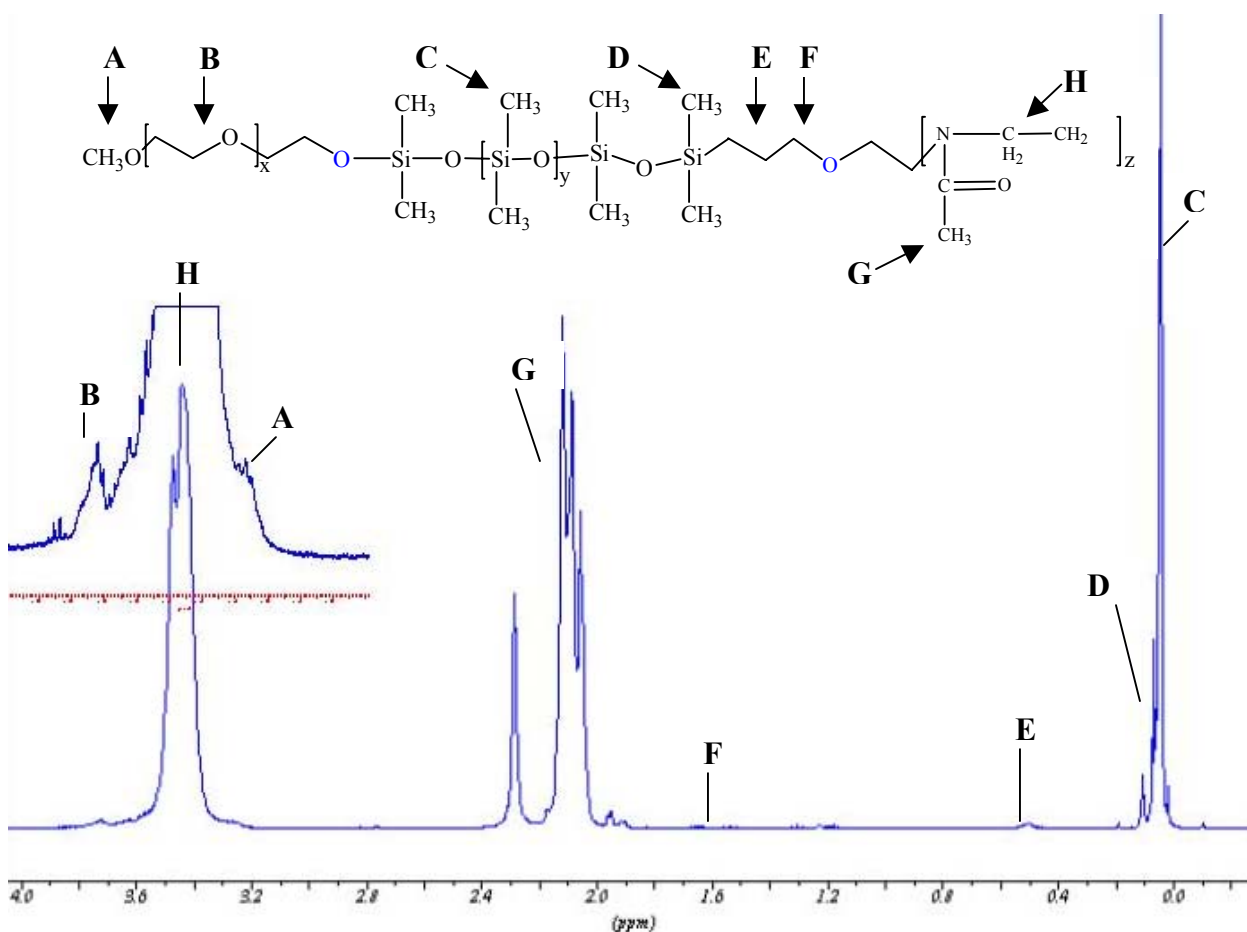


Figure 5.11 ^1H NMR spectra of ABC triblock copolymer ($\text{POE}_{25}\text{PDMS}_{19}\text{PMOXA}_{110}$)

Table 5.5. Molecular weight estimation by ¹H NMR and MALDI-TOF analysis

Units number	M _n (¹ H NMR) (g/mol)	M _n (MALDI TOF) (g/mol)	PD.I*
A ₂₅ B ₈₀ C ₂₈₅	31347	34000	1.25
A ₄₅ B ₁₀₀ C ₇₁₅	70175	67456	1.19
A ₂₅ B ₁₉ C ₁₁₁	11856	10010	1.21
A ₂₅ B ₈ C ₆₂	7064	7600	1.33
A ₄₅ B ₅₀ C ₄₇	9888	8823	1.41

* calculated from MALDI TOF

MALDI-TOF (matrix-assisted laser desorption/ionization time-of-flight) mass spectrometry is generally an effective tool for determination of the molar mass of polymers. One major concern is the ability of MALDI-TOF to provide accurate molar mass measurements. It has been shown¹⁶² that for the polydispersities above $M_w/M_n \geq 1.1$, there is a significant discrepancy between molar mass calculated from size exclusion chromatography (GPC) and MALDI TOF. In the present case, the overall detection sensitivity for different polymers is not the same. However, information on polymer mass and distribution were obtained, by optimizing the detection range and developing appropriate sample protocol in terms of matrix (dihydroxybenzoic acid) and quantities.

5.2.4 Thermal analysis (DSC)

Differential scanning calorimetry was used in order to study the thermal behavior of the amphiphilic copolymers. The constitutive segments of the ABC triblock copolymer could be identified using this method, by comparison with standards (i.e., with characteristic temperatures for homopolymers which form the triblock).

The table below (Table 5.6) presents the characteristic transition temperatures obtained for each of the constituents of the triblock copolymer.

Table 5.6 Characteristic transition temperatures for the homopolymers in the composition of ABC triblock copolymers

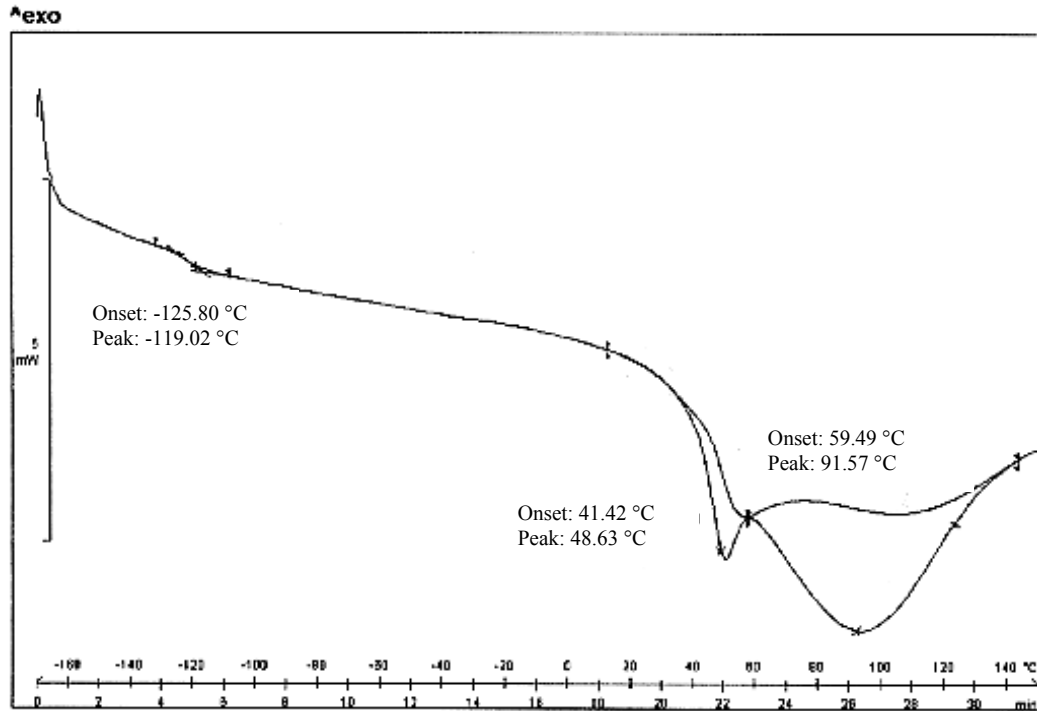
Component	Units number	M _n [*] , g/mol	Temperature (°C)	Transition type, reference
Polydimethylsiloxane	75	5550	- 124	T _g , ¹⁶³
Polyethylene oxide	45	2000	51	T _m , ¹⁶⁴
Polymethyl oxazoline	22	1880	85	T _m , -

^{*}T_g = glass transition, T_m = melting point

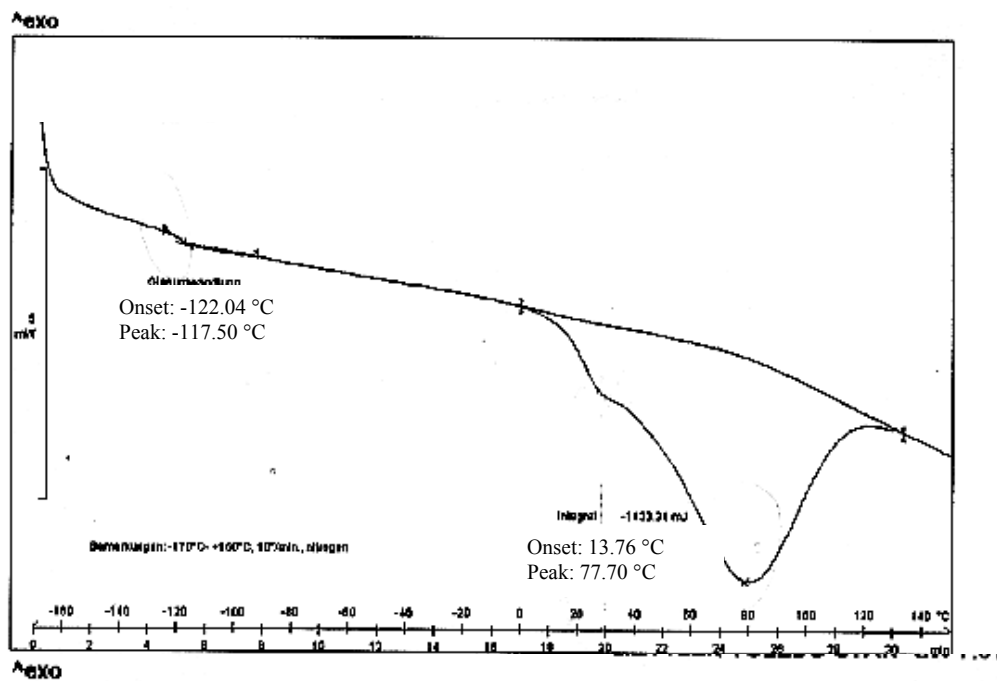
^{*} molecular weight from supplier (for PDMS and PEO) and from ¹H NMR data for PMOXA

In most cases, the DSC curves of the asymmetric copolymers show all three transitions (Figure 5.12 a), b), c)).

a) POE₂₅PDMS₁₉PMOXA₁₁₀ (white powder)



b) POE₂₅PDMS₈₀PMOXA₂₈₅ (white powder)



c) POE₂₅PDMS₈PMOXA₆₂ (white powder)

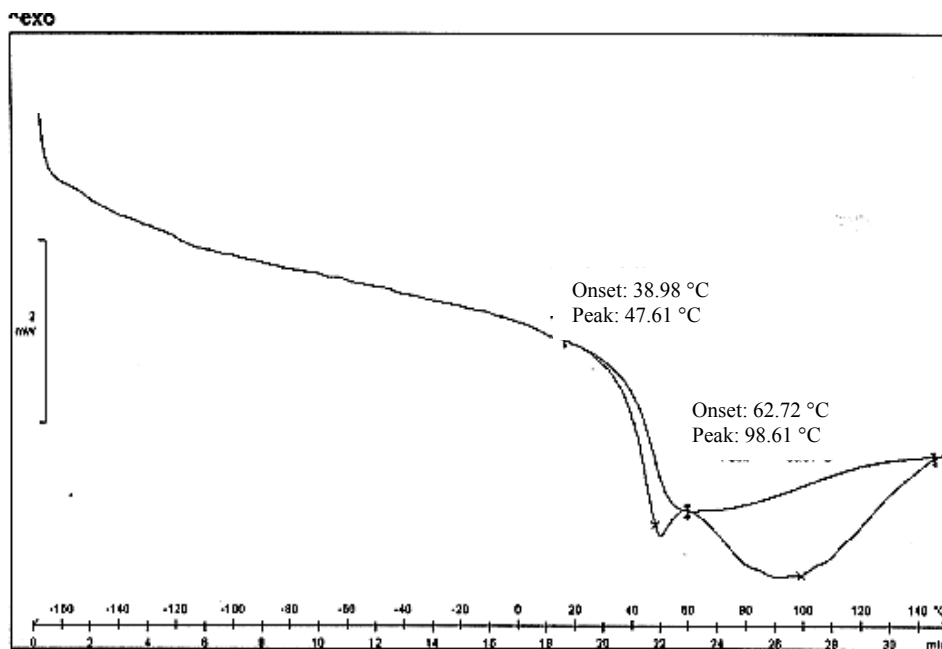


Figure 5.12 DSC analysis of asymmetric triblock copolymers; heating rate: 10°C/min

The melting point for poly2-methyl oxazoline segment is well visible for all the copolymers analyzed. The melting point for the polyethylene oxide segment in the copolymer chains compared to the one from polyethylene oxide homopolymer decreases from 51°C to 47- 48°C, while for polymethyl oxazoline, the melting point increases by 6-8°C. This phenomenon is believed to be the result of the lower molecular weight of PEO block compared to the reference polymer and higher molecular weight in the case of PMOXA block.

The DSC curves, obtained under the same conditions as for the homopolymers show three transition temperatures for the triblock copolymers at ca. 50°C, corresponding to the melting of the crystalline phase of the polyethylene oxide, -124°C corresponding to the glass transition of the polydimethyl siloxane and at 80°C, the characteristic temperature for polymethyl oxazoline. These DSC clearly indicate that the obtained copolymer contains all three segments in its chain. These indicate a phase separation between the hydrophilic and the hydrophobic domains and/or also between the different hydrophilic domains in the bulk.

5.3 Labelled triblock copolymers

The ABC triblock copolymers were labelled at the hydroxy terminated poly 2-methyl oxazoline end. The labelled triblock copolymers were used in order to prove the asymmetric orientation of hydrophilic blocks. Three fluorescent dyes were used for labelling: 7-methoxy coumarin azide, tetramethyl rhodamine and a derivative of fluorescein. The coumarin azide was chosen for its commercial availability and known reactivity. The latter two, fluorescein and rhodamine derivative were employed because of their high reactivity against alcohol functions and their fluorescent properties (i.e., wavelength). The chemical modification of hydroxy terminus with azides (coumarin-and rhodamine-azide) requires the reaction of alcohols with azide at high temperature. Acyl azides can rearrange in inert solvents in the presence of alcohols. They react via intermediate isocyanates to carbamic acid esters¹⁶⁵. 5-(4,6-dichlorotriazinyl)aminofluorescein (5-DTAF) was coupled to the block copolymers in a single step, via a nucleophilic aromatic substitution mechanism¹⁶⁶. These intermediary species are used to react with hydroxy function of ABC triblock copolymers.

Figure 5.13 shows ¹H NMR spectra the coumarin labelled-ABC-triblock copolymer. The presence of the aryl protons specific for coumarin molecules clearly indicates the modification of the triblock copolymers (conversion of hydroxy groups was 28% for POE₄₅PDMS₆₇PMOXA₃₄₆ and 12% for POE₄₅PDMS₄₀PMOXA₆₇ triblock copolymers).

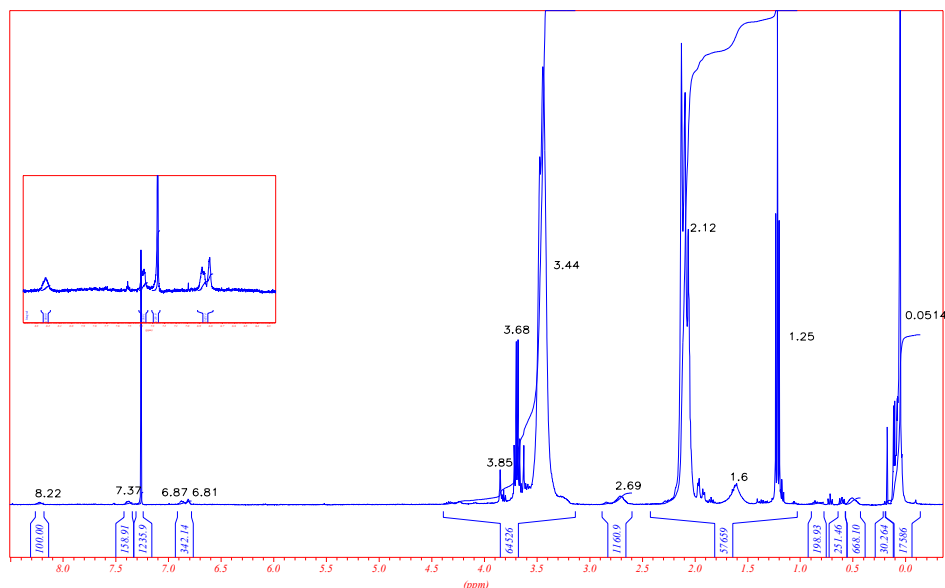


Figure 5.13 ¹H NMR spectra of PEO₄₅PDMS₄₀PMOXA₆₇-7-methoxy coumarin labelled copolymer

The second fluorescent dye used for the modification of ABC triblock copolymers was tetramethyl rhodamine.

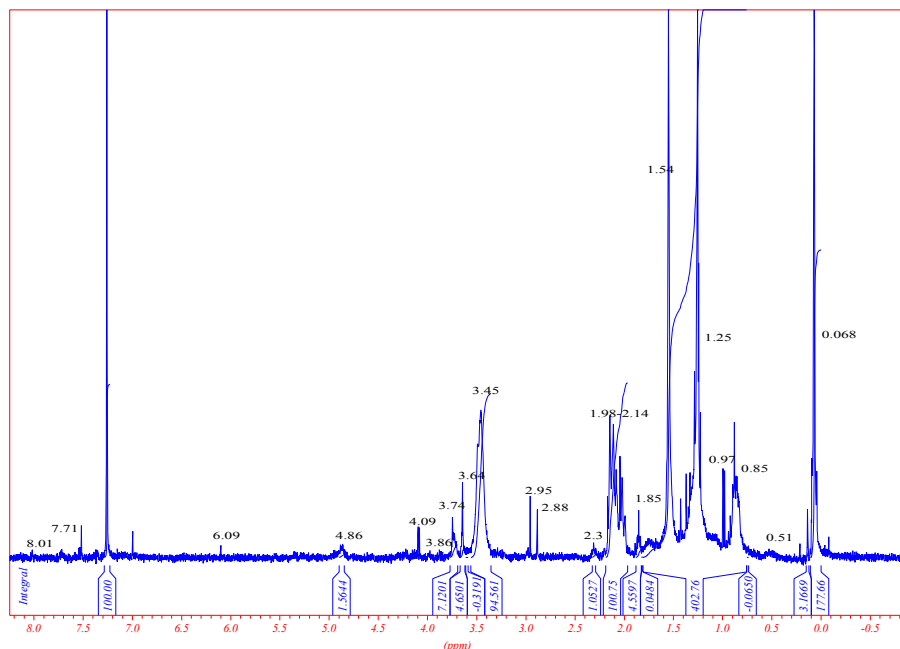


Figure 5.14 ^1H NMR spectra of $\text{PEO}_{25}\text{PDMS}_{80}\text{PMOXA}_{285}$ -tetramethyl rhodamine labeled copolymer

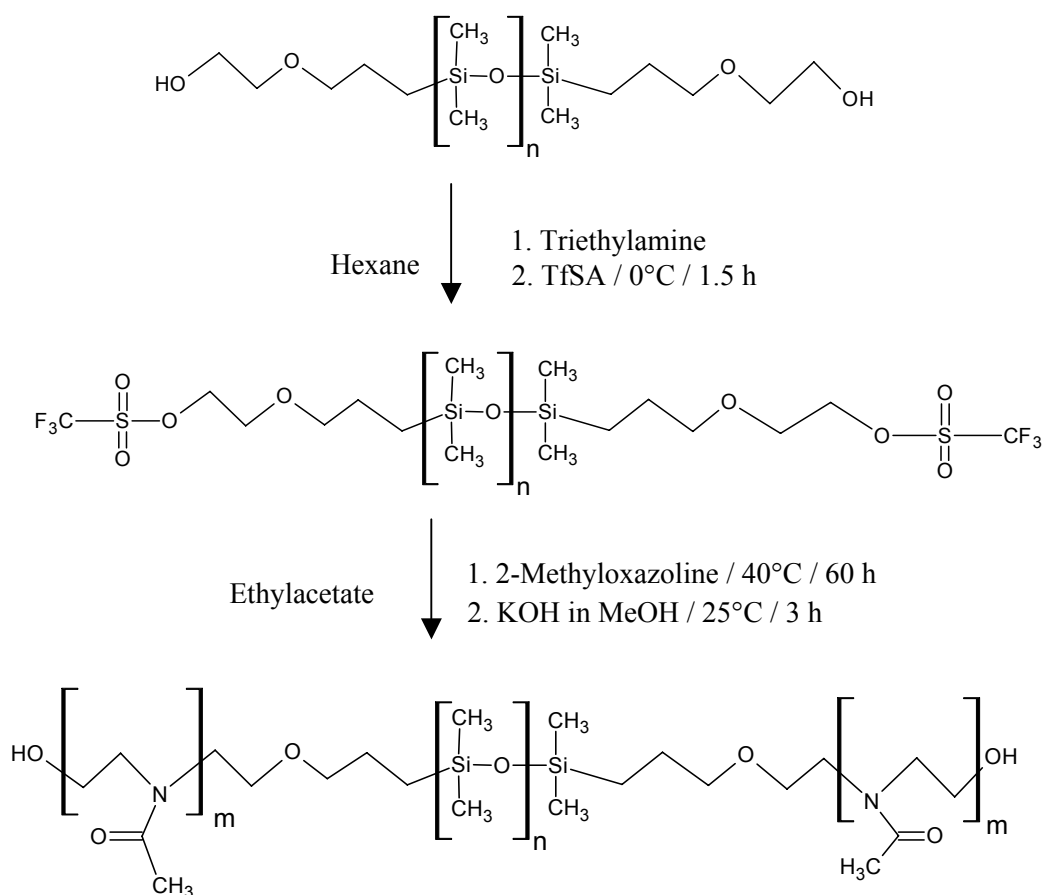
^1H NMR (Figure 5.14) shows that 41% of the polymer chains were functionalized.

The last fluorescent dye used was 5-(4,6-dichlorotriazinyl)aminofluorescein (5-DTAF). The reaction implies a single step reaction and mild conditions.

The NMR analysis of labelled copolymers does not reveal the presence of peaks in the aromatic range between 6.1 and 11.1 ppm, which could confirm the presence of 5-DTAF molecules in the final product. However, giant vesicles prepared with this polymer, in mixture with unlabelled analogues, show intense fluorescence emission in microscopy (as showed further in Chapter 7). In accordance with literature, this reaction leads to very low conversions¹⁶⁶.

5.4 ABA triblock copolymer:

The symmetric triblock copolymer was obtained by a similar procedure used for the attachment of the polymethyl oxazoline to the diblock copolymer in order to obtain an ABC triblock copolymer (Scheme 5.3).



Scheme 5.3 Flow chart for the preparation of PMOXA-PDMS-PMOXA symmetric triblock copolymers

The only difference is the macroinitiator: here the hydrophobic middle chain polydimethyl siloxane bears two hydroxy groups. This macroinitiator was functionalized with triflic anhydride at both ends to allow methyl oxazoline polymerization to an ABA triblock copolymer. The molecular weight of ABA triblock copolymers was determined by ^1H NMR spectroscopy (Figure 5.15): PMOXA-PDMS-PMOXA ($M_{n,\text{PMOXA}} = 1700 \text{ g mol}^{-1}$; $M_{n,\text{PDMS}} = 5600 \text{ g mol}^{-1}$); (19%PMOXA-62%PDMS-19%PMOXA), $M_w^{(1\text{H NMR})} = 9000 \text{ g/mol}$

Gradient COSY :

^1H NMR, CDCl_3

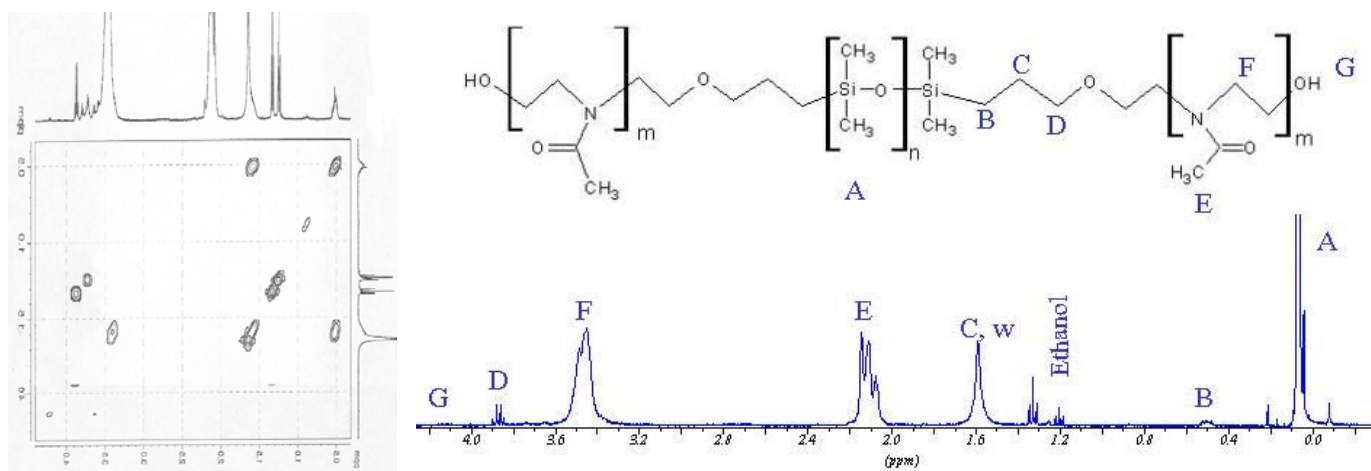


Figure 5.15 2D NMR (COSY) and ^1H NMR spectra of ABA symmetric triblock copolymer ($\text{PMOXA}_{19}\text{PDMS}_{75}\text{PMOXA}_{19}$)

5.5. Conclusions

We developed a new synthetic procedure for amphiphilic ABC triblock copolymers, with different composition and block length ratio. Amphiphilic triblock copolymers with alternating hydrophilic and hydrophobic blocks were produced via a combination of anionic and cationic polymerization. The method allows the synthesis of well-defined asymmetric block copolymers. Due to their amphiphilic nature and to the tailor-made chemical structure, the ABC triblock copolymers are potentially able to form well-defined supramolecular structures (vesicular structures) in water, as will be discussed later (Chapter 6).

Moreover, the triblock copolymers were modified with dyes at the free hydroxy group of methyl oxazoline segment. The coumarine-, fluoresceine- and rhodamine - labelled triblock copolymers were used in further studies concerning the asymmetric character of the membrane formed by these copolymers in aqueous solutions.

CHAPTER 6

SELF-ASSEMBLED STRUCTURES FROM AMPHIPHILIC BLOCK COPOLYMERS IN AQUEOUS SOLUTION

Poly(ethylene oxide)-*b*-poly(dimethyl) siloxane-*b*-poly(methyl) oxazoline ABC triblock copolymers are amphiphilic. Due to the hydrophilicity of the PEO and PMOXA blocks and the strong hydrophobicity of PDMS block, they form superstructures in diluted aqueous media. A special feature of these triblock copolymers results from the two different hydrophilic blocks (PEO and PMOXA chains) which tend to segregate, due to their molecular incompatibility. This could lead to noncentrosymmetric aggregates similar to Janus micelles¹⁶⁷, membranes or highly complex lyotropic mesophases. Currently, investigations of the bulk phase morphologies of ABC triblock copolymers have been expanded to include more complex polymeric architectures such as linear and branched copolymers composed of more than two incompatible chains. This led to the discovery of a large number of new three-dimensional structures¹⁶⁸. The formation of these morphologies is due to the inherent incompatibility of most polymers above a certain molecular weight threshold, which, because of the covalent attachment of the segments, leads to micro phase separation³⁸.

Investigations concerning the solution properties and surface activity of these polymer architectures, however, are still at the very beginning. We studied the behaviour of ABC triblock copolymers in diluted aqueous solutions. Surface activity and aggregation behaviour of the triblock copolymers were characterized by means of monolayer investigations, light scattering, and transmission electron microscopy. More precisely, the size of vesicular structures formed by ABC triblock copolymers was measured by dynamic light scattering, transmission electron microscopy, and light microscopy. Static light scattering measurements allowed establishing the critical micelle (aggregation) concentration of the triblock copolymers. A comparison between monolayer properties at the air-water interface and membrane morphology was made to check transmembrane protein incorporation into the asymmetric triblock copolymers monolayers.

Results and Discussion

Dynamic Light Scattering

Dynamic light scattering measurements allow the determination of the dynamics of macromolecules in solution. The mean apparent hydrodynamic radius of the aggregated structures can be determined¹⁶⁹. The model used for DLS measurements is based on the exponential expression for a single species field autocorrelation function (Williams-Watts function) as described in literature^{8a}:

$$g^{(1)}(\tau) = \exp[-Dq^2\tau]$$

where τ is the decay time and $q=(4\pi n/\lambda)\sin(\theta/2)$, with the solvent refractive index n , the wavelength of the incident light λ , and the scattering angle θ . The scattering amplitude is proportional to the molar mass of the species, and the scattering intensity I replaces the concentration c . In the case of the diffusion coefficient distribution, D is directly used in the model for the autocorrelation function, in the case of R_h distribution; D is calculated via Stokes-Einstein equation. The analysis of the autocorrelation functions measured at different angles (30, 60, 90, 100, 120 and 150°) shows only one peak. An example for the results on analysis used for determination of the hydrodynamic radii is shown in Figure 6.1 (for a sample obtained after filtration).

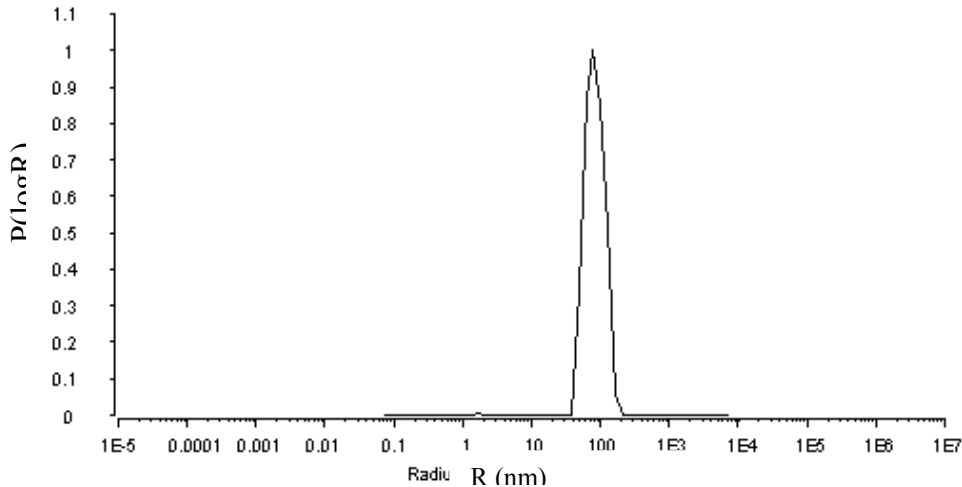


Figure 6.1 Distribution function of the radii of the $POE_{25}PDMS_{19}PMOXA_{110}$ triblock copolymer vesicles in water after filtration (from analysis of autocorrelation function $g^2(t)-1$; $c = 1$ g/L; $\theta = 90^\circ$)

The hydrodynamic radius of the corresponding species in solution was found by extrapolation $R_h(q^2)$ to $q^2 \rightarrow 0$. Because the experiments were done at concentrations $c \geq c_{ac}$ and because the

hydrodynamic radius determined by light scattering is z-averaged, only aggregates were observed.

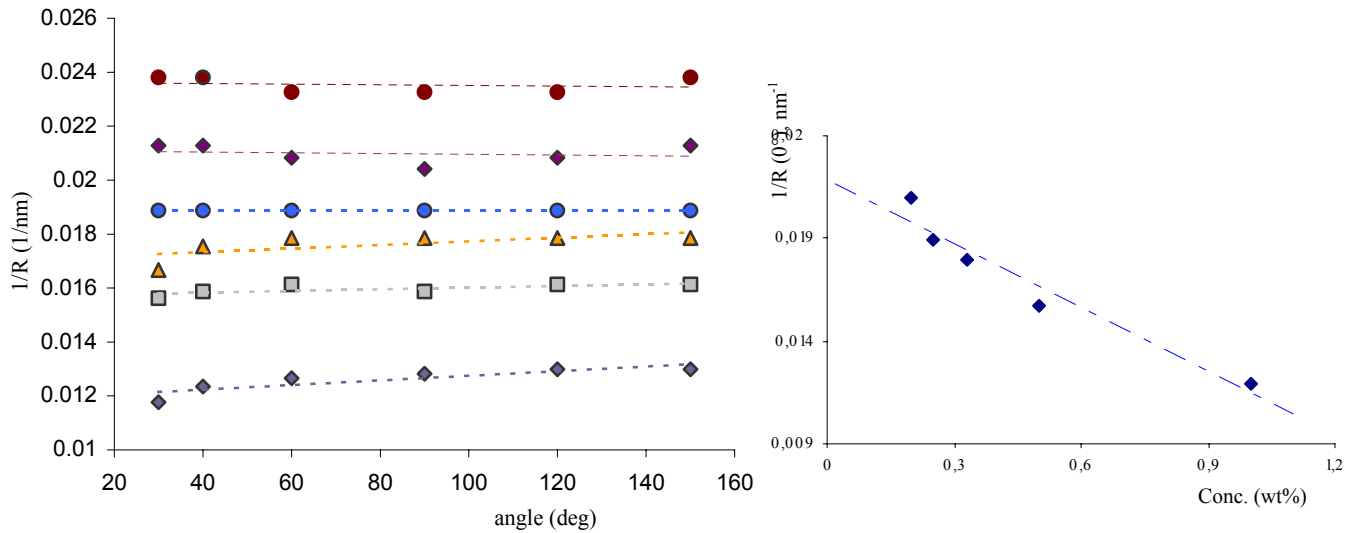


Figure 6.2. Determination of hydrodynamic radius for $POE_{25}PDMS_{19}PMOXA_{110}$ triblock copolymer

Dynamic light scattering on vesicles formed for example by $POE_{25}PDMS_{19}PMOXA_{110}$ triblock copolymer in water yield a hydrodynamic radius of $R_h = 44$ nm (Figure 6.2). The value of extrapolated reversed radius increases with decrease of the concentration, normal phenomenon when the concentrations approach the cac. The polydispersity of resulting vesicles was found to be about 20% from dynamic light scattering for the same polymer.

Table 6.1 shows the composition of the triblock copolymers analysed and their hydrodynamic radii.

Table 6.1 The hydrodynamic radii of the asymmetric triblock copolymers with A: POE, B: PDMS and C: PMOXA determined by dynamic light scattering

Polymer	Molar mass (g/mol)	Blocks composition (%)			R_h (nm)	HPL/HPB*
		%A	%B	%C		
$A_{45}B_{67}C_{346}$	36 300	5	14	81	69	5,8
$A_{113}B_7C_{590}$	50 000	10	1	89	95	100
$A_{25}B_{19}C_{110}$	11 941	10	12	78	44	7,1
$A_{45}B_{100}C_{715}$	70 145	3	10	87	65	7,6
$A_{25}B_{80}C_{285}$	31 245	4	18	78	23	3,8
$A_{25}B_7C_9$	2 383	46	22	32	46	4,8

*HPL/HPB = hydrophilic/hydrophobic ratio

As a general tendency, from the table 6.1, one could notice that for the increase of the hydrophilic/hydrophobic ratio, the diameter of the vesicles seems to increase. Since the hydrophilic fractions of the triblock copolymers presented in Table 6.1 increase, these chains could influence the size of vesicles.

DLS indicates that the amphiphilic triblock copolymers form aggregates in aqueous solutions. These results could possibly help choosing of a particular composition of asymmetric blocks in order to estimate a specific diameter of vesicular structure, important for specific applications. It is worth to make the observation that not only hydrophobic chains influence substantially the curvature of vesicles; also the distribution and length of hydrophilic chains are important. A more precise study in order to establish directly the influence of these parameters on the diameter of vesicles is subject of forthcoming research.

To further elucidate the radius of gyration and critical aggregation concentration, SLS experiments were performed. Determination of radius of gyration of vesicles and critical aggregation concentration for ABC triblock copolymer follow the experimental approach using SLS described in reference 8a. Figure 6.3 shows a typical Zimm diagram. For clarity, only the extrapolated values at zero scattering angles are plotted. The radius of gyration from static light scattering (i.e., $R_g = 47$ nm) and the hydrodynamic radius from dynamic light scattering are almost identical values, thus leading to a ratio $\rho = R_g/R_h = 1.068$. The ρ parameter is a structure sensitive property, which reflects the radial density distribution of the scattering particle (a ratio $\rho = 1$ is characteristic for hollow spheres).

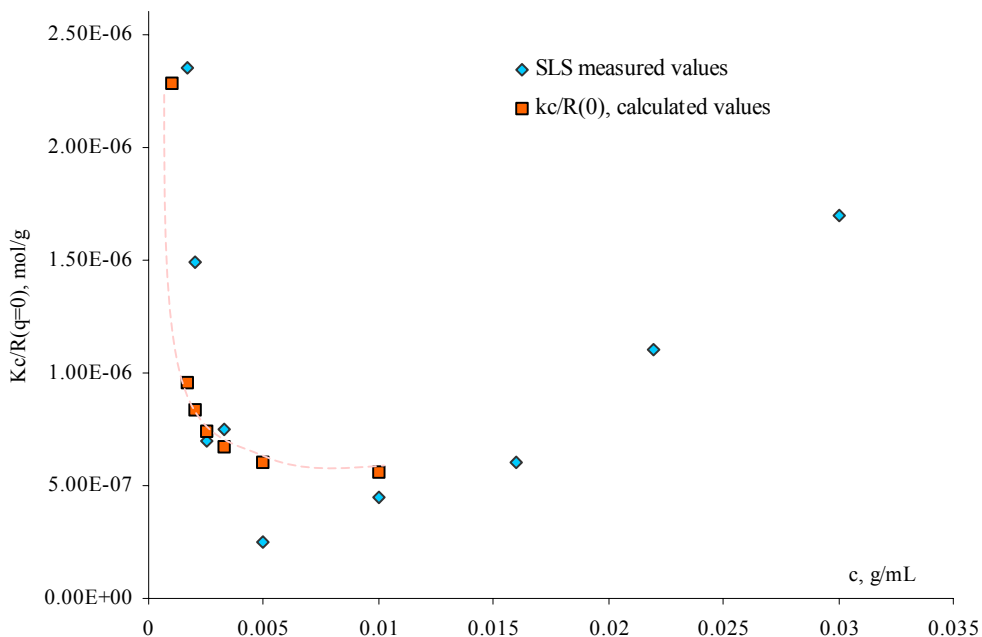


Figure 6.3 Concentration profile of the static light scattering intensity $(Kc)/R(0)$ by nanovesicles formed from $POE_{25}PDMS_{19}PMOXA_{110}$ triblock copolymer; the radius of gyration was found 47 nm

Static light scattering intensity exhibits a minimum in the range of concentration 0-0.01 g/mL. That means that there exists a critical aggregation concentration below that the vesicular aggregates disintegrate into dissolved triblock copolymer molecules.

A fit of the experimental data shows the critical aggregation concentration to be $c_{ac} = 0.78 \times 10^{-3}$ g/mL (7.8×10^{-6} mol/L). This value is comparable to that of low molecular weight lipids¹⁷⁰ and depends significantly on the length of the individual hydrophilic and hydrophobic blocks of a triblock copolymer molecule¹⁷¹. The c_{ac} at this concentration was also confirmed by surface tension measurements on the vesicle dispersions.

Critical Micellar (Aggregation) Concentration

The surface tension of the vesicle dispersion for one representative ABC triblock copolymer (POE₂₅PDMS₁₉PMOXA₁₁₀) was measured (Figure 6.4). The critical aggregation concentration (c_{ac}) of the triblock copolymer dispersions was deduced from the correspondent tangent to the γ ($\ln c_{polymer}$) curve, following a model described in reference 8a.

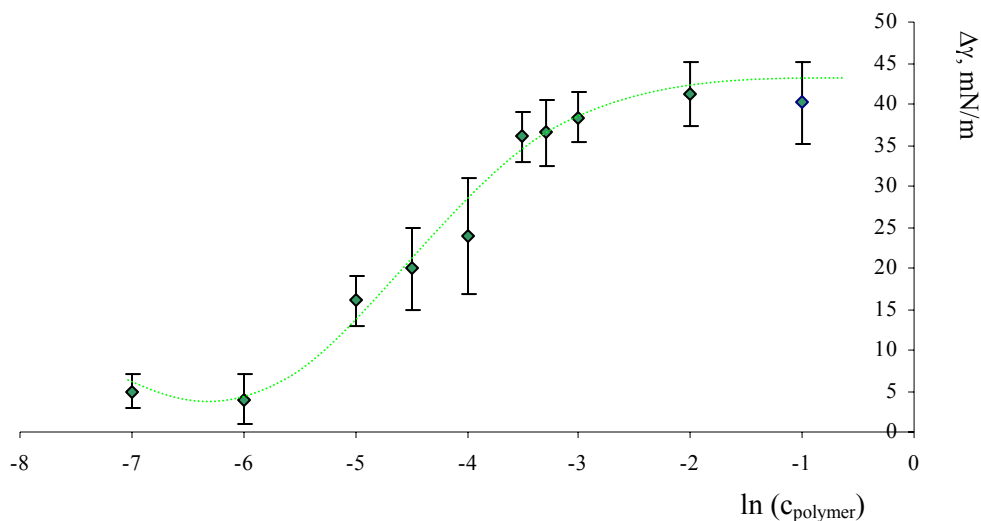
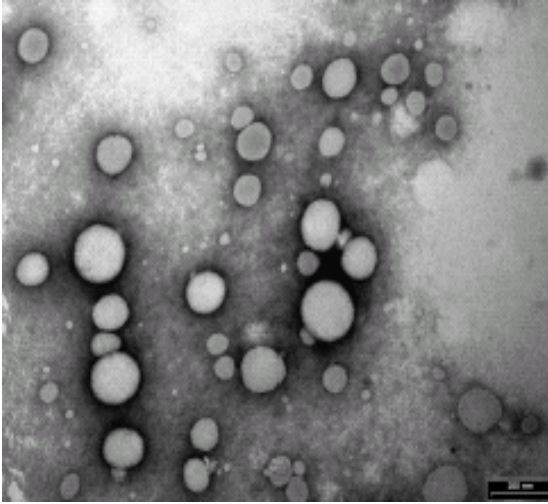


Figure 6.4 Surface tension measurements ($\gamma(\ln c_{polymer})$); the critical aggregation concentration of the triblock copolymer dispersion was deduced from the tangent to the curve, corresponding to a change in the curve profile.

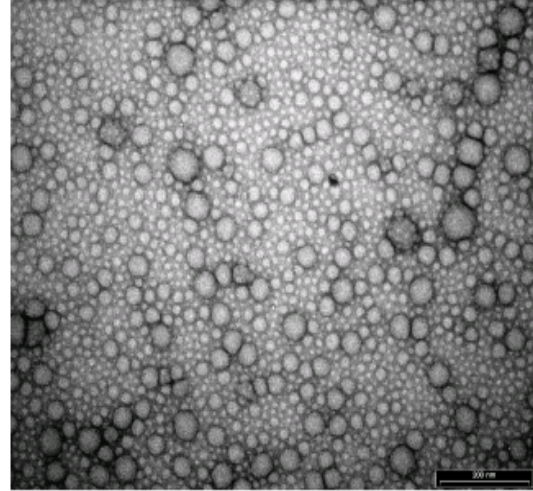
The occurrence of c_{ac} at 0.78×10^{-3} g/mL found in SLS experiments was confirmed by surface tension measurements on the vesicle dispersion. In surface tension measurements, the c_{ac} was found to be 0.675×10^{-3} g/mL (6.75×10^{-6} mol/L). The method offers a good control for the static light scattering experiments. The only disadvantage of this method consists in the fact that it is time consuming, due to long time needed to equilibrate the individual solution.

Transmission electron microscopy (TEM)

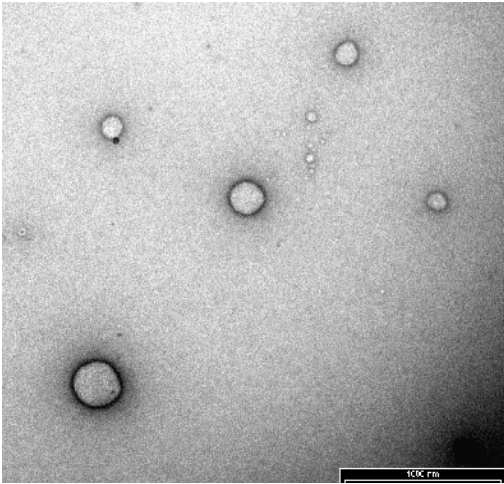
Complementary to dynamic light scattering measurements, dispersions were analysed by electron microscopy (Figure 6.5). The figures below are examples of vesicular structures formed by triblock copolymers in water.



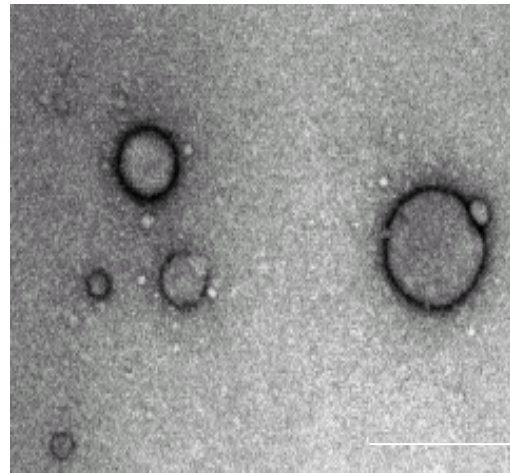
$A_{25}B_{113}C_4$; bar 200 nm;
 $D_h^{\text{DLS}} = 100 \text{ nm}$; $D^{\text{TEM}} = 150 - 174$



$A_{45}B_{67}C_{346}$; bar 500 nm;
 $D_h^{\text{DLS}} = 140 \text{ nm}$; $D^{\text{TEM}} = 100 - 160 \text{ nm}$



$A_{45}B_{40}C_{97}$; bar 1000 nm;
 $D_h^{\text{DLS}} = 180 \text{ nm}$; $D^{\text{TEM}} = 132 - 400$



$A_{25}B_{19}C_{111}$, bar 333 nm;
 $D_h^{\text{DLS}} = 90 \text{ nm}$; $D^{\text{TEM}} = 100 - 280$

Figure 6.5 Transmission electron micrographs of negatively stained vesicular structures from ABC triblock copolymers

Figure 6.5 shows a TEM micrograph of samples of PEO-PDMS-PMOXA triblock copolymers vesicles prepared by extrusion through filters with pore width of 200 nm, in aqueous solutions.

The figure clearly demonstrates that the preparation procedure yields spherical vesicles. The diameters of the particles are in the range from about 100 nm to about 250 nm. The values found by TEM are in good agreement with DLS results. The presence of smaller vesicles could find an explanation in the filtration procedure: vesicles with diameter larger than the pore diameter of filters are affected by the extrusion, while smaller vesicles can pass without being influenced.

Light microscopy (LM)

Identically as for vesicles, the PEO-PDMS-PMOXA triblock copolymers may also form giant vesicles by electroformation. The amphiphiles produced giant vesicles with diameter between 2 – 5 μm and a reasonable polydispersity. Below, phase contrast (Figure 6.6 a. and b.) and differential interference contrast (Figure 6.7) images of vesicles obtained via electroformation are presented.

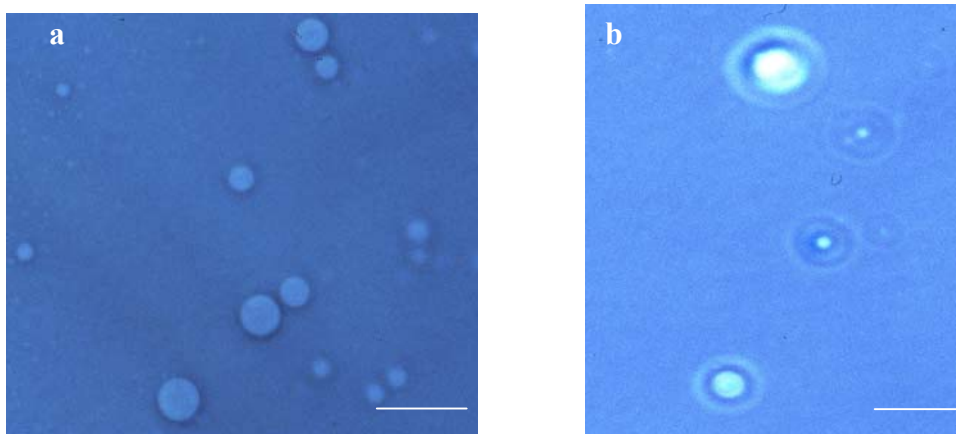


Figure 6.6 a) Phase contrast images of giant vesicles formed from $\text{POE}_{25}\text{PDMS}_{19}\text{PMOXA}_{110}$ and b) $\text{POE}_{25}\text{PDMS}_{80}\text{PMOXA}_{285}$. Scale bars are 2 μm for picture a) and 3 μm for picture b).

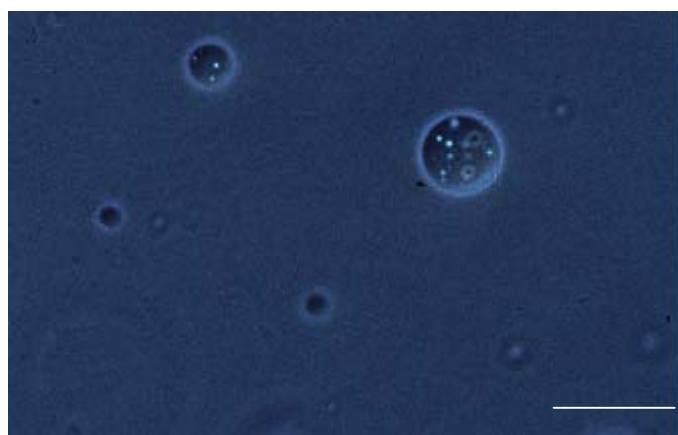


Figure 6.7 DIC image of giant vesicles formed from $\text{POE}_{45}\text{PDMS}_{67}\text{PMOXA}_{346}$ triblock copolymer. Scale bar is 5 μm

Giant vesicles are the most convenient systems for studying bilayer membranes. They have a series of very interesting features: they can be analysed by (light) microscopy, are appropriate for electrophysiological/microinjection studies (for instance, the giant vesicles from these copolymers, similarly with smaller vesicles, allow Cy5-dye encapsulation (Figure 6.8)) and are the closest to natural cells (concerning their curvature and volume).

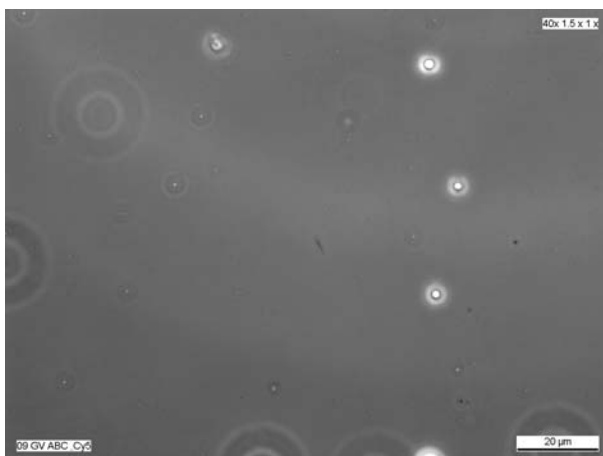


Figure 6.8 Light micrograph of giant vesicles from asymmetric triblock copolymers $POE_{25}PDMS_{19}PMOXA_{110}$ containing encapsulated chromophore Cy5. Scale bar is 20 μm . The dye encapsulation allows the visualization of vesicles on the surface by mean of fluorescence microscopy.

The interest for the formation of giant vesicles from an asymmetric triblock copolymer arises from its intrinsic membrane properties. Since giant vesicles are mimicking the best natural cells, we can imagine an impressive number of technical applications for biology. Since the triblock copolymer form asymmetric membranes, as it will be described later (Chapter 7), the insertion of membrane proteins could be controlled. For biomineralization studies, for instance, the giant vesicles formed by PEO-PDMS-PMOXA triblock copolymers offer a very interesting alternative.

Surface Pressure-Area Isotherms

The monolayer study offers information relative to the film-forming character of triblock copolymers, stability of these films. The technique was also used to study the interaction of LamB transmembrane protein with the asymmetric polymers. This part has the purpose to investigate film formation by these asymmetric copolymers and to follow the increase in the surface pressure of the monolayer, which may indicate the insertion of a tetrameric transmembrane protein.

The amphiphilic triblock copolymer form monolayers at the air-water interface and that were studied by Langmuir balance¹⁷². These monolayers are influenced by molecular parameters of triblock copolymers and the interactions between the chains.

Figure 6.9 presents π -A isotherms for a series of asymmetric triblock copolymers, with the same chemical compositions, but different length of POE, PDMS and PMOXA chains.

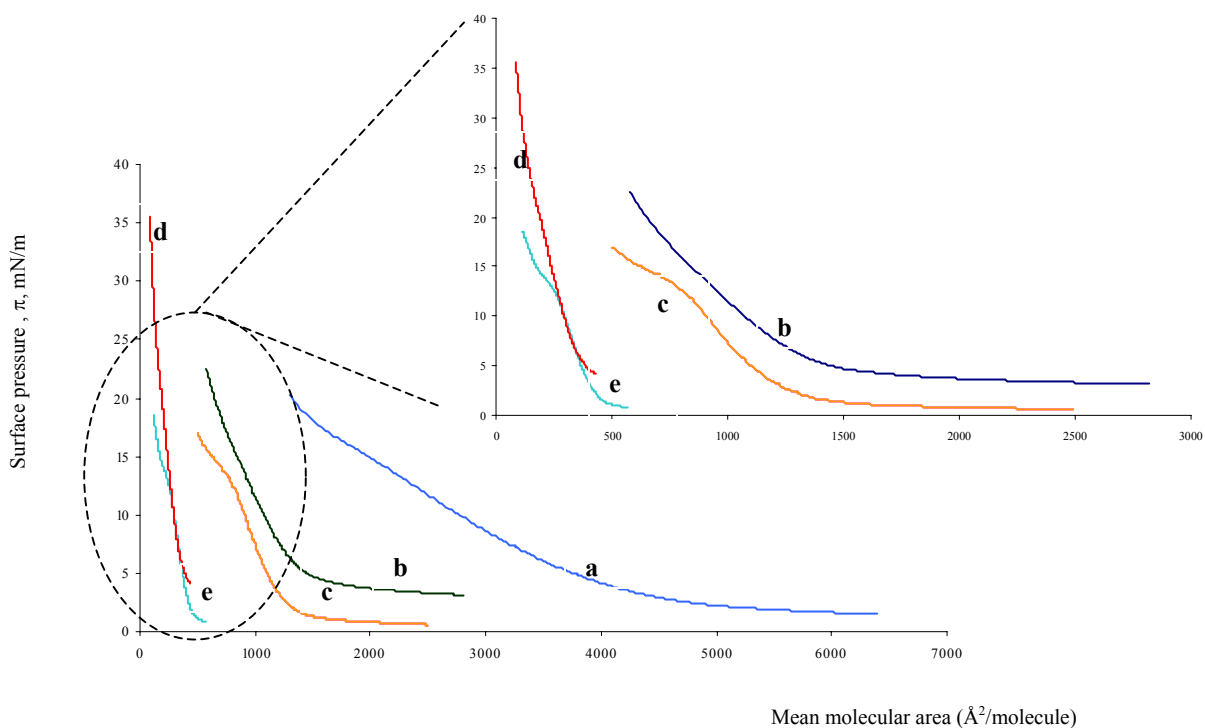


Figure 6.9 Compression isotherms of amphiphilic triblock copolymers forming stable Langmuir films

where: a) $\text{POE}_{45}\text{PDMS}_{100}\text{PMOXA}_{700}$; b) $\text{POE}_{25}\text{PDMS}_{76}\text{PMOXA}_{250}$;
 c) $\text{POE}_{45}\text{PDMS}_{65}\text{PMOXA}_{346}$; d) $\text{POE}_{45}\text{PDMS}_{40}\text{PMOXA}_{67}$; e) $\text{POE}_{25}\text{PDMS}_{19}\text{PMOXA}_{100}$

When the polymer was spread at the air-water interface, a “gaseous” monolayer was formed, in which the molecules occupy a large area per molecule. Upon compression of the monolayer (by moving the barriers towards each other) the area per molecule decreases and at a certain area per molecule the surface pressure starts to increase because the polymer molecules exert a repulsive effect on each other. The triblock copolymer molecules are in “liquid condensed” phase. When the area is further reduced, it is a sharp discontinuity of the slope of the π -A isotherm, with indication that the lower pressure condensed phase is reached. The surface pressure increases very rapidly with a small change in area per molecule. The polymer molecules are arranged in their closest possible packing, which is highly incompressible.

Compression isotherms show that the mean molecular area of ABC triblock copolymers varies, depending on the molecular weight. The highest molecular weight leads to the largest molecular area (i.e., $\text{POE}_{45}\text{PDMS}_{100}\text{PMOXA}_{700}$ triblock copolymer), as expected. For all the polymers studied, the surface-pressure area isotherms have a similar profile. The only exception are the polymers $\text{PEO}_{45}\text{PDMS}_{65}\text{PMOXA}_{346}$ and $\text{PEO}_{25}\text{PDMS}_{19}\text{PMOXA}_{100}$, where at the pressure of 13 mN/m a shoulder is visible, indicating a passage of liquid condensed phase to “condensed” region of isotherm. These polymers have a similar behaviour in monolayer experiments. Figure 6.10 shows their isotherms. For both polymers, the ratio between the polymethyl oxazoline segment and polydimethyl siloxane segment is 5.3; the composition of these triblocks is also similar (see table 6.2). At a surface pressure up to 13 mN/m, there is a change in the polymer arrangement into monolayers; the polymeric chains pass from liquid condensed phase into condensed phase. The variation of the mean molecular area, proportional to the surface pressure, is appreciable relative to the other polymers studied. The polymeric chains tend to arrange themselves into a convenient conformation to pass in “lower-pressure condensed phase”.

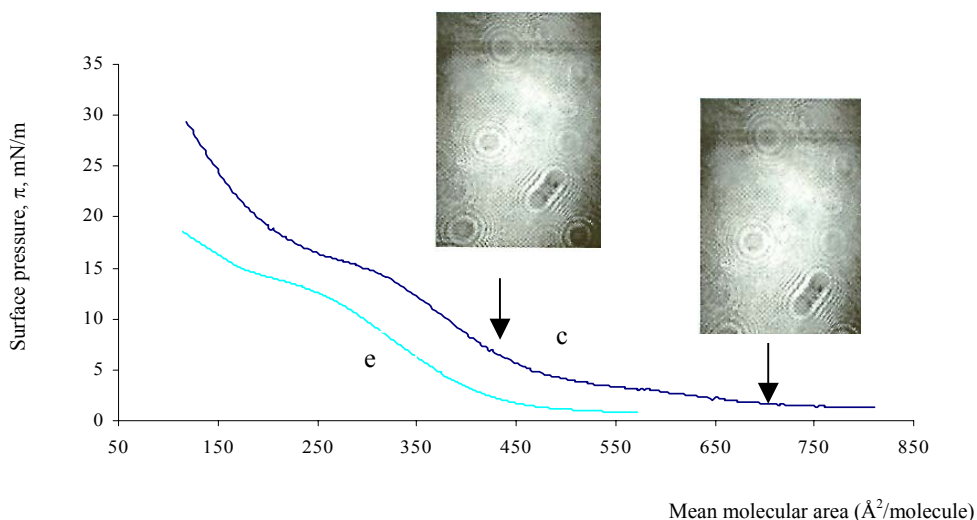


Figure 6.10 Compression isotherms for e) $\text{PEO}_{45}\text{PDMS}_{65}\text{PMOXA}_{346}$ and c) $\text{PEO}_{25}\text{PDMS}_{19}\text{PMOXA}_{100}$; the pictures have been taken using a Mini BAM, image size 4x6 mm

From these comparative examples, one can conclude that PDMS and PMOXA chains have an important contribution to chain arrangement in monolayers upon compression (i.e., liquid condensed phase). Brewster angle microscopy (Fig. 6.13) shows that the asymmetric triblocks form smooth and homogeneous films without domains. The microscopy analysis of copolymers shows that monolayers are stable. There are not significant changes of the monolayer structure during the compression.

The table 6.2 lists the mean molecular area at surface pressure of 15 mN/m (pressure when the polymer monolayer for the series of triblock copolymers are in condensed-liquid phase, similarly to biological membranes).

Table 6.2 ABC triblock copolymers studied in monolayers experiments

Units number	Composition			Ratio (A+C)/B (in units number)	Mean Molecular Area (Å ² /molecule)
	%POE	%PDMS	%PMOXA		
POE ₄₅ PDMS ₁₀₀ PMOXA ₇₁₅	3	10	87	7.6	1964.81
POE ₂₅ PDMS ₈₀ PMOXA ₂₈₅	4	18	78	3.8	617.79
POE ₄₅ PDMS ₆₅ PMOXA ₃₄₆	6	14	80	6.0	848.7
POE ₄₅ PDMS ₄₀ PMOXA ₆₇	16	22	62	2.8	239.15
POE ₂₅ PDMS ₁₉ PMOXA ₁₁₀	10	12	78	7.1	171.87

The values from Table 6.2 indicate that there is a direct contribution of PDMS and PMOXA chains to the changes of mean molecular area per molecule. The mean molecular area increases with increasing number of hydrophobic units, as expected, since this chain have the tendency to group together from the aqueous/buffer medium by hydrophobic forces. The composition of triblock copolymers in terms of number of units of each segment seems to have a considerable influence especially in the case of the PMOXA chain: the higher the percentage of this hydrophilic chain, the larger area will the triblock copolymer occupy. This might be due because of conformational changes in the molecule of polymethyl oxazoline; moreover, the hydration effect could have also an important effect.

It seems that, for a bigger hydrophilic/hydrophobic ratio, the triblock have the tendency to rearrange in the monolayer structure (the rearrangement could be I form of the polymer); this could possible explain the transition shoulder noticed for two polymers. The rest of analysed triblocks have a hydrophilic/hydrophobic ratio 3 times smaller and they behave in monolayer experiments as very classical short amphiphiles.

The monolayer technique proves that ABC triblock copolymers form stable monolayers. Especially with water-soluble molecules, this stability comes from a competition between hydrophobic interactions, hydrophilic-water and hydrophilic-hydrophilic interactions.

The influence of the temperature on the structures of monolayers could be interesting. Generally, the variation in the isotherm curve with temperature allows establishing the kind of transition between the phases (condensed and lower pressure condensed phase): first order transition of

chains or conformational rearrangement of chains. A study of the molecular area as a function of temperature shows a minor influence on the monolayer films (Figure 6.11) in a range from 15-30°C.

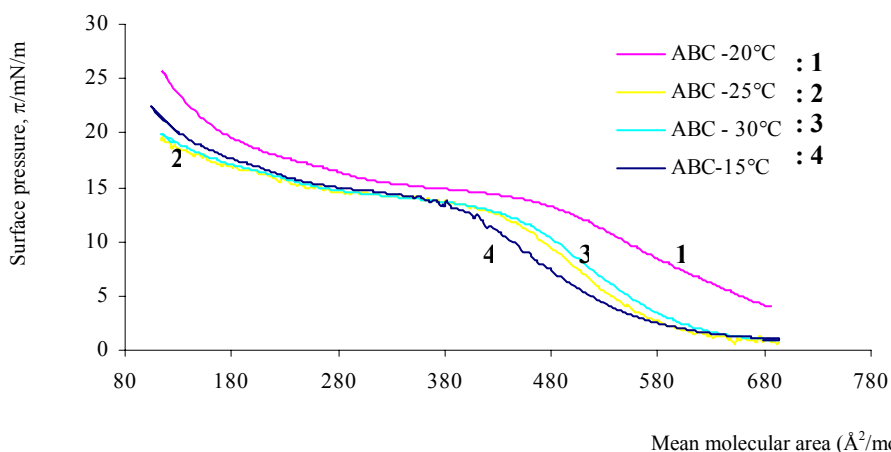


Figure 6.11 The influence of temperature on the monolayers from $POE_{25}PDMS_{19}PMOXA_{110}$ triblock copolymer

Increasing the temperature from 15° to 30°, increases the solubility hydrophilic chains increases, with effect on the mobility of these chains. These phenomena could be explained with the assumption that water plays an important role in chain hydration, as we can postulate a dislocation of water molecules from the hydrophilic chains upon disruption of the physical network of hydrophilic chains and water molecules.

In contrast, a decrease of the temperature forces the chains to rearrange to occupy a smaller molecular area, since their mobility is less obvious. Another potential explanation could concern the rigidity of the chains with minimization of the free energy of the hydrophilic chains at 15°C. Still the question remains open how a broader range of temperature affects the mean molecular area of the monolayer. The temperature range 15°-30° seems not to be enough to define this dependency in quantitative terms, however, the technique is limited to temperatures up to 35°C due to water evaporation.

For comparison, also, the behavior of the amphiphilic ABA symmetric triblock copolymer ($PMOXA_{17}PDMS_{75}PMOXA_{17}$), was analyzed by the monolayer technique. It presents a classical isotherm (Figure 6.12). At high pressure, polymethyl oxazoline chains allow the symmetric blocks to arrange in a manner that the polymer is in “condensed phase”: the chains are arranged

almost parallel. BAM does not indicate clear changes in the monolayer upon compression. This behaviour brings us to the conclusion that the monolayer is very stable and has the necessary characteristics of a fluid membrane. The chain rearrangement is more obvious in the case of ABA than for ABC triblock copolymers. All three distinct transitions are well visible and the transition between liquid condensed and low pressure condensed phase show that the polymeric chains rearrange in a well-defined manner into the monolayer film. Unlike for ABC triblock copolymers monolayers, when the mobility of the two hydrophilic different chains (PEO and PMOXA, respectively) is different, the monolayer formed by ABA triblock copolymer seem to adopt a more stable conformation. For ABC triblock copolymer monolayers, the surface pressure starts to rise at molecular areas much larger then those required for a close packing of molecules and the chains have the tendency to pass into a “liquid expanded” region of the isotherm, without an additional transition. This could be due to the random orientation of hydrophobic moieties, in competition with the opposite effect of hydrophilic chains.

In the ABA triblock copolymer monolayer, this phenomenon is not present.

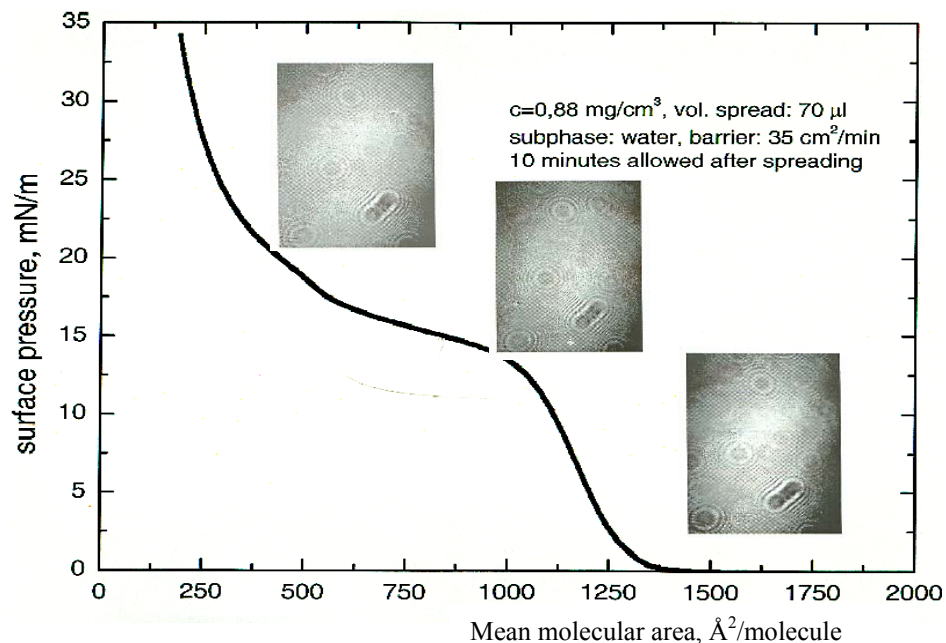


Figure 6.12 Compression isotherm and Brewster angle microscopy for symmetric ABA triblock copolymer

To check whether membrane proteins insert into ABC block copolymer monolayers, we used LamB, a transmembrane protein¹⁷³ as model system. The protein was incorporated from the subphase, and the process was followed via the pressure changes. The resulting compression

isotherms curves of triblock copolymers were recorded in the absence (at a initial pressure of 14 mN/m) or presence of different amounts of purified LamB in the subphase.

The changes of monolayer surface pressure upon the introduction of the protein in the subphase show (Figure 6.13) that there is an interaction between the polymer monolayer and the protein; consequently, the insertion of transmembrane proteins into a new asymmetric triblock copolymer may be possible.

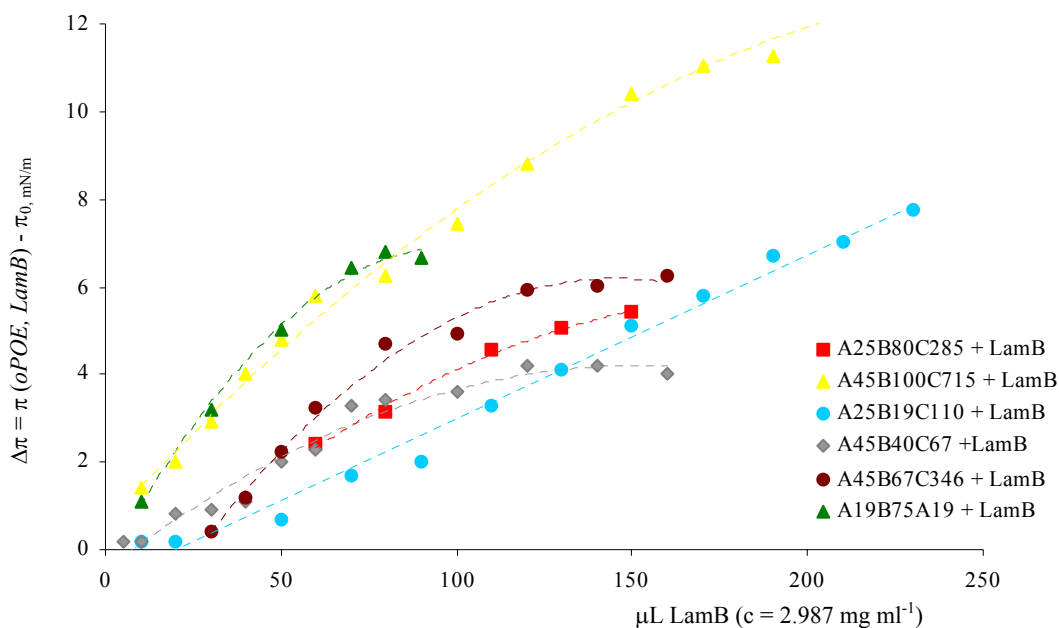


Figure 6.13 Influence of LamB protein on a triblock copolymer film. The surface pressure increases as a function of the protein concentration, which could indicate the protein insertion¹⁷³; $\Delta\pi$ represents the difference between the measured pressure, π (after subtraction of pressure for the detergent control experiments and addition of LamB protein) and π_0 , the pressure of the polymer film without protein or detergent

The molecular weight of triblock influences the surface pressure of insertion: the difference of the surface pressure increase with the increase of molecular weight, from 4 mN/m for a molecular weight of 10 600 g/mol to 11 mN/m for a molecular weight of 68 000 g/mol.

However, how the composition of the triblock copolymers influences the insertion yields and in which way this insertion is possible into a polymeric matrix formed by these ABC triblock copolymers are subjects to be developed in a forthcoming research.

CHAPTER 7

ASYMMETRIC MEMBRANES FROM ABC TRIBLOCK COPOLYMERS

7.1. Labelled asymmetric triblock copolymers

Two hydrophilic blocks form the ABC triblock copolymer: polyethylene oxide and polymethyl oxazoline, separated by a hydrophobic middle block, polydimethyl siloxane. The triblock copolymers self-assemble in aqueous solutions into vesicles-like aggregates with asymmetric distribution of vesicular walls, since the hydrophilic blocks have a molecular incompatibility. These hydrophilic blocks segregate to different sides of the hydrophobic block, thus leading to an asymmetric distribution across the membrane. The distribution of the hydrophilic chains in the vesicular wall is unknown. Using fluorescent measurements (with coumarin fluorescent labelled polymers) and a similar approach as described in reference 37, it is possible to prove which of the hydrophilic blocks is oriented toward the outside or the inside of vesicular walls respectively.

7.2 Validation of the asymmetry via fluorescence measurements of labeled polymers

The fluorescence spectra of the unlabelled and coumarin labelled asymmetric triblock copolymers are shown in Figure 7.1. Compared to the unlabelled triblock copolymer, the fluorescence intensities for the labelled polymers are 3 times higher.

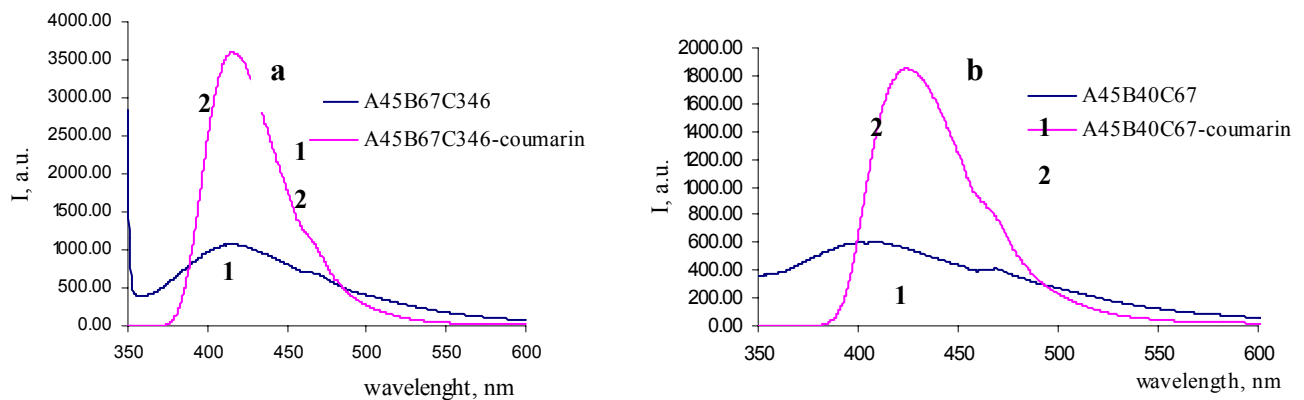


Figure 7.1 Fluorescence spectra of labelled and non labelled triblock copolymers vesicles used for quenching experiments (a: $PEO_{45}PDMS_{67}PMOXA_{346}$; b: $PEO_{45}PDMS_{40}PMOXA_{67}$). The unlabelled triblock copolymer presents a residual fluorescence, due to the functional groups in the molecule of polymethyloxazoline.

For quenching experiments, labelled polymers were mixed with the corresponding non-labelled copolymers in a molar ratio 300:1. Light scattering proved that diameters of the labelled vesicles were similar to those of the non-labelled (*i.e.*, 69 nm for PEO₄₅PDMS₆₅PMOXA₃₄₆ / POE₄₅PDMS₆₅PMOXA₃₄₆-coumarin compared to 80 nm for POE₄₅PDMS₆₅PMOXA₃₄₆ and 74 nm for POE₄₅PDMS₄₀PMOXA₆₇ / POE₄₅PDMS₄₀PMOXA₆₇-coumarin vs. 115 nm for POE₄₅PDMS₄₀PMOXA₆₇). Obviously, the presence of the fluorescent dye does not disturb the self-assembly of the polymers. Co²⁺ is known to quench the fluorescence of coumarin¹⁹², and, as only PMOXA chains bear a coumarin group, one can identify which block is at the outside of the vesicles because only “outside” coumarin will be quenched by addition of Co²⁺ ions. Control experiment with the non-labelled polymer vesicles prove that also the autofluorescence of the polymer is affected by the presence of cobalt ions (Figure 7.2), however, the change is small compared to differences obtained for labelled polymers. We assume that the cobalt ions are impermeable to the polymeric membrane.

Figures 7.2 and 7.3 present the fluorescence spectra of the two labelled ABC triblock copolymers used in this study. As expected, fluorescence intensities decrease with increasing Co²⁺ ion concentration in the vesicle solution, much more than for non-labelled polymer. Table 7.1 below presents the relative fluorescence intensities for labelled triblock copolymers and control experiments in the presence of cobalt ions.

Table 7.1 Calculated values of relative intensities, as cobalt ions concentration for the studied polymeric vesicles; I_0 represents the steady state fluorescence of mixed labelled-non-labelled polymers, before addition of the quenching solution; I is the fluorescence of the mixed copolymers in the presence of different concentrations of cobalt ions; the values represents the ratio I_0/I function of cobalt ions concentration for three copolymer vesicles. These values are nearly the same for the unlabelled long PMOXA triblock copolymer and labelled short PMOXA blocks; for the labelled PMOXA blocks, the ratio I_0/I is 2 times higher

System studied	$c (Co^{2+}), mM$				
	10	20	70	200	400
	I_0/I				
A ₄₅ B ₆₇ C ₃₄₆	-	1.3	1.7	2.4	2.5
A ₄₅ B ₆₇ C ₃₄₆ -coumarin	1.2	1.4	2.3	3.6	5.6
A ₄₅ B ₄₀ C ₆₇ -coumarin	1.2	1.5	1.6	2.35	2.5

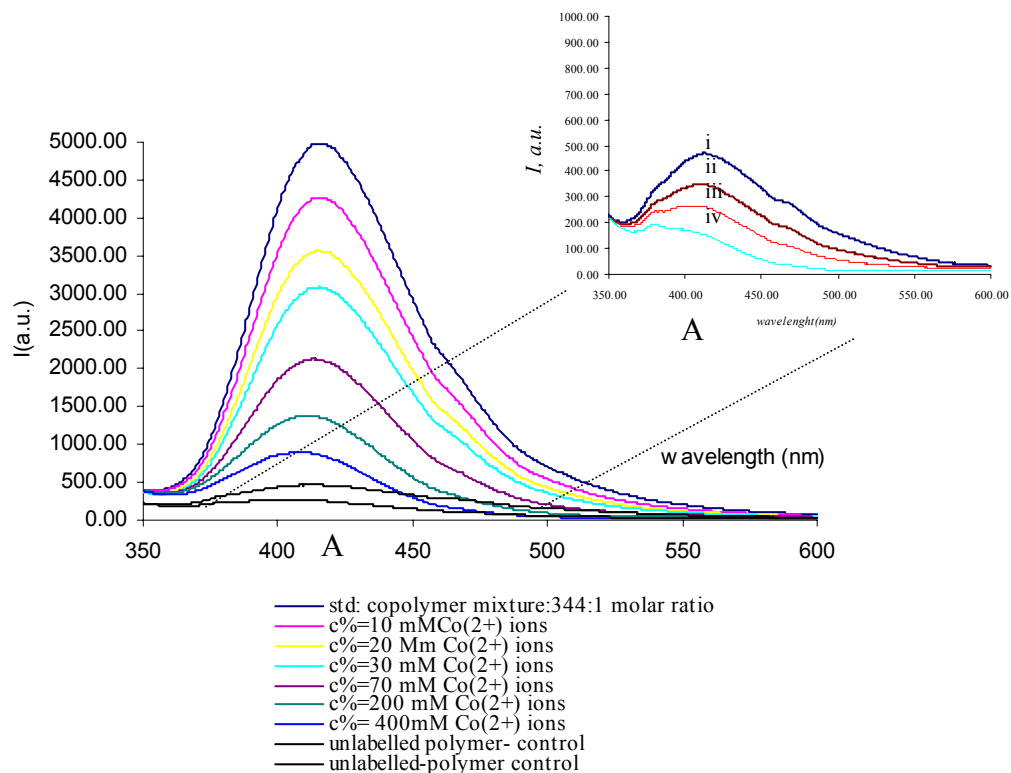


Figure 7.2 Fluorescence spectra for the $PEO_{45}PDMS_{67}PMOXA_{346}$ -coumarin labelled triblock copolymer (quenching with cobalt ions). The inset indicates the fluorescence spectra for control experiment of $PEO_{45}PDMS_{67}PMOXA_{346}$ unlabelled triblock copolymer (in the presence of cobalt ions). i): polymer control $A_{45}B_{67}C_{346}$: 0.55 wt%, $I_0 = 469.2$; ii): Polymer $A_{45}B_{67}C_{346}$: 40 μL Co^{2+} 1M; $c=0.02$ M; $I_0 = 350.60$; iii): Polymer $A_{45}B_{67}C_{346}$: 140 μL Co^{2+} 1M; $c=0.07$ M; $I_0 = 266.90$; iv): Polymer $A_{45}B_{67}C_{346}$: 500 μL Co^{2+} 1M; $c=0.25$ M; $I_0 = 195.7$

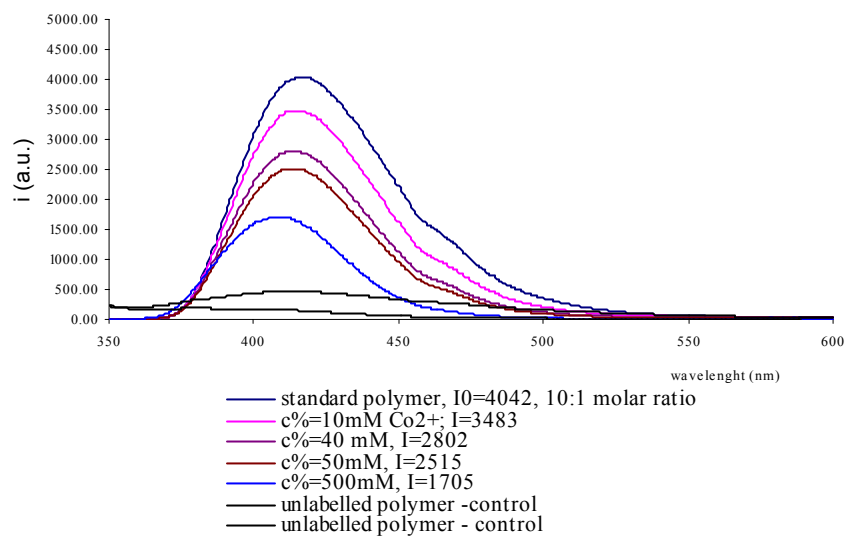


Figure 7.3 Fluorescence spectra for the $PEO_{45}PDMS_{40}PMOXA_{67}$ -coumarin labelled triblock copolymer (quenching with cobalt ions).

Figure 7.4 shows the results of the quenching experiments for the labelled $\text{PEO}_{45}\text{PDMS}_{67}\text{PMOXA}_{346}$ and the $\text{PEO}_{45}\text{PDMS}_{40}\text{PMOXA}_{67}$ systems together with data for non-labelled block copolymer vesicles. The non-labelled vesicles of the control experiment showed a fluorescence emission around ca. 420 nm, however, with a ten times lower intensity than the coumarin-labelled polymers. This is presumably due to traces of impurities in the block copolymers. The presence of Co^{2+} ions influenced the “polymer” fluorescence to a very small degree.

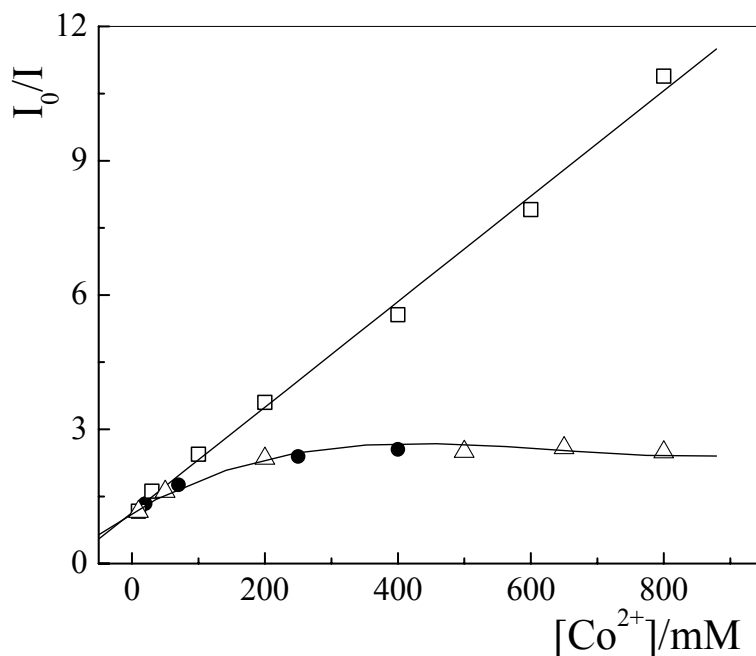


Figure 7.4 The variation of steady state fluorescence with concentration of Co^{2+} ions quencher for spherical vesicles: $\text{POE}_{45}\text{PDMS}_{67}\text{PMOXA}_{346}/\text{POE}_{45}\text{PDMS}_{67}\text{PMOXA}_{346}$ -coumarin (-□-); $\text{POE}_{45}\text{PDMS}_{40}\text{PMOXA}_{67}/\text{POE}_{45}\text{PDMS}_{40}\text{PMOXA}_{67}$ -coumarin (-△-); unlabelled polymer $\text{POE}_{45}\text{PDMS}_{67}\text{PMOXA}_{346}$, control experiment (-●-)

Interestingly, the data for $\text{PEO}_{45}\text{PDMS}_{40}\text{PMOXA}_{67}/\text{POE}_{45}\text{PDMS}_{40}\text{PMOXA}_{67}$ -coumarin vesicles were identical with the control experiment within the experimental error, i.e., the fluorescence emission remains nearly unaffected by the presence of the quencher ions (see Figure 7.5).

In contrast to that, for the $\text{PEO}_{45}\text{PDMS}_{67}\text{PMOXA}_{346}/\text{POE}_{45}\text{PDMS}_{67}\text{PMOXA}_{346}$ -coumarin vesicles, with the longer PMOXA block, the data follow a Stern-Volmer relation and the fluorescence is quenched by Co^{2+} ions¹⁹³. This leads to the conclusion that, in the case of the $\text{POE}_{45}\text{PDMS}_{67}\text{PMOXA}_{346}$ triblock copolymer, the PMOXA chains are on the outer surface of the vesicles, while the PEO chains are oriented in the inner surface of vesicles. For the

POE₄₅PDMS₄₀PMOXA₆₇ triblock copolymer, this situation is reversed, with PMOXA chains oriented to the inner of vesicular walls and PEO outside of vesicles.

Fluorescence microscopy

Giant vesicles fluorescent-dye labelled could be visualized in fluorescence microscopy. Using the fluorescence quenching technique, they could offer additional information relative to the orientation of labelled chains (i.e., PMOXA chains).

Fluorescence and confocal fluorescence microscopy analysis of giant vesicles prepared by electroformation from fluorescein- and rhodamine-conjugated ABC triblock reveal fluorescent giant vesicles (Figures 7.5 and 7.6).

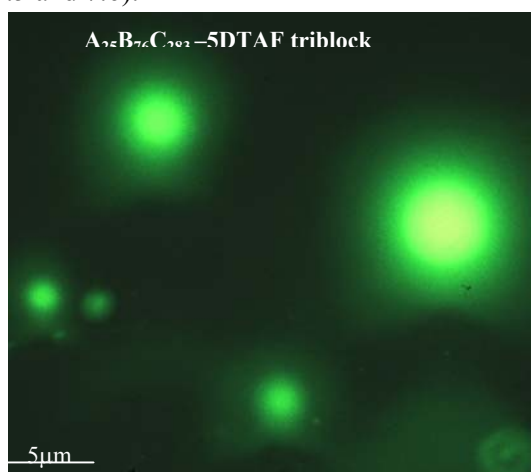


Figure 7.5 Fluorescence microscopy of giant vesicles prepared from ABC-fluorescein labelled triblock copolymers (mixture of labelled/non-labelled polymer 300:1 molar ratio)

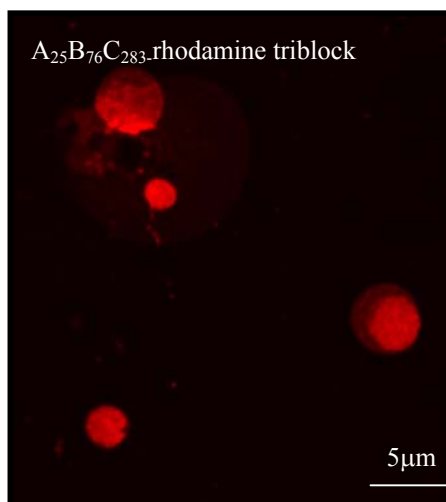


Figure 7.6 Fluorescence microscopy of giant vesicles prepared from ABC-rhodamine labelled triblock copolymers (mixture of labelled/non-labeled polymer 100:1 molar ratio)

Due to the preparation for microscopy, the quenching experiments were not successful. The assays for quenching the fluorescence directly on the microscopy slides induce a dilution of the sample, which increases the motion of the aggregates on the microscopy slides. This makes the analysis very difficult.

However, confocal fluorescence microscopy offered the possibility to analyze our system in 3D. Giant vesicles of rhodamine-labelled triblock copolymers are completely spherical, with a diameter of 5 μm and show a uniform distributed fluorescence.

Conclusions

Fluorescence measurements indicate that in the $A_{45}B_{67}C_{346}$ (i.e. long PMOXA chain) system all PMOXA blocks are oriented towards the outside of the vesicles and consequently the PEO blocks towards the inside. For the shorter PMOXA blocks of the $A_{45}B_{40}C_{67}$ system, the arrangement is reverse, i.e., PEO points outwards and PMOXA towards the interior. This agrees with geometrical considerations: due to the curvature of the vesicle walls, it is favourable when the hydrophilic blocks with lower volume segregate towards the interior.

The two hydrophilic blocks, PEO and PMOXA chains are incompatible and they segregate in both sides of the hydrophobic middle chain. Thus leads to an asymmetry across the polymeric membrane.

The segregation between the two PEO and PMOXA blocks in triblock copolymers is also in qualitative agreement with the recent observation that aqueous solutions of poly(ethylene oxide)-*b*-poly(2-methyloxazoline) diblock copolymers can form lyotropic mesophases at higher concentration¹⁷⁴. These peculiar water-in-water mesophases are again a direct result of microphase separation of the two incompatible polymer chains.

CHAPTER 8

BIOLOGICAL APPLICATIONS OF ASYMMETRIC MEMBRANES

8.1 Introduction

This chapter describes a new approach to induce a directed insertion of membrane proteins into asymmetric membranes formed by amphiphilic ABC triblock copolymer with two chemically different water-soluble blocks A and C. In a comparative study we have reconstituted Aquaporin 0 in lipid, ABA block copolymer, and ABC block copolymer vesicles. By analogy with biological systems, the inner and outer leaflets of biological membranes are strictly asymmetric with respect to lipid composition and distribution. However, most artificial membranes are symmetric with respect to their midplane. Breaking this symmetry of the membrane either by external (e.g., electric) fields or the chemical composition of the two membrane leaflets can influence the insertion and orientation of integral proteins^{175,176,177}. These methods require, however, rather complicated and protracted procedures that are not well suited for technical applications. ABC block copolymers offer more interesting approach, as they spontaneously form asymmetric vesicular structures in aqueous solution (Fig. 8.1).

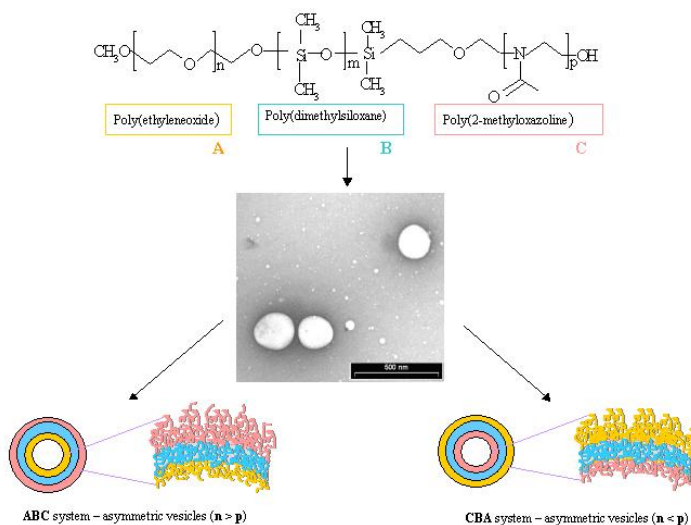


Figure 8.1 Chemical constitution of the ABC triblock copolymers ($n = 25$, $m = 20$, $p = 110$ and $n = 45$, $m = 40$, $p = 67$, respectively). Upon dispersion in water, triblock copolymers form nanometer-sized vesicles (see TEM micrograph; scale bar: 500 nm), with an asymmetric membrane. Curvature forces the less voluminous hydrophilic chains to segregate towards the inner side and the longer hydrophilic chains towards the outer side of the vesicles. This leads to 'ABC' block copolymer vesicles with the poly(ethylene oxide) blocks A on the outside and 'CBA' block copolymer vesicles with the inverse orientation, i.e., the poly(ethylene oxide) blocks A on the inside of the vesicle walls.

Insertion of proteins into membranes is promoted in cases of membranes with spontaneous curvature¹⁷⁸. This phenomenon has been related to the effect of asymmetric fluctuations of the amphiphilic molecules across the membrane. The present work extends the concept to asymmetric ABC triblock copolymer membranes.

The general concept for the following studies was as follows:

Firstly, polymer vesicles were prepared with reconstituted Aquaporin0 protein. The protein contains a His-Tag unit at one end that, in natural environment (cells) will be directed to the cytoplasmic side. This His-Tag can be used as specific ligand for antibodies. Labelling the antibody allows to follow its binding to His-Tag, and thus –indirectly- conclude about protein orientation.

Three detection methods were applied:

1. Immunogold detection: antibody was labelled with nanogold (6 nm), which is possible to monitor via TEM
2. Immunoassay: antibody was labelled with HR peoxidase. In this case, HR peroxidase serves as substrate for TMB, the content of which can be followed by UV Vis spectroscopy. Only the HR peroxidase antibodies present outside vesicles (outer membrane) will undergo this reaction, because they are the only accessible to the antibodies.
3. Immunofluorescence: antibody was labelled previously with a dye (Alexa Fluor 555). This way, fluorescence could be detected, but again, only from those proteins, whose His-Tag points to the outside of the vesicles.

Combining the results from above measurements, allows conclusions concerning the protein orientation in asymmetric ABC membranes, and also gives overview of the applicability of the chosen methods through comparison of the obtained values.

As a model system to investigate directed protein insertion we performed reconstitution experiments with Aquaporin 0, a channel-forming integral membrane protein. Aquaporins are transmembrane protein water channels. They are responsible for osmoregulation and water balance of microorganisms, plants, and animal tissues¹⁷⁹. All aquaporins studied to date are thought to be homotetramers with each monomer containing a separate water pore^{180,181}

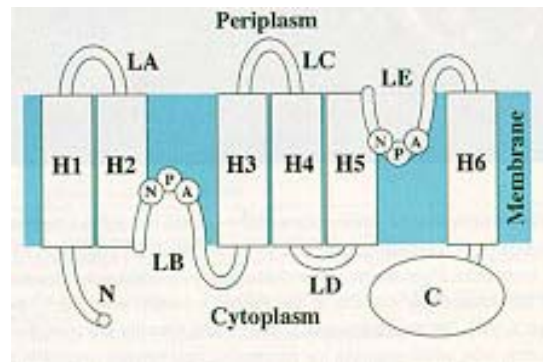


Figure 8.2 Representation of aquaporin 1, similar to aquaporin 0. Top: model showing the predicted position of the helices and loops (from [Walz et al., 1997](#))¹⁸²

We used Aquaporin that has been genetically fused to a His-Tag unit consisting of ten consecutive histidine residues on its amino terminus (i.e., the His-Tag appears on the cytoplasmic side for a physiological orientation of the protein). We wanted to compare the orientation distribution of Aquaporine 0 in the walls of ‘symmetric’ lipid (phosphatidyl choline) and ABA block copolymer vesicles to the orientation distribution in ‘asymmetric’ ABC and CBA block copolymer vesicles with a reversed membrane orientation.

Generally, the proteins are incorporated into the symmetric membranes with a random insertion (Fig.8.3), i.e., Aquaporin could be then incorporated with the His-Tag end in both (outside and inside) directions.

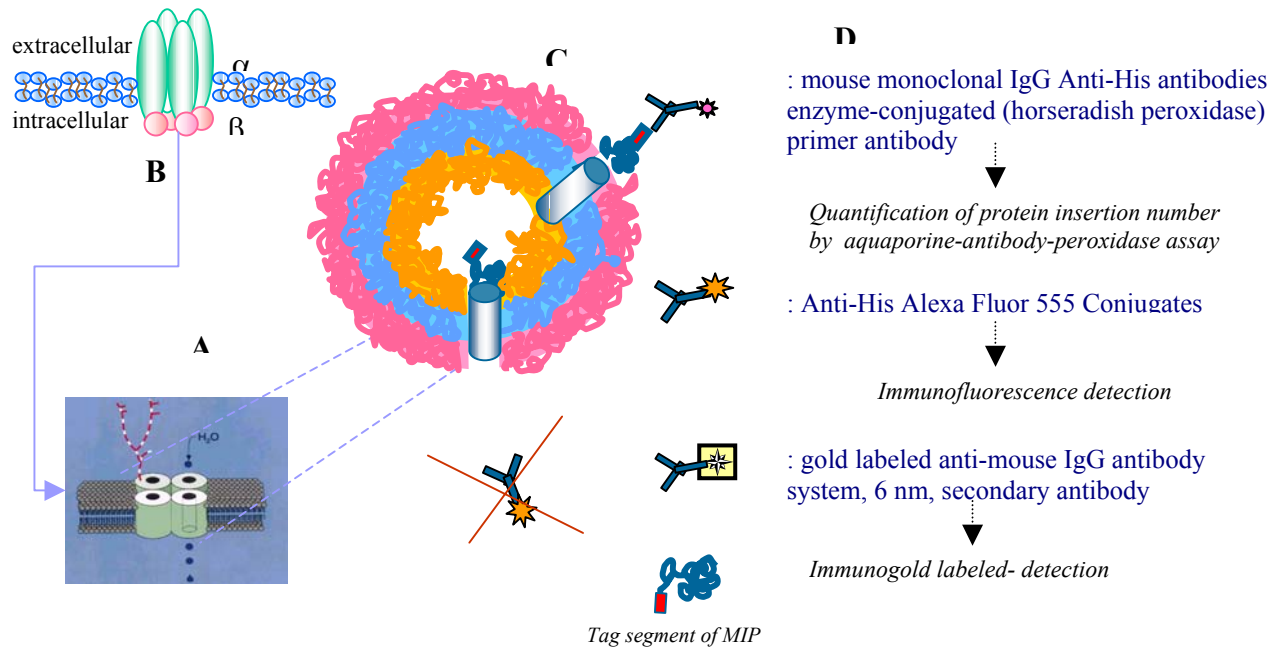
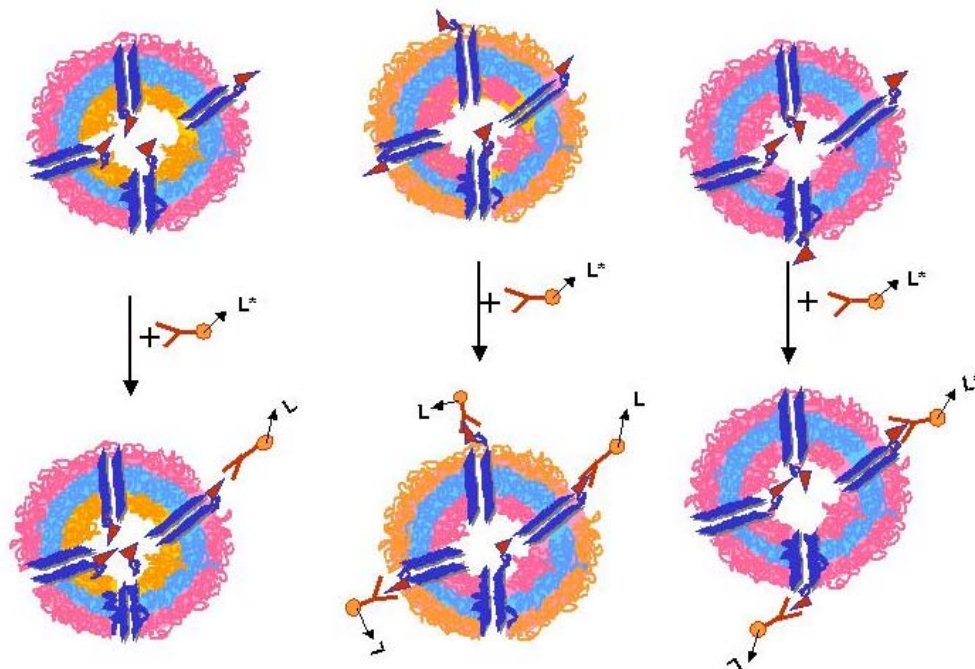


Figure 8.3 Schematic representation of proteovesicles reconstituted with aquaporin. His-Tag head is oriented in both sides: inside and outside the vesicular walls. A) schematic representation of biological

insertion of aquaporin with N- and C- termini oriented in cytoplasm space; B) the aquaporins are tetrameric assemblies, forming water channels; C) reconstituted proteovesicles (protein insertion in the polymeric matrix); D) principle of detection of His-Tag outside oriented tails by anti-his antibodies labeled enzymatically, with fluorescent dye and gold carriers.

The His-Tags of Aquaporin0 proteins could be located inside and outside of the vesicles for both symmetric and asymmetric vesicles. The percentage of this orientation is reversed for symmetric and asymmetric matrices. This location of His-Tag tail will not interfere with the conformation of the proteins upon immobilization and will preserve bioactivity for immunoreactions and antigen-antibody interactions. By the use of Penta-His antibodies we were able to identify the Aquaporin His-Tag tail as anti-Penta-His antibodies¹⁸³ recognize specifically the antigen determinant of the protein exposed to the outer side of the asymmetric membrane. All Anti-His antibodies used are mouse monoclonal IgG1 with high affinity and specificity for His Tags. Therefore, these antibodies can bind to even partially hidden His-Tags that other anti-His antibodies could not recognize. These antibodies recognize an epitope of at minimum five consecutive histidine residues. Upon addition to the external solution the antibodies can bind, however, only to those His-tag units that are located on the outer surface of the vesicles (Fig. 8.4); His-Tags inside the vesicles are not accessible.



Where L^* : nanogold-6 nm; horseradish peroxidase or Alexa Fluor 555, respectively

Figure 8.4 Schematic (not to scale) representation of the orientation of His-Tag labeled Aquaporin 0 in 'symmetric' ABA and 'asymmetric' ABC triblock copolymer vesicles. A preferred orientation is expected

only for the ABC block copolymer vesicles. Monoclonal anti-His antibodies can bind only to proteins that expose their His tag unit to the external vesicular side.

Control experiments with lipid and block copolymer vesicles without Aquaporin revealed that unspecific binding of the antibodies was generally below the detection limit of our different assays. The antibody concentration has been optimized with respect to the protein concentration to guarantee that all experiments were performed with an excess of antibody.

8.2. Results and discussions

In order to establish if there is an interaction between Aquaporin 0 protein and polymer monolayer, we use a similar approach as the one described for the interaction of LamB protein with triblock copolymers monolayers (chapter 6) and described in reference 173. Also here, the interaction of the protein with the monolayer of the asymmetric triblock copolymer indicates that it can incorporate into the vesicle walls formed by the polymers. The AQP0 was added to the subphase at 13 mN/m, where the monolayer has the “fluid-properties” of a biological membrane. The addition of AQP to the subphase of the monolayer induced a shift toward higher surface pressure in the compression isotherms, indicating AQP0-monolayer interaction (Fig. 8.5). Furthermore, the surface-pressure increase was protein concentration dependent (Fig. 8.6).

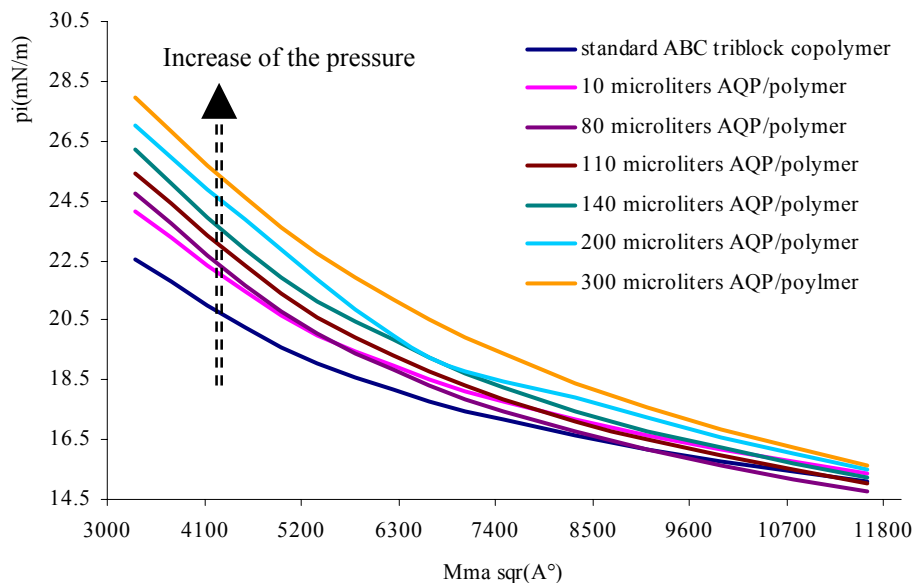


Figure 8.5 Compression isotherms of the polymer monolayer ($PEO_{25}PDMS_{19}PMOXA_{110}$) in presence of different amount of injected protein in the PBS-buffer subphase ($500 \mu\text{L}$ polymer spread to reach a starting pressure of 13 mN/m).

The presence of the detergent has influence on the polymeric monolayer, however the increase of the surface pressure is relatively small: 1.7 times compared to the one observed for the AQP interaction 7 times (moreover, the mean molecular area per molecule does not have a high increase). A maximum surface pressure difference of 2.7 mN/m has been reached at 300 μ L (4.3 nmoles) protein for the polymer film (Figure 8.6), in contrast with 0.9 mN/m reached for 300 μ L detergent.

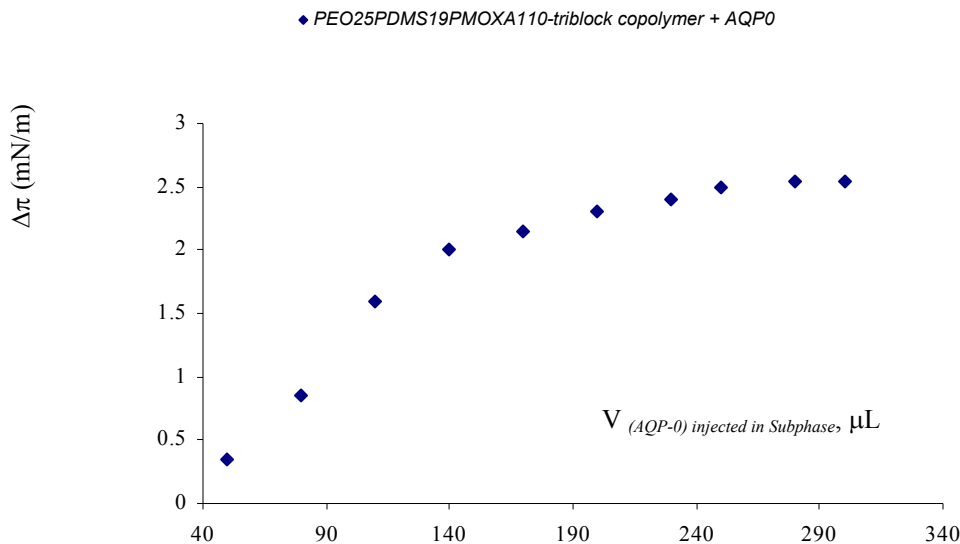


Figure 8.6 Influence of AQP0 on triblock copolymer monolayer. The surface pressure increases as a function of protein concentration because of possible protein insertion. The values for control measurements using detergent (*n*-decyl maltoside) have been subtracted from the values for the copolymer after the injection of the protein in the sub phase.

Monolayer experiments demonstrate that AQP interacts with monolayers made from polymers, in a similar mode with other transmembrane proteins in symmetric triblock copolymers¹⁷³.

Protein detection in proteovesicles

To check whether the protein is inserted into the vesicular walls of polymeric vesicles after the purification of the vesicles from the unincorporated protein, we have used SDS PAGE experiments. The detection of Aquaporin in proteovesicles was revealed using as staining agent Commassie Blue dye in 50% methanol. The detected quantity of Aquaporin0 from 2 μ L sample spread on the gel has been 10-15 ng/mL (from an initial total quantity of the protein of 50 μ L protein for the reconstitution of proteovesicles and after removal of unincorporated protein by

size exclusion chromatography) (Fig. 8.7). Thus indicates that the protein is present into the vesicle walls (proteovesicles).

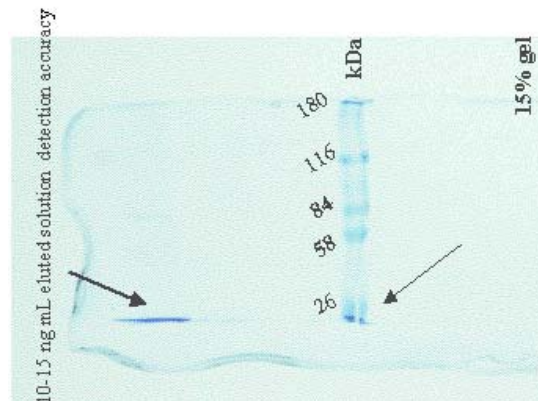


Figure 8.7 Purified 10-tagged proteins (10 μ l of 1.6 mg/mL) were applied to a 15% SDS-Page gel.

Experiments with pure polymeric vesicles and pure protein showed no signal for polymeric vesicles (without protein) and allow a control for the protein (especially interesting concerning the protein's purity).

Immunogold assay

We have used a 6-nm colloidal gold anti-mouse Penta-His antibody as a secondary antibody and free-tagged oriented antibody as a primary Aquaporin antibody. The incubation was done directly on the microscopy grids, following the specific procedure for the immunogold labelling. These procedures request a two-step incubation using a primary antibody and a gold-labelled secondary antibody conjugate.

In the first set of measurements, we used a double immunolabeling with colloidal gold as a probe in combination with transmission electron microscopy to visualize the presence of Aquaporin 0 in the triblock copolymer vesicles. First, we added the monoclonal Penta-His antibody to the external volume of proteo-vesicle dispersion. This antibody binds to His-Tag units on the outer surface of the vesicles i.e., to proteins that have a 'non-physiological' orientation. As a secondary antibody we used GAM Aurion IgG coupled to 6 nm gold particles.

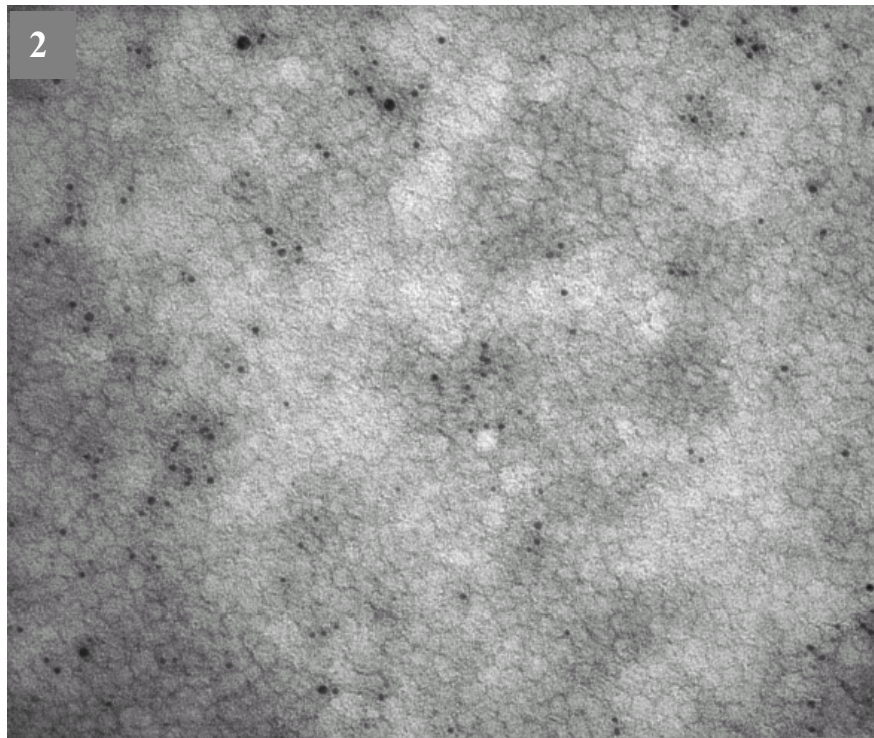
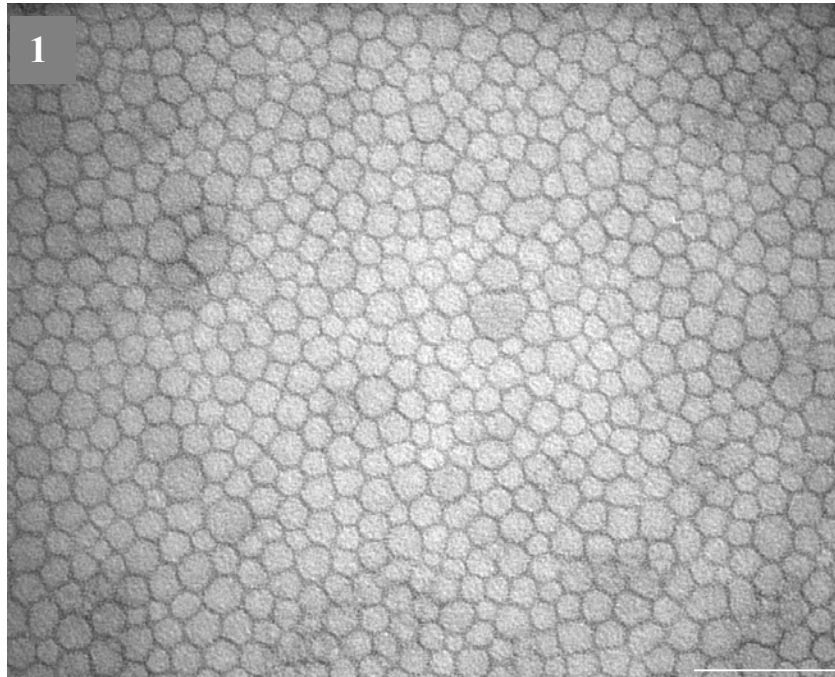


Figure 8.8 Transmission electron microscopy images of ABA triblock copolymer vesicles. 1) negative control of ABA polymer vesicles after incubation with the primary antibody, non-carrier of nanogold, bar 200 nm; 2) nanogold labelled secondary antibody of ABA triblock copolymer vesicles, bar 100 nm

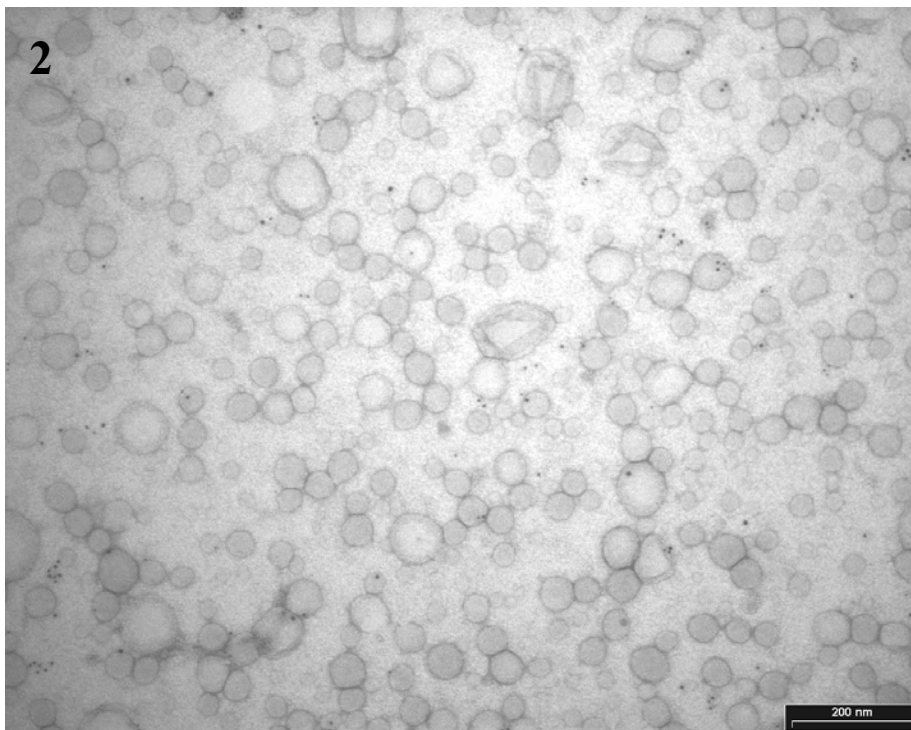
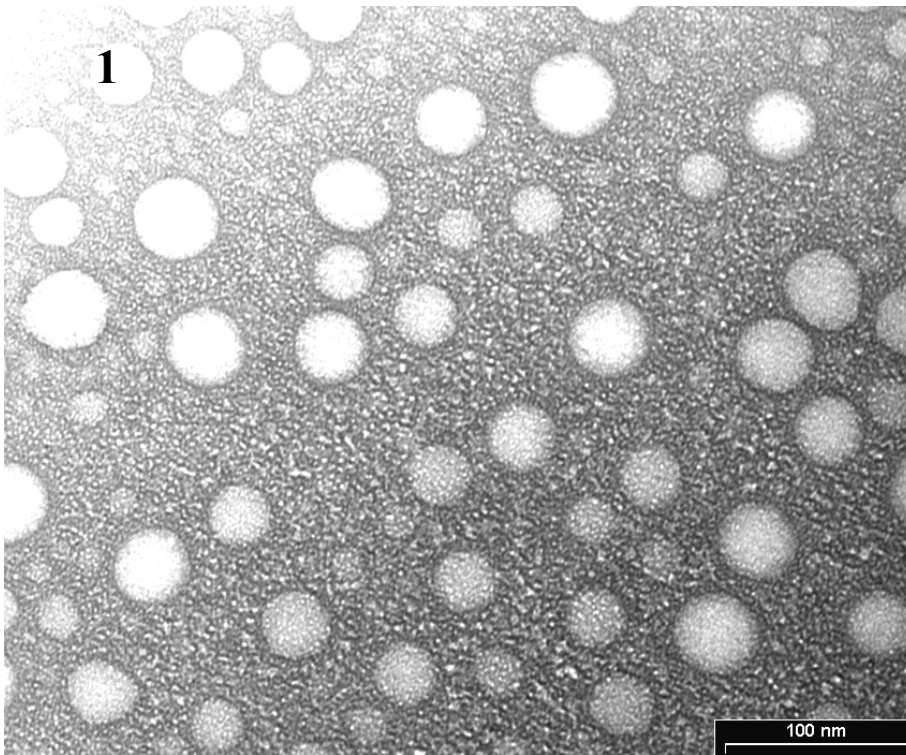


Figure 8.9 Transmission electron microscopy images of ABC triblock copolymer vesicles. 1) negative control of ABC polymer vesicles after incubation with the primary antibody, non-carrier of nanogold; 2) nanogold labeled secondary antibody of ABC triblock copolymer vesicles

Transmission electron microscopy (see Fig. 8.8 and Fig. 8.9) shows the presence of gold particles attached to the surface of ABA and ABC triblock copolymer vesicles. As expected, control experiments with pure block copolymer vesicles and proteo-vesicles without primary antibody never showed binding of colloidal gold. As the micrograph analyses showed, not every individual vesicle contains nanogold particles. According to previous studies concerning the general preparation of gold labelled-antibodies, the gold antibody stock solution contained a significant fraction of non-bound antibody¹⁸⁴. This could explain the considerable number of vesicles without gold nanoparticles found in Fig. 8.9 (ABC triblock copolymer vesicles and ABA triblock copolymer vesicles). There is a difference in what concerns the density of nanogolds for symmetrical (i.e., ABA) and asymmetrical (i.e., ABC) vesicles. Despite the resolution of these micrographs, the results of TEM analyses indicate that there is a first qualitative difference between these two systems.

For quantitative information about the amount and orientation of reconstituted protein we performed complementary colorimetric and fluorescence investigations. In colorimetric assays, we used a monoclonal IgG1 anti-His mouse antibody coupled to horseradish peroxidase. This approach circumvents the need of a secondary antibody. The purification of proteovesicles after the binding of antibodies, in order to remove the unattached excess antibodies, was achieved using size exclusion chromatography (Fig. 8.10) from Sepharose 4B. The separation procedure relies on the differences of molecular weight of the systems constituents.

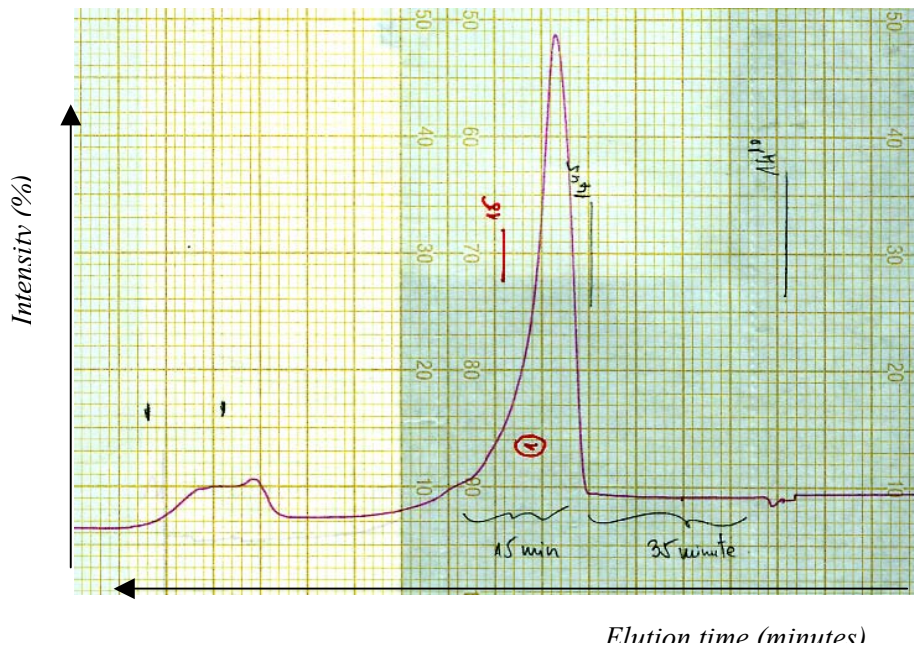


Figure 8.10 Chromatogram (SEC) of purified HRC antibody –proteovesicles complexes.

The first peak corresponds to the proteovesicles which bound to peroxidase labelled antibodies. The second peak is composed to free-nonbound antibodies (it has to be taken in account that the excess of antibodies has been important concerning the quantification of the protein, to assure that all accessible His-Tag tails have been attached to antibodies).

As a well-established, specific substrate for horseradish peroxidase we used 3,3'-5,5'-tetramethyl benzidine (TMB). The enzymatic reaction was stopped after 90 seconds by diluting the vesicle dispersion to twice the original volume with 5M HCl¹⁸⁵. Subsequently the extinction of the yellow reaction product was measured at its absorption maximum at 450 nm. This allowed the calculation of (via the Lambert-Beer law) the concentration of dye produced; this is directly proportional to the concentration of the enzyme-antibody conjugate in the system (Figure 8.11).

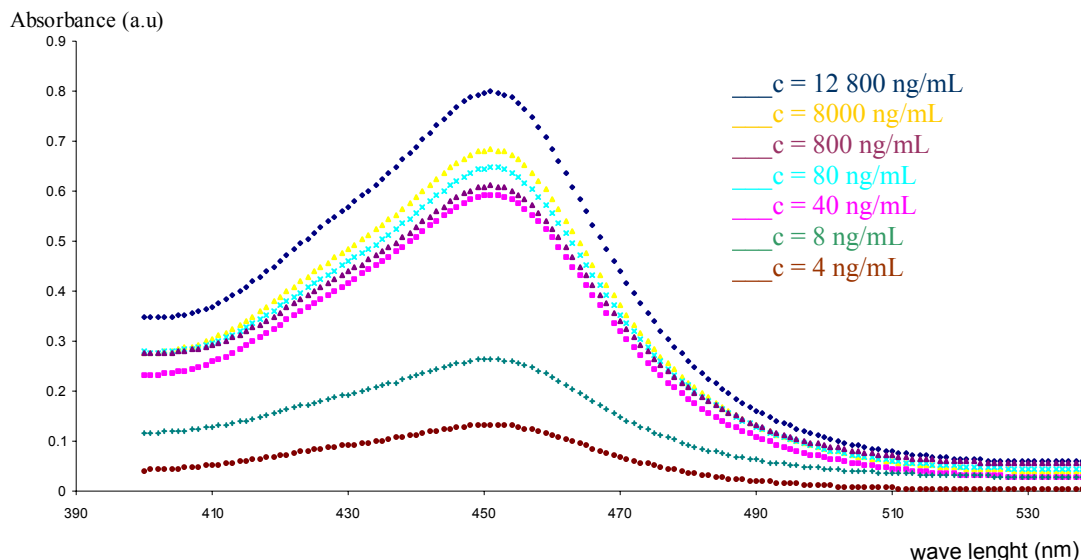


Figure 8.11 UV Vis spectra of the Aquaporin-labelled antibodies for calibration standard.

As a calibration standard in the concentration range from 4 ng/mL to 80 μ g/mL we used dilutions of detergent solubilized Aquaporin 0 in phosphate buffer. Figure 8.12 presents the calibration standard of Aquaporine-HRC antibodies. The total and partial amount and the orientation of AQP0 inserted into vesicles has been calculated from this calibration.

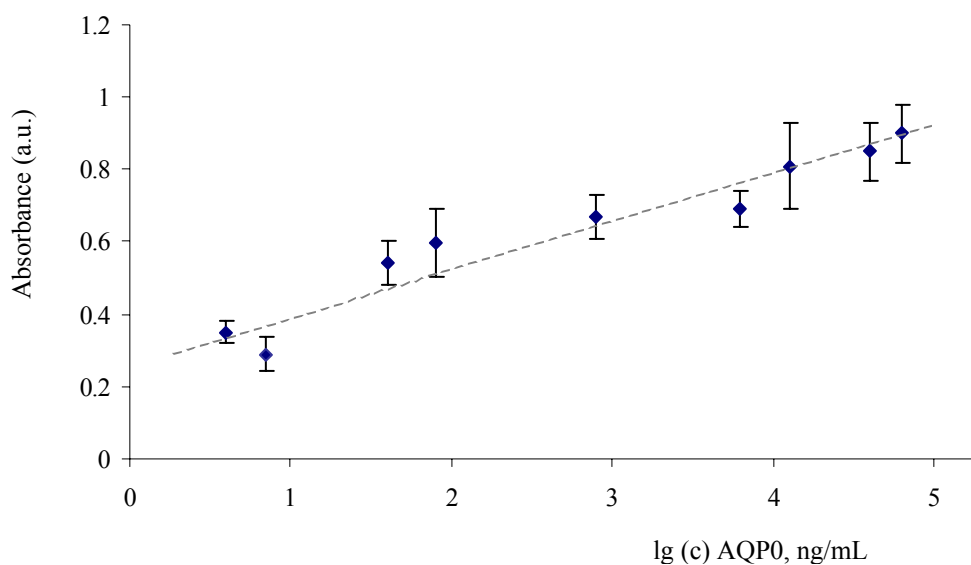


Figure 8.12 Calibration standard for binding of the horseradish peroxidase labelled antibody using detergent-solubilized Aquaporin 0. 3,3'-5,5'-tetramethyl benzidine (TMB) was used as a specific substrate for horseradish peroxidase. The enzymatic reaction was stopped after 90 seconds. The plot shows the absorption at 452 nm as a function of Aquaporin 0 concentration.

We determined the overall concentration of Aquaporin 0 in the protein-containing vesicles by addition of octyl-polyoxyethylene (octyl-POE) up to a concentration of 3 wt.% prior to antibody incubation. Light scattering experiments indicated that at this detergent concentration both the lipid and the block copolymer vesicles are disrupted. Hence the antibody has access to all His-tag units of Aquaporin (even those that were originally on the inner surface of the vesicles¹⁸⁸), which allows for a quantitative Aquaporin concentration determination. The choice of octyl-polyoxyethylene (octyl-POE) as destructive agent for the membranes of proteovesicles has been supported by dynamic light scattering studies. Octyl-POE has been preferred to n-decyl-maltoside¹⁸⁶ for solubilizing the vesicles: dynamic light scattering indicated that there is no significant decrease of hydrodynamic radius upon addition of n-decyl-maltoside. It seems that the detergent only partially solubilize the vesicles.

The results for the lipid, ABA, ABC and CBA triblock copolymer vesicles are summarized in Table 8.1. All data given are mean values of repetitive measurements using independently

prepared samples. Interestingly, we observed that, generally for lipids the Aquaporin added to the system was completely incorporated into the vesicles. In contrast to that, the overall amount of protein incorporated into the ABA, ABC and CBA block copolymer membranes was lower by approximately 30%. This is also in agreement with observations on the insertion of other membrane proteins into these systems¹⁸⁷. Presumably, this effect is related to the considerably higher energy necessary to create the required defect allowing protein incorporation into the polymer layer^{8a}.

Table 8.1 Amount and orientation of His-tag labeled Aquaporin 0 in lipid, ABA, ABC and CBA triblock copolymer vesicles. The error given is the maximum deviation observed during three independent measurements.

System	Total amount of protein with His-Tag out and inside vesicles		The amount of protein with His-Tag outside vesicles		Fraction (%) of protein with non-physiological orientation
	Absorbance (x 10 ² a.u.)	Concentration (x10 ⁻⁴ ng/mL)	Absorbance (x 10 ² a.u.)	Concentration (x10 ⁻⁴ ng/mL)	
<i>ABC</i>	90 ± 18	6 ± 1	63 ± 3	1.1 ± 0.5	19 ± 8
<i>CBA</i>	96 ± 1	7 ± 0.1	85 ± 0.2	5 ± 0.5	72 ± 5
<i>ABA</i>	94 ± 24	7 ± 2	73 ± 1	3.4 ± 2	47 ± 5
<i>Lipos</i>	105 ± 11	9 ± 1	82 ± 14	4.9 ± 0.9	55 ± 7

With respect to the orientation of the His-Tagged Aquaporin, we observed a substantial difference between the ‘symmetric’ and the ‘asymmetric’ vesicles. In reasonable agreement with random insertion in lipid and ABA block copolymer vesicles, 55±7% and 47±5% respectively, of the protein had a non-physiological orientation with the His-tag exposed to the external solution. In strong contrast for the asymmetric ‘ABC’ and ‘CBA’ triblock copolymer systems we clearly found a direct correlation between the orientation of the membrane and that of the protein. While the ABC system induces a preference of the ‘physiological’ orientation with only 19±8% of the His-Tag moieties on the outside of the vesicles, the CBA system induces the reversed, ‘non-

physiological' orientation of the protein with $72 \pm 5\%$ of the His-Tag moieties on the outside of the vesicles.

As a control we performed a set of experiments where we investigated antigen binding to a fluorescence labelled antibody. This technique is widely used for the detection and quantification of cell surface antigens¹⁸⁹ and allows a direct determination of the amount of bound antibody. We used a Penta-His antibody labeled with Alexa Fluor 555. To allow antibody binding we followed the same incubation and purification procedure as described above. The fluorescence spectra for Aquaporin-Alexa Fluor antibody complex for four different systems are presented in Figure 8.13. The correlation between the fluorescence intensity of each of immunolabelled systems and the fluorescence intensity of the used antibody stock solution allowed the estimation of the percentage of His-Tag tails oriented outward of vesicular walls. The pure antibody solution served as a reference.

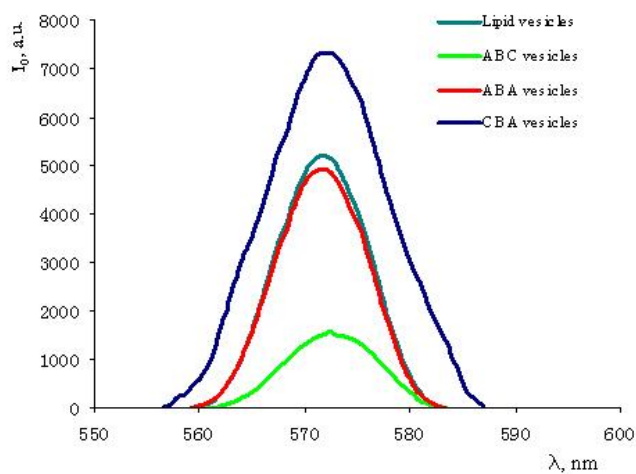
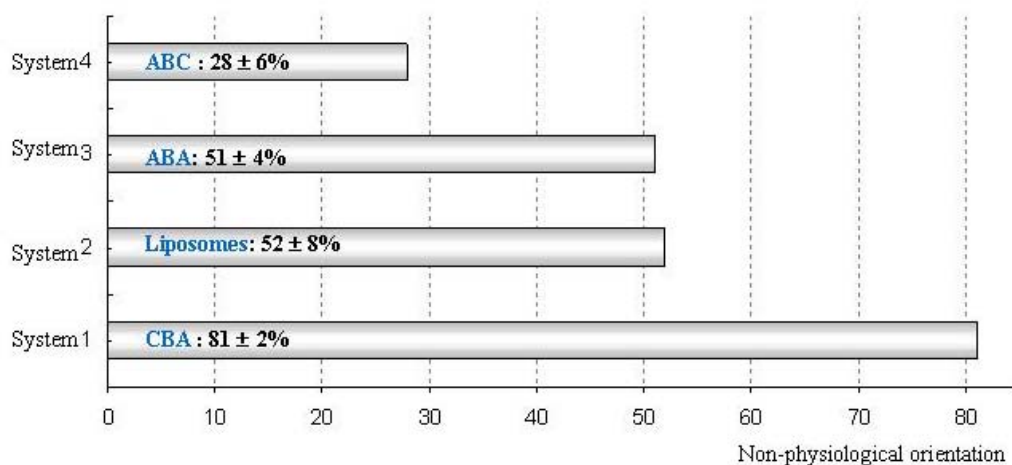


Figure 8.13 Fluorescence spectra of Aquaporin 0 contained in ABA, ABC, CBA and lipid vesicles (excitation/emission maxima: 450 / 572 nm) after incubation with the Alexa Fluor 555 labeled antibodies. Prior to measurements, the vesicles were purified chromatographically

The results were in strikingly good agreement with the previous investigation using horseradish peroxidase modified antibody (see Figure 8.15). Again the results for the lipid and ABA block copolymer vesicles indicate a random insertion of Aquaporin with $52 \pm 8\%$ and $51 \pm 4\%$ native orientation, respectively. In the ABC (CBA) system clearly a preferred orientation with $28 \pm 6\%$ ($81 \pm 2\%$) of 'non-physiological' orientation could be detected.



Figure

8.15 Fraction of His-tag labeled Aquaporin 0 with a ,non-physiological' orientation (His tag outside) for lipid, ABA, ABC and CBA triblock copolymer vesicles. Data were obtained by binding of AlexaFluor 555-labeled antibody to the His tag moiety of Aquaporin. The error given is the maximum deviation during three independent measurements

Conclusions

The above experiments indicate that the symmetry and orientation of the membrane plays a crucial role for the insertion of integral membrane proteins into artificial membrane systems. While these experiments reveal a statistical incorporation of Aquaporin 0 with approximately 1:1 distribution of proteins with the His-tag unit at the outer and inner surface of walls of the lipid and ABA block copolymer vesicles, the asymmetric ABC or CBA-triblock copolymer membranes always favor one orientation. Such a preferred orientation of the proteins intrinsically induces a directional functionality in block copolymer vesicles, which may be used to mimic biological processes. Unlike biological systems, we can also induce “anti-biological” functionalities, i.e. functions that are inverted compared to the natural systems.

There are many potential applications for these reconstituted systems depending on the correct orientation of proteins, including sensors (directed epithelial fluid transport, selective channels) and pharmacy (in the treatment of human pathophysiology; cell-to-cell adhesion behavior)¹⁹⁰. Besides applications, the new ABC triblock copolymer membranes could be interesting to investigate protein incorporation since polymer chemistry allows a convenient molecular tailoring (e.g., chemical nature and sequence of the repeat units, or the lengths of the individual blocks) of the polymers with respect to their desired properties. In a recent paper, molecular dynamics simulations suggest a two-step process for the protein insertion where the proteins are first adsorbed onto the membrane surface and then they rotate into their final transmembrane configuration¹⁹¹. Our study could provide interesting approach following the fundamental

problem of direct incorporation of integral proteins into an artificial environment. This work is believed to motivate further studies for understanding the interaction between asymmetric amphiphilic molecules and membrane proteins.

CHAPTER 9

Summary and conclusions

We developed a synthetic pathway to new amphiphilic ABC triblock copolymers with water-soluble blocks A and C and a hydrophobic middle block B. The synthesis involves a two-step polymerization. The prepolymer AB, constituted of poly(ethylene) oxide –b– poly(dimethyl) siloxane was prepared by anionic ring-opening polymerization of cyclic siloxanes, with 3 and 4 siloxane units. The polymerization of strained cycles (e.g., D₃) leads to polysiloxanes with monodisperse chains; the reaction time for anionic polymerization is lower and the yield of polymerization improved. Finally using the AB diblock copolymers as macroinitiators, a cationic polymerization of 2-methyloxazoline leads to asymmetric ABC triblock copolymers.

As a model polymer we used an amphiphilic polyethylene oxide-*b*-polydimethylsiloxane-*b*-poly 2-methyloxazoline (PEO-*b*-PDMS-*b*-PMOXA) triblock copolymer. In aqueous solutions, this triblock copolymer self-assembles into well defined supramolecular aggregates. For certain compositions, the triblock copolymers form membrane like-superstructures and spherical vesicles in aqueous media. With the help of fluorescently labelled polymers, we were able to prove that the walls of these vesicles are asymmetric, due to the incompatibility between the hydrophilic chains: the blocks A and C are segregated on two different sides of the membrane.

In case of nanometer-sized vesicles where membrane-curvature plays an important role we were even able to achieve a control over the membrane orientation, i.e., which of the two hydrophilic block is at the inner and which at the outer surface. This seems to be mainly governed by steric considerations: generally the smaller hydrophilic blocks are forced to the inner side where less space is available.

Interestingly, the intrinsic asymmetry of the vesicular walls induced a directed insertion of transmembrane proteins. Using Aquaporin 0 as a model system we employed immunoassay, immunofluorescence and immunogold labelling, to quantify the amount and the orientation of these proteins in the walls of the asymmetric ABC-block copolymer vesicles. The results clearly show a direct correlation between the membrane orientation and the preferred direction of the proteins.

These studies indicate clearly that amphiphilic ABC triblock copolymers provide a convenient way to come to new materials with a directional functionality. Since they allow even a control over the orientation, they could allow to realize systems with a functionality that is reversed with respect to the biological model.

CHAPTER 10

FUTURE WORK

As a new block copolymer, a few properties of POE-b-PDMS-b-PMOXA triblock copolymer have been determined. The behavior of this polymer type in aqueous or non-aqueous solutions needs more studies.

Therefore, the following research is foreseen:

- Preparation of a series of block copolymers with different length of the central and tail blocks to establish the relationship between microstructure and physical properties
- Detailed investigation of alternative possibilities of synthesizing this polymers type by other synthetic approaches, other than anionic or cationic polymerisations (i.e. hydrosilylation, emulsion polymerization).
- Using those block copolymers as matrix for directed insertion of transmembrane proteins and find out A) what is the suitable composition for an optimum insertion of this proteins; B) the behaviour of particular classes of transmembrane proteins relative to a predetermined asymmetric matrix, C) whether the functionality of this proteins is not disturbed by the oriented insertion.
- Development of alternative applications within these amphiphiles (solubilization of inorganic compounds, e.g. carbon nanotubes; loading or binding to block copolymers weakly coordination metals or preparation of amphiphilic semiconductors or electrolytes, by replacement of hydrophobic or hydrophilic chains).

CHAPTER 11

EXPERIMENTAL SECTION

Yields are reported as the ratio between the weight of recovered polymeric material and the total weight of polymeric material.

Chemicals and Purification

Tetrahydrofuran (THF, C₄H₈O, F.W. 72.11 g/mol, b.p. 65-67°C, d. 0.889g/cm³) – RdH

Major impurities in THF include inhibitors, peroxides, and water. To remove these impurities, commercial THF (RdH 99,5%) was refluxed over sodium mirrors (Aldrich, 40 wt% in paraffin), under argon in the presence of benzophenone, until a bright deep purple color is attained. Pure THF was distilled from this deep purple solution immediately prior to use in a round-bottom flask containing fresh finely ground CaH₂ and next distilled over 3 Å molecular sieve.

Dichloromethane (CH₂Cl₂, F.W. 84.93 g/mol, b.p. 40°C, d. 1.325 g/cm³)

Dichloromethane (Merck, 99.8%) was washed several time with concentrated sulfuric acid until the sulfuric phase was no longer yellow, then washed several times with water to remove residual acid and pre-dried with anhydrous magnesium sulfate. Finally pure dichloromethane was distilled over calcium hydride (Fluka, 99.5%) under argon. Purified dichloromethane was stored under argon in a septum-capped container filled with a molecular sieve (3 Å).

Toluene (C₆H₅CH₃, FW 92.14 g/mol, b.p. 110.6°C, d. 0.867 g/cm³)

Toluene (Fluka, 99%) was washed twice with concentrated sulfuric acid at room temperature, then several times with water until neutral, predried with anhydrous magnesium sulfate and distilled over calcium hydride.

Hexane (C₆H₁₄, F.W. 86.18 g/mol, b.p. 69°C, d. 0.659 g/cm³)

Hexane (Fluka, 99.5%) was distilled over Na/benzophenone and further stored over molecular sieve under argon in a septum-capped container.

Ethyl acetate (C₄H₈O₂, F.W. 88.11 g/mol, b.p. 76-77°C, d. 0.900 g/cm³)

Ethyl acetate (Fluka, 99.5%) was stored over activated molecular sieve before use.

Ethanol (C₂H₅OH, F.W. 46 g/mol, b.p. 78°C, d. 0.807 g/cm³)

Ethanol (Fluka, 96%) was distilled over sodium and dipropionyloxybenzene mixture and kept under argon before use.

Triethyl amine ($C_6H_{15}N$, F.W. 101.19 g/mol, b.p. 89°C, d. 0.726 g/cm³)

Triethylamine (Fluka, 99.5%) was distilled over CaH₂, exposed to several sodium mirrors and finally distilled into ampoules under argon.

Lutidine (2,4-dimethyl pyridine) (C_7H_9N , F.W. 107.16 g/mol, b.p. 145°C, d. 0.923 g/cm³)

Lutidine (Fluka, 98%) was distilled over calcium hydride prior to use.

Molecular sieves (Fluka, UOP Type 3A-1/8'' rods, pore diameter 3 Å and UOP Type 4A, pore diameter 4Å°). Before use the sieves were activated at 200°C/0.5-1 torr for 48 hours.

12-Crown-4 ether ($C_8H_{16}O_4$, F.W. 176.22 g/mol, b.p. 68°C, d. 1.108 g/cm³, Fluka 98%) and **18-Crown-6 ether** (Fluka, 99%, $C_{12}H_{24}O_6$, F.W. 264.32 g/mol, m.p. 41°C) were used as received in p.a. grade.

Lithium hydride (LiH, F.W. 7.95 g/mol)

Lithium hydride (Riedel-de-Häen, 98%) has been dried under vacuum for 24h prior use.

Potassium hydride (KH, F.W. 40.11 g/mol)

Potassium hydride (Fluka, 35 % dispersion in mineral oil) was washed multiple times with dry THF until no color of the solvent could be detected. The powder obtained after washing was dried in a special glassware filter-ampoule under vacuum for 48 h before use. The presence of mineral oil residue has been checked by ¹H NMR / CDCl₃ after filtration of a sample into the NMR tube.

Trifluoromethansulfonic anhydride ($C_2F_6O_3S_2$, F.W. 282.14 g/mol, b.p. 82-85°C, d. 1.71 g/cm³). Triflic acid (Fluka, 98%) was used as received.

Ethyl trifluoromethane sulfonate ($C_3H_5F_3O_3S$, F.W. 178.13 g/mol, b.p. 115°C/760 Torr, d. 1.378 g/cm³)

Ethyl trifluoromethane sulfonate (Fluka, 98%) was used as received.

2-Methyloxazoline (C_4H_7NO , F.W. 85.11 g/mol, b.p. 110°C, d. 1.00 g/cm³)

Methyl oxazoline (Fluka, 98%) was stirred for 3h over calcium hydride and distilled from the heterogeneous mixture under argon. The monomer was kept into sealed ampoules under argon.

1,1',3,3',5,5'-Hexamethyltricyclosiloxane (D₃), (C₆H₁₈O₃SiO₃, F.W. 222.47 g/mol, F.p. 35°C (95°F), b.p. 134°C/760 mmHg)

Solid D₃ (Aldrich) was diluted in THF, stirred over CaH₂ overnight and then fractionally distilled under consecutive reduced pressure in argon atmosphere. The fraction of D₃ distilling at 132-136°C is collected into the same flask containing THF. The last flask is kept during all distillation at 0-5°C, in order to avoid the contamination of connection tubes or glassware being parts of the apparatus. The balloon containing D₃ solution in THF with a predefined concentration is kept under argon.

Octamethyltetracyclosiloxane (D₄), (C₈H₂₄O₄Si₄, F.W. 296.62 g/mol, m.p. 19°C, b.p. 175°C, d. 0.955 g/cm³); D₄ was distilled under reduced pressure over calcium hydride. Previously it has been stirred over CaH₂ overnight.

Methacryloxypropyldimethylchlorosilane (C₉H₁₇ClO₇, F.W. 220.77 g/mol, d. 1.012 g/cm³)

This terminating agent (Fluka, 85%) was degassed and used without further purification.

Poly(ethylene oxide) monomethyl ether (PEO), (Fluka, M_w: 1100 g/mol; 2000 g/mol; 5000 g/mol); PEO was freeze-dried from benzene solution. The remaining powder was dried for 48 hours before use.

Poly(dimethyl siloxane) bis(hydroxyalkyl) terminated (F.W. 5600 g/mol, d. 0.98 g/cm³)

The hydroxy terminated poly(dimethyl) siloxane polymer (Aldrich) was degassed for 24 hours under high vacuum, passed through a silica gel column and dried for 10 hours under high vacuum.

Preparation of triblocks (ABC type)

Preparation of poly(ethylene oxide) macroinitiator

a) In a typical synthesis, 1.3 g of KH (32.5 mM) was placed in a round-bottom flask under inert atmosphere. Anhydrous THF was added via a double-tipped needle, the resulting dispersion briefly stirred and then a 1/3rd of the corresponding total calculated amount of 18-crown-6 ether (6.3 mg, 2.39×10⁻² mM) added. To this heterogenous dispersion of potassium hydride in dry THF,

a solution of 6.2 g poly (ethylene oxide) monomethyl ether ($M_n = 2 \times 10^3$ g/mol, $M_n/M_w = 1.03$) in THF was added ($[PEO]_0 = 125$ g/L). The reaction mixture was stirred for ca. 12-24 hours at 25-35°C*. Subsequently, 1.2 mL of 2,6-dimethylpyridine (lutidine) was added dropwise (50 μ L/min) and stirred for another hour. The heterogenous dispersion became yellow-orange. After warming to the room temperature, the dispersion was transferred to another flask and the remaining 18-crown-6 ether (12.7 mg; 4.8×10^{-2} mM) was added.

All steps were carried over argon atmosphere. The resulting potassium alcoholate anion was used as an initiator for the anionic ring opening polymerization of octamethyltetracyclosiloxane.

Yield: 68%, conversion of hydroxyl groups 80%.

$^1\text{H NMR}$ (DMSO- d_6): $\delta = 3.36$ (s, 3H, $\text{CH}_3\text{-O-}$); 3.55-3.7 (s, $-\text{CH}_2\text{-CH}_2\text{-O-}$); before activation, the signal of hydroxy end groups appears at 4.57 (t, 1H, OH-).

FT-IR (KBr, cm^{-1}): 3490 ($\nu_{\text{O-H}}$ asymmetric), 2990–2790 (ν aliphatic C-H), 2820 ($\nu_{\text{ass}} \text{CH}_3\text{-O}$), 1467 ($\delta_s \text{CH}_2$), 1343 (δ_{OH}), 1097 ($\nu_{\text{as}} \text{C-O-C}$), 1115, 963, 841 ($\nu_s \text{C-O-C}$).

b) The activation of poly (ethylene) oxide by LiH is similar to the one described previously for KH. However, lutidine was not used anymore this time; the reaction time increases (from 12-24 hours to 24-36 hours); the 18-crown-6 ether quencher of K^+ ions has been replaced by 12-crown-4 ether quencher of Li^+ ions; the separation of the dispersion (LiH/ in PEO solution in THF) was carried out by means of a special filtration-apparatus using vacuum line (for the filtration of dispersion in a determined time).

The lithium alcoholate containing solution in THF was colorless in this case. The resulting lithium alcoholate anion was further used as an initiator for ring opening polymerization of hexamethyltricyclosiloxane.

Yield: 66%; conversion of hydroxyl groups 60%.

Polymerization of D_4 and D_3 cyclosiloxanes

a) Anionic ring opening polymerization of octamethyltetracyclosiloxane

To 4.2 g (2.1 mM) potassium alcoholate precursor described previously (5.4.1.a.) and kept under argon atmosphere, 18.7 mg, 63 mM of 4-ring member cyclosiloxane (D_4) was added in one quick shot (using a syringe) under argon atmosphere. The polymerization was carried out at 50-55°C for 20 hours. After the first 10 hours, the viscosity of homogenous medium increased; however, the increase of the stirring rate compensates the growing-chains mobility

*The variation of the heating temperature and stirring time is dictated by the solubility of the poly (ethylene) oxide chains: for a homopolymer with 110 units the solubility rate is lower in THF than for a chain of 25 units.

in the polymerized mixture. The chain growth was terminated by addition of 2.8 g (12.6 mM) methacryloyloxypropyldimethylchlorosilane. Immediately after addition of the terminating agent, salt formation was observed and the change of the reactions' color, indicating the presence of active centers and their disappearance. The stirring was maintained for another 5 hours.

The reaction mixture was centrifuged at 4 000 rpm for 20 min. The liquid was collected and the THF solvent evaporated. The oily product was dissolved in hexane, in order to precipitate the unreacted poly (ethylene) oxide monomethyl ether precursor. The precipitation, followed by centrifugation was repeated several times, until no solid phase was present after addition of n-hexane.

After hexane evaporation the mixture of AB-oligomers and polymers was obtained.

Yield: 40%.

1H NMR (CDCl₃, 400 MHz): δ = 6.09 ppm (CH₂=C<), 5.52 (CH₂=C<), 4.08 (-CH₂-CH₂-O-), 3.72 (-CH₂-CH₂-O-), 3.4 (CH₃-O-), 1.92 (CH₃-C=), 1.68 (-CH₂-CH₂-CH₂-O-), 0.55 (-Si(CH₃)₂-CH₂-CH₂-CH₂-), 0.067 (-Si (CH₃)₂-O-), 0.07 (O-Si(CH₃)₂-CH₂-).

^{29}Si NMR (CDCl₃, 500MHz): δ = -19.008 (D₄ cycle, unreacted), -21.453 (secondary product, oligomer), -21.896 (polysiloxane), -22.12 – 22.437 (D₅,D₆,D₁₀(?) side cycles).

FT-IR (KBr, cm⁻¹): 2990-2790 (v aliphatic C-H), 1719 (C=O), 1637.6 (C=CH₂), 1460 (δ_s CH₂), 1264 (δ_s Si(CH₃)₂-O), 1097-1020 (Si(CH₃)₂-O in polysiloxanes), 947, 850 (v_s C-O-C).

b) *Anionic ring opening polymerization of hexamethyltricyclosiloxane*

To 40 g (0.182 M) of lithium alcoholate prepared as previously (5.4.1.b.), solution of 100 g (0.449 M) D₃ in THF was introduced under argon. This step should be carried out rapidly and cautiously: D₃ monomer in THF solution has the tendency to crystallize if the concentration is too high or if the temperature is low (even below 25°C). On the other hand, the polymerization of this monomer is carried out at 0-5°C in order to avoid the side-products formation. The polymerization was pursued at the mentioned temperature for 24 hours. The same terminating agent as used in the polymerization of D₄ was used here. The reaction mixture was centrifuged, separated, evaporated and precipitated further like in the case of octamethyl tetracyclosiloxane. The mixture obtained after the last precipitation from hexane was turbid and viscous.

Yield: 30%.

$^1\text{H NMR}$ (CDCl_3 , 400 MHz): $\delta = 6.09$ ppm ($\text{CH}_2=\text{C}<$), 5.52 ($\text{CH}_2=\text{C}<$), 4.08 ($-\text{CH}_2-\text{CH}_2-\text{O}-$), 3.72 ($-\text{CH}_2-\text{CH}_2-\text{O}-$), 3.4 ($\text{CH}_3-\text{O}-$), 1.92 ($\text{CH}_3-\text{C}=>$), 1.68 ($-\text{CH}_2-\text{CH}_2-\text{CH}_2-\text{O}-$), 0.55 ($-\text{Si}(\text{CH}_3)_2-\text{CH}_2-\text{CH}_2-\text{CH}_2-$), -0.067 ($-\text{Si}(\text{CH}_3)_2-\text{O}-$), 0.069 ($\text{O}-\text{Si}(\text{CH}_3)_2-\text{CH}_2-$).

$^{29}\text{Si NMR}$ (CDCl_3 , 500MHz): $\delta = -8.194$ ppm (D_3 cycle unreacted), -19 (D_4 cycle, side product), -20.7 (secondary product, oligomers), -21.25 –21.43 (D_5 , D_6 side cycles), -21.859 (polysiloxane chain).

Poly(ethylene) oxide-b- poly(dimethyl) siloxane copolymers

a) POE-b-PDMS ester terminated chains were purified using column chromatography. 15 g of silica gel 6 (Fluka, pore size 230-400 mesh) was added to the dichloromethane solution of block copolymer (5g/mL) and unreacted homopolymers under stirring. The solvent (dichloromethane) was evaporated to obtain the polymer-coated silica gel as dry powder, which was added to the top of a chromatographic column (diameter 17 cm, filled with 25 cm silica gel in toluene). The elution started with toluene, fractions of 200 ml were collected. The solvent was replaced by a mixture of THF/MeOH 8:2 (v:v) to yield pure PEO-PDMS-ester diblock copolymer followed by unreacted PEO.

Compositions of fractions were checked by $^1\text{H NMR}$.

Yields of pure diblock copolymers were about 10%.

- a) An additional purification step was carried out using ultrafiltration from a diluted ethanol/water solution (0.5 g/mL) of the PEO-PDMS samples, to assure that the unreacted PEO and monomeric cycles have been removed during the chromatographic separation. The ultrafiltration was carried out using a 300 mL ultrafiltration module (Millipore, 76 mm diameter) and ultrafiltration (UF) membranes from regenerated cellulose, with a molecular cut off between 1000- 5000 g/mol, under stirring at 3-bar pressure.

After ultrafiltration, the product was lyophilized from the water/ethanol mixture and dried under vacuum for 24 hours.

Reduction of AB-diblock copolymer: hydroxyl function

For the cationic ring opening polymerization of 2-methyl oxazoline, one needs a hydroxy group “spaced” from the rest of the chain by an alkylene bridge.

The AB diblock copolymer has an unsaturated ester at one end of the chain. Using the Bouveau Blanc reduction of esters¹⁷¹ (Na (in toluene)/EtOH), the AB diblock copolymer was successfully converted in a hydroxy-end terminated diblock copolymer. The methods of Schlesinger (via LiAlH₄) or basic hydrolysis were unsuccessful.

An excess of sodium (20% above stoichiometric requirement; relative to the quantity of diblock copolymer used for reduction) was placed into a sealed three-necked flask in toluene under argon atmosphere. The sodium mirror was heated to 120°C, without stirring. The purpose of stirring after melting the sodium is production of finely dispersed sodium particles. After melting of sodium, the heating bath is removed and the mixture is allowed to cool to 50°C. Stirring must be continued during the cooling in order to keep sodium finely divided. After cooling to 50°C, a solution of unsaturated AB copolymer in absolute ethanol (2 g/mL), then more alcohol was added very rapidly (ca. 2 min.). After 20 hrs, the mixture was steam distilled to remove toluene and ethanol. The content of the flask was transferred to a separator funnel while still hot and washed 3 times with 200 mL of hot water. The obtained AB-hydroxy terminated was extracted with diethyl ether from the washings. The combined ether extracts were washed with water, 1N sodium carbonate solution, again with water and dried over magnesium sulfate, followed by evaporation of ether and the distillation of alcohol under reduced pressure.

Yield: 31%, conversion 98%.

¹H NMR (CDCl₃, 400 MHz): 3.8 (-CH₂-CH₂-OH), 3.72 (-CH₂-CH₂-O-), 3.4 (CH₃-O-), 1.8 (-CH₂-CH₂-CH₂-O-), 0.54 (-Si(CH₃)₂-CH₂-CH₂-CH₂-), 0.05-0.07 (-Si (CH₃)₂-O-), 0.07 (O-Si(CH₃)₂-CH₂-). The complete disappearance of the olefin protons (5.3 and 6.09 ppm) proves the conversion of the unsaturated ester to the corresponding alcoholic functional groups.

FT-IR (KBr, cm⁻¹): 3450 (ν O-H_{ass}), 2990-2790 (ν aliphatic C-H), 1452 (δ_s CH₂), 1220 (dband, δ_s -Si(CH₃)₂-O), 947, 850 (ν_s C-O-C).

Attachment of block C: polymerization of methyl oxazoline

The polymerization of methyl oxazoline was done according to a literature procedure¹⁷². Anhydrous conditions are required.

1.3 g (0.19 mM, M_{w(AB)} = 6810 g/mol) AB-diblock copolymer in hexane were added by Soxhlet extractor filled with molecular sieve (3 Å) for 20 hours in argon atmosphere. Subsequently, the solution was concentrated, cooled to 0°C and 76.8 mg (0.76mM) triethyl amine was added. After 3 hours of stirring, 0.1 mL (0.703 mM) trifluoromethansulfonic anhydride was added within 15 minutes and the mixture was stirred for 1 hour at 0°C. After a new addition of dry hexane to

improve the solubility of activated macroinitiator, the suspension was filtered under vacuum using a G4 glass filter funnel and then evaporated at high vacuum (0.6-2 mbar). The evaporation of the solution gives yellowish oil.

$^1\text{H NMR}$ (CDCl_3 , 400 MHz): $\delta = 0.057$ ppm ($\text{CH}_3\text{-Si}$); 0.55 ($-\text{CH}_2\text{-CH}_2\text{-Si}-$); 1.85 ($-\text{CH}_2\text{-CH}_2\text{-CH}_2-$); 4.4 ($\text{CF}_3\text{SO}_3\text{-CH}_2\text{-CH}_2-$), 3.72 ($-\text{CH}_2\text{-CH}_2\text{-O}-$), 3.4 ($\text{CH}_3\text{-O}-$).

To this oil solution in dichloroethane 2-methyl oxazoline was added. After stirring the solution for 2 hours at room temperature, the temperature was increased to 45°C. After 48 hours, the solution was cooled to room temperature and 0.5N KOH/EtOH solution was added. This solution was stirred for one hour and subsequently the solvent evaporated at high vacuum. The colorless solid obtained was further dissolved in a 1:1 (v:v) EtOH/water solution, centrifuged to remove the homopolymer of polyoxazoline and ultrafiltrated until a concentrated solution of polymer was obtained.

Yield: 35 %.

$^1\text{H NMR}$ (Figure 5.1), (CDCl_3 , 400 MHz): $\delta = 0.057$ ppm (s, $\text{CH}_3\text{-Si}$), 0.55 (m, 4H, CH_2), 1.56 (m, 4H, CH_2), 2.0-2.2 (m, $\text{CH}_3\text{-CON}<$), 3.3-3.5 (s, $>\text{N-CH}_2\text{-CH}_2\text{-N}<$), 3.74 (m, $\text{CH}_2\text{-CH}_2\text{-O}$).

FT-IR (KBr, cm^{-1}): 3453 (δ O-H), 2990-2790 (ν aliphatic C-H), 1734 (C=O), 1418 (δ_s CH_2), 1260 (dband, δ_s $\text{Si}(\text{CH}_3)_2\text{-O}$), 1020 ($\text{Si}(\text{CH}_3)_2\text{-O}$ in polysiloxanes), 800, 702.5 (ν_s C-O-C).

Synthesis of ABA triblock copolymers

The synthesis of the symmetric ABA triblock copolymer used further as a reference in the experiments concerning the protein insertion was performed in a similar manner as described in section 5.3.5. The polydimethyl siloxane macroinitiator used had two hydroxyl-end terminated groups, both modified with triflic acid. In a 250 mL round bottom two-necked flask with a Soxhlet extractor filled with a molecular sieve (4 Å) and equipped with condenser and a septum on the second joint, 24.25 g (4.33 mM) α,ω -bis(3-hydroxypropyl)-polydimethylsiloxane, $M_n = 5600$ g/mol) were dissolved in 100 mL hexane and distilled under reflux for 17 hours in argon atmosphere. Subsequently, the solution was concentrated to 100 mL, cooled to 0°C and 1.3 g (12.9 mM) triethylamine were added. Then 3.79 g (15.15 mM) trifluoromethanesulfonic acid anhydride was added over 20 minutes and the mixture was stirred for another 30 minutes at 0°C. The suspension was filtered under vacuum using a G4 glass filter funnel and evaporated. 15.4 g (0.18 M) methyl oxazoline and 22.3 g of the macroinitiator were added to 50 mL 1,2-dichloroethane at room temperature. After stirring the solution at room temperature for 30

minutes, the temperature was increased to 40°C. After 48 hours, the solution was cooled at room temperature and 15.5 mL 0.5 N KOH/MeOH were added. After evaporation of the solvent and purification by ultrafiltration, a white glassy solid was obtained.

Yield: 80 %.

¹H NMR (Figure 5.2), (CDCl₃, 400 MHz): δ = 0.07 ppm (s, CH₃-Si, A), 0.52 (m, 4H, CH₂), 1.59 (m, 4H, CH₂), 2.14 (m, CH₃-CON<), 3.45 (s, >N-CH₂-CH₂-N<), 3.87 (m, CH₂-).

FT-IR (KBr, cm⁻¹): 3453 (δ O-H), 2963 (ν aliphatic C-H), 1634 (s, C=O), 1418 (δ_s CH₂), 1260 (δ_s Si(CH₃)₂-O), 1021 (Si(CH₃)₂-O in polysiloxanes), 800 (s, Si(CH₃)₂), 702 w.

Synthesis of Poly(methyl) oxazoline

The homopolymer was used as control for ¹H NMR, DSC measurements. Polymerization was performed in dried chloroform. Ethyltrifluoromethane sulfonate was cautiously added to the solvent and then methyl oxazoline was introduced in the initiator solution. The polymerization time was 48 hours and temperature 55°C. Polymerization has been terminated using a 0.5N solution KOH/MeOH. After the evaporation of the solvent, the polymer was precipitated in ethyl ether from a very concentrated solution of chloromethylene.

The molecular weight of polymers can be varied by the amount of initiator and monomeric cycle. Yield: 90%.

¹H NMR: 2.17-1.94 (m, CH₃-CON<), 3.45 (s, >N-CH₂-CH₂-N<), 1.19 ((C₂H₅)₂O), 3.75 (m, CH₂-O).

Synthesis of labelled triblock copolymers

Synthesis of 7-methoxy coumarine labelled polymers

Polymer labelling was necessary for visualization/quantification of block segregation in vesicles. 7-methoxycoumarin-3-carbonyl azide (Molecular Probes, M.W. 245.19 g/mol) was used without further purification. Standard solutions of triblock copolymer (38 mg/mL CH₂Cl₂ for POE₄₅PDMS₆₇PMOXA₃₄₆ triblock copolymer and 7.5 mg/mL CH₂Cl₂ for POE₄₅PDMS₄₀PMOXA₆₇ triblock copolymer) and reagents (25 mg/mL coumarin azide) were prepared. A mixture of each of the triblock copolymers with the corresponding solution of coumarin azide was heated at 80°C for 90 minutes. The product obtained was verified by TLC plates (K6 silica gel) in toluene: ethyl acetate (4:1). The bright blue fluorescent spot near the top of the plate (r_f = 0.9) was visualized by UV long exposure. The product was eluted from silica gel

with 2 mL isopropanol and further studied by ^1H NMR. The product obtained was purified from ethanol solution by ultrafiltration. The permeate was constantly checked by UV- Vis and conductivity measurements (the conductivity value should be identical as the one for pure water (1.1 $\mu\text{S}/\text{cm}$, at 20°C)). When no traces of free coumarine derivative could be detected, the ethanol was evaporated under high pressure. The conversion of hydroxy groups was 28% for $\text{POE}_{45}\text{PDMS}_{67}\text{PMOXA}_{346}$ (6% POE; 13% PDMS; 81% PMOXA) and 12% for $\text{POE}_{45}\text{PDMS}_{40}\text{PMOXA}_{67}$ (16% POE; 22% PDMS; 62% PMOXA) triblock copolymers.

^1H NMR (CDCl_3 , 400MHz): δ = 0.06 ppm (s, $\text{CH}_3\text{-Si}$); 0.55 (m, 4H, CH_2); 1.56 (m, 4H, CH_2); 2.0-2.2 (m, $\text{CH}_3\text{-CON}<$); 2.7 (broad m, NH-); 3.3-3.5 (s, $>\text{N-CH}_2\text{-CH}_2\text{-N}<$); 3.72 (m, $\text{CH}_2\text{-CH}_2\text{-O-}$); 3.85 (s, O-CH_3); 6.77-6.85 (2H, m, C_6 and $\text{C}_8\text{-H}$); 7.5 (1H, d, $\text{C}_5\text{-H}$); 8.4 (1H, s, $\text{C}_4\text{-H}$).

Synthesis of 5-DTAF labelled polymers

5-(4,6-dichlorotriazinyl) aminofluorescein (DTAF) – single isomer dye was purchased from Molecular Probes (M.W. 495.28 g/mol) and was used without further purification.

The conjugation of asymmetric triblock copolymer with a fluorescein derivative was proceeded at room temperature under aqueous conditions, according to a literature procedure¹⁷³.

Stock solutions of 5 w/v % triblock copolymers ($\text{POE}_{25}\text{PDMS}_{80}\text{PMOXA}_{285}$ and $\text{POE}_{25}\text{PDMS}_{19}\text{PMOXA}_{110}$) were prepared by dissolving the polymers in 0.1M sodium bicarbonate solution at $\text{pH} \approx 9.5$. A stock solution of 20 g/L of 5-DTAF was prepared by dissolving the fluorescein in dimethyl sulfoxide. The 5-DTAF solution was diluted in 0.1M sodium bicarbonate solution and added to triblock copolymers solution so that the molar ratio triblocks:DTAF was 5:1. The reaction has been allowed to proceed in the dark at room temperature for 10 hours.

Ultrafiltration of the solution mixture from a concentrated solution of dimethyl formamide was unsuccessful: traces of unconjugated fluorescein derivative being present in the product mixture. A second assay for purification was done using size exclusion chromatography on Sephadex G-50 with 1x10 cm columns, in dark, to avoid the photobleaching of the fluorescent tag. The eluent was 0.05 M sodium chloride. The column effluents were collected and further concentrated using Centricon centrifugal filter devices (Millipore Corp.) with a molecular cutoff of 3000 Daltons. The overall labelling efficiency of triblock copolymers was small, ca. 0.3%.

^1H NMR (CDCl_3 , 400MHz): δ = 0.06 ppm (s, $\text{CH}_3\text{-Si}$); 0.55 (m, 4H, CH_2); 1.56 (m, 4H, CH_2); 2.0-2.2 (m, $\text{CH}_3\text{-CON}<$); 2.7 (broad m, NH-); 3.3-3.5 (s, $>\text{N-CH}_2\text{-CH}_2\text{-N}<$); 3.64-3.72 (m, $\text{CH}_2\text{-CH}_2\text{-O-}$); 4.88 -shifted (m, ring- $\text{O-CH}_2\text{-CH}_2\text{-N}$); 6.24-7.26 (aryl protons, undetectable).

Synthesis of tetramethyl rhodamine-5-carbonyl azide labelled polymers

The rhodamine conjugated PEO₂₅PDMS₈₀PMOXA₂₈₅ and PEO₂₅PDMS₁₉PMOXA₁₁₀ triblock copolymers were synthesized by employing a modified version of an existing procedure¹⁷⁴.

20 mg of triblock copolymers and 10 mg tetramethylrhodamine-5-carbonyl azide were dissolved in 10 mL of freshly distilled toluene under argon atmosphere. After heating at 80°C for 8 hours, the reaction mixture was diluted with dimethyl formamide and ultrafiltered over membranes with molecular cutoff 3000 Da, until no traces of rhodamine in the permeate could be detected by ¹H NMR. Then, the ultrafiltration solution was changed with bidistilled water in order to remove any organic solvent. The residual aqueous solution has been freeze-dried. The rhodamine conjugated block copolymers were obtained in 20% yield.

¹H NMR (CDCl₃, 400MHz): δ = 0.06 ppm (s, CH₃-Si); 0.51 (m, 4H, CH₂); 1.25 – ethanol traces; 1.53 (s, 6H, =N⁺(CH₃)₂); 1.98-2.14 (m, CH₃-CON<); 2.95 (s, -N(CH₃)₂); 3.45 (m, >N-CH₂-CH₂-N<); 3.64-3.74 (m, CH₂-CH₂-O-); 4.88 -shifted (m, ring-O-CH₂-CH₂-N); 6.37-8.28 (aryl protons of rhodamine molecule).

Characterization techniques

¹H NMR

All ¹H NMR spectra were obtained on a Varian Unity 400 NMR spectrometer; the NMR instrument was operated (with 5 mm multinuclear probe) at 400 MHz with a sweep width of 8278.146 Hz and a 22° pulse width of 2.96 μs. For simple compounds, CDCl₃ was used as solvent and sample concentrations were in the range of 1-10 wt.%. For end group detection, CDCl₃ was used as solvent, but the sample concentrations were increased to 20-30-wt % to improve the signal-to- noise ratio of the end groups.

²⁹Si NMR

All ²⁹Si NMR spectra were collected on a Bruker 500 NMR spectrometer operated at 99.36 MHz with a spectral width of 9920.35 Hz, 90° pulse with a width of 13.6 μs.

Samples were dissolved in deuterated chloroform and sample concentrations were in the range of 10-20 wt%. The parameters' optimization has been enough to allow very good detection and resolution. During experiments, the relaxation delay was set to five times as large as T₁ (spin-lattice relaxation time).

Gel Permeation Chromatography (GPC)

Gel permeation chromatography experiments were done with a Dionex Instrument with a set of three PL gel mixed-D (5 μm x 300, Polymer Laboratories) columns at 20°C with a flow rate 1mL/min. A refractive index detector (Viscotek Laser Refractometer) was used for signal detection. Other experiments have been carried out using an Agilent Technologies GPC Instrument with a ODS Hypersil column (5 μm). Here, a refractive index detector and the UV-Vis detector were linked in parallel for detection. Polystyrene standards were used to establish a universal calibration curve. The regression curve had 10 points, with the correlation coefficient of 0.99920.

Samples were prepared by dissolving 20-40 mg in 10 mL HPLC grade THF or chloroform. Sample solutions were filtered through a 0.45 μm filter before loading into the GPC autosampler.

Infrared Spectroscopy (IR)

IR spectra were acquired on a Nicolet Impact Fourier transform infrared spectrometer. Potassium bromide plates were used as sample holders.

MALDI-TOF spectrometry (Matrix-Assisted Laser Desorption/ Ionization Mass Spectroscopy – Time of Flight)

Spectra were recorded on a Voyager-DE Pro instrument (Perseptive Biosystems). The irradiation source was a pulsed nitrogen laser with a wavelenth of 337 nm. The length of one laser pulse was 1ns. The measurements were carried out using the following conditions: polarity-positive mode, flight path-linear, mass-high (15 kV acceleration voltage), 150 –300 pulses per spectrum. The delayed extraction technique was used applying the delay time of 300 ns. The matrix dihydroxybenzoic was added coaxially on a MALDI TOF targets (2 μL into a gold plate).

Differential Scanning Calorimetry (DSC)

Differential scanning calorimetry was performed using a Mettler Toledo instrument and aluminium crucibles. Samples (19-20 mg) were quickly quenched to liquid nitrogen temperature and then scanned from –130°C to 150°C, at the rate of 10°C/min. Each sample was scanned twice and no obvious differences were found between the first and the second scan.

Light Scattering Measurements

Dynamic and static light scattering experiments were performed using a commercial goniometer (LALV-Langen) equipped with a frequency-doubled Nd:YAG laser (ADLAS, wavelength $\lambda = 632.8$ nm) at scattering angles between 30° and 150° . An ALV-5000/E correlator calculates the photon intensity autocorrelation function $g^2(t)$.

Samples were prepared by filtering the solutions through Millipore filters ($0.45\mu\text{m}$) into 10 mm cylindrical glass cells. These cells were mounted in a thermostated optical matching with a temperature accuracy of $T = \pm 0.02$ K. The experiments were performed at $T = 293\text{K}$.

For SLS measurements, a mathematical model described in reference 8a. was used. c_{ac} was determined following this model.

Transmission electron microscopy (TEM) and phase contrast microscopy (PC)

TEM was done with a Philips EM 400 operated at 80 kV. Images were taken using the Morgani 268D software, with a magnification of $\times 44\ 000$. $2\ \mu\text{L}$ of the vesicle dispersion were brought onto a 400 mesh copper TEM grid, shadowed previously with W/Ta at angle of 30° . The samples were negatively stained with 2% uranyl acetate solution and allowed to dry in air before analysis. Images in phase contrast analysis (Ph3) were acquired with a Zeiss Axiophot microscope, with a 100x10 objective – ocular. Images have been taken using a CCD camera. $10\ \mu\text{L}$ of the dispersion of giant vesicles were analysed.

Critical Micelle Concentration

Surface tension γ of the vesicles dispersions was determined with a Krüss K8 Interfacial Tensiometer with a platinum-iridium ring of radius 9.545 mm and $R/r = 51.6$ at 25°C . The surface tension was measured by Du-Nuöy-ring method. The critical aggregation concentration (c_{ac}) of the triblock copolymer dispersions was deduced from the discontinuity in the γ ($\ln c_{\text{polymer}}$) curve.

Fluorescence spectroscopy

The fluorescence experiments were carried out with a spectrofluorimeter Jasco F-P-773 in a 1×0.4 cm cuvette. Excitation and emission wavelengths were 335 and 350 nm, respectively and slits were 5 nm for both excitation and emission.

Quenching experiments

The decrease of fluorescence signal was recorded for different concentrations of aqueous solution 1M CoCl₂:

- Control experiments (0.55 wt% PEO₄₅PDMS₆₇PMOXA₃₄₆): 0.02M, 0.07M, 0.25M CoCl₂ solution
- Long PMOXA chains (labeled –unlabeled mixtures): 10mM to 400 mM 1M Co²⁺ ions solution
- Short PMOXA chains (labeled-unlabeled mixtures): 10 mM to 500 mM 1M Co²⁺ ions solution

A control experiment established the fluorescence intensity of the vesicles formed by non-labeled copolymers.

Fluorescence Microscopy

Fluorescence microscopy images were been acquired with a Zeiss Axiophot microscope with a 100x/1.3 oil plan neofluar Ph3 objective. The images were taken using a CCD camera, using phase contrast and differential interference contrast (DIC) techniques. 10 μL of the dispersion of labeled giant vesicles was deposit between two microscopy slides and the system was analyzed. The fluorescent background was removed by filtration of the vesicle dispersion on mini-columns (1 x 5 cm) over Sephadex G100, at 2500 rpm.

Confocal fluorescence microscopy images were taken with a Leica TCS-NT/SP1 in confocal optical mode with 63x/1.32-0.60 oil plan apochromat objective in FITC (excitation: 450 - 490 nm, emission: 515 nm) fluorescence mode. The optical sections, collected from out-of-focus fluorescence from adjacent layers have been projected to give a 3D image of the vesicular structures.

Langmuir Surface-Pressure Isotherms

For surface pressure-area measurements, a thermostated KSV Minithrough (364x75 mm, from solid PTFE) was used. Surface pressure was measured by the Wilhelmy plate method, with Whatman filter paper as sensor and at a barrier speed of 10 mm/min. Concentration of polymers in chloroform solution was 1g/mL and the spreading volume 100 μL.

Furthermore, the polymers were spread from chloroform solution (1mg/mL) on a Nima Langmuir through (1200 cm²) filled with ultra pure water. After at least 20 minutes the surface area/pressure isotherms were recorded with a compression rate of 100 cm²/min (using two independent barriers

which allow a symmetrical compression of the monolayer). The protein (LamB protein) was injected with a microsyringe directly to the PBS subphase. Measurements were started 30 minutes after.

Protein insertion studies: Langmuir-Blodgett monolayers experiments

The monolayers experiments were similar to the ones described in Chapter 6. Aquaporin 0 protein in n-decyl-maltoside detergent was used.

Vesicle Preparation

Unilamellar vesicles from ABC triblock copolymers were obtained as follows: the triblock copolymer was dissolved in ethanol to yield a clear homogenous solution containing 12-wt% of polymers. This solution was added drop-wise to the corresponding volume of doubly distilled water (5-wt% polymer) under vigorous stirring. The vesicles were filtered repeatedly through Nucleopore filters (Millipore, 2 x 0.45 μm , 2 x 0.22 μm , 3 x 0.1 μm if filtration still possible).

Giant vesicle preparation

Giant vesicles were prepared by electro-formation. 1 mL of 1% triblock copolymer solution in CHCl_3 :MeOH (9:1) were homogeneously added under nitrogen stream on a conductive ITO (indium tin oxide) electrode to form a uniform film. This film was phoresed from the electrode by an alternating current (AC) into the aqueous solution or PBS buffer solution (phosphate buffer, pH 7.4). AC voltage was 5V at 10 Hz for 2 hours, followed by 30 minutes at 5V and 5 Hz. Phase contrast microscopy investigations indicated that the resulting dispersion contained giant vesicles with diameters between 1 and 2 μm .

Labelled vesicle preparation

For quenching experiments labelled (PEO₄₅PDMS₆₇PMOXA₃₄₆-7-methoxycoumarin and PEO₄₅PDMS₄₀PMOXA₆₇-7-methoxy coumarin) with the corresponding non-labelled polymers (PEO₄₅PDMS₆₇PMOXA₃₄₆ and PEO₄₅PDMS₄₀PMOXA₆₇, respectively) in molar ratios of 300:1 and 10:1. From these mixtures, vesicles were prepared following the procedure described. The variation in vesicle diameter was followed by dynamic light scattering.

Labelled giant vesicles preparation

As described in Chapter 6, labelled giant vesicles were prepared by electro-formation, using 1 ml solution of 1% triblock copolymer mixture: the mixture is formed by non-labelled ABC triblock copolymer and labelled triblock copolymer in a molar ratio of 350:1 in CHCl₃:MeOH (9:1). Confocal fluorescence microscopy investigations indicated that the resulting dispersion contained fluorescent giant vesicles with diameters between 1 and 4 μm .

Preparation of triblock copolymer vesicles for experiments - Chapter 8

The polymer was dissolved in ethanol and then sonicated to yield a clear, homogeneous solution containing 30-wt % polymers. The solution was added dropwise to a PBS buffer solution under vigorous stirring. The resulting vesicle dispersion (3% polymer, respectively) was equilibrated for 12h at room temperature. The vesicles size was adjusted by several extrusion cycles through 0.45 μm and 0.22 μm Nucleopore filters (Millipore). Vesicles containing AQP-0 were prepared by injecting a stock solution of the purified protein (1.6 mg/mL, 0.4 % n-decyl- β -maltoside, 150 mM NaCl, 50 mM KH₂PO₄ pH 8.0) simultaneously with the 30% ethanol-polymer solution into the PBS buffer. Non-incorporated proteins and detergent were removed by gel filtration chromatography using a Sepharose 4B (SIGMA) column. Incorporation of intact protein was monitored by polyacrylamide gel electrophoresis. Molar ratio of triblock copolymers to AQP-0 of about 5×10^3 was kept constant throughout all experiments.

Preparation of lipid vesicles

20 mg of a lipid (Egg-phosphatidylcholine from SIGMA, purity > 99%) in chloroform stock solution of 10 mg/mL was dried under reduced pressure using rotary evaporation at 40°C. To remove the last traces of chloroform, the lipid film was further dried under high vacuum for 12h at room temperature. To obtain protein-containing vesicles, 50 μl of the 1.6 mg/mL stock solution of AQP-0 was added to the film and then vortexed to yield a homogeneous mixture, which was dried for a short period under vacuum. The dry mixed lipid/protein film or the pure lipid film, respectively, were dispersed in 2 mL of PBS buffer solution. This yields a dispersion containing multilamellar, polydisperse proteovesicles or vesicles. A freeze-thaw cycle was applied to the dispersion consisting of five cycles of freezing in liquid nitrogen and thawing in a water bath at 30°C. Finally, the dispersion was repeatedly extruded through polycarbonate filters (Nucleopore filters (Millipore)) with a pore size of 0.45 μm and 0.22 μm to obtain unilamellar vesicles of rather uniform size.

Expression and purification of Aquaporin 0 (AQP-0)

Aquaporin-0 was expressed in *S. Cerevisiae* strain BY 4732, a S288C derivative owing the genotype: MAT α *his3* Δ 200 *met15* Δ 0 *trp1* Δ 63 *ura3* Δ 0. The strain was transformed using 2 μ l of the plasmid pYES2 multicopy which codes for Aquaporin-0. AQP-0 expression and purification were performed by F. Casagrande. (*Biocenter, University of Basel*) following a procedure described in literature¹⁸⁴.

Aquaporin–Antibody–Horseradish peroxidase (HRC) conjugate assay

To quantify the amount of incorporated AQP-0 in ABC, CBA, ABA and lipid vesicles we used an antibody directed against the AQP-0 specific His-tag sequence. The anti-His antibody has a very high binding affinity so that dissociation of the antibody from His-Tag vesicles can be excluded during gel filtration. Here we used an antibody (Anti-His HRP Conjugates (Qiagen, AG)) coupled to horseradish peroxidase (HRP). The enzymatic activity of this enzyme was used to quantify antibody binding.

As a calibration standard in the concentration range from 4 ng/mL to 80 μ g/mL we used 9 well-defined dilutions of detergent solubilized Aquaporin 0 in phosphate buffer.

The Anti-His HRP Conjugate stock solution was diluted to 1/100 with PBS/blocking reagent buffer as recommended by the supplier. AQP-0 was then incubated with a 1/2000-antibody dilution at 4°C (i.e., an excess of antibody according to the protein-antibody saturation curve).

After 10 h of incubation, the samples were purified by gel filtration chromatography Sepharose 4B to remove the non-attached antibodies. Here we used PBS buffer containing 0.2 % Bovine Serum Albumin (BSA) to prevent non-specific binding of the antibody. After purification, the samples were incubated with 3,3',5'-trimethylbenzidine (TMB, Sigma), as a substrate for horseradish peroxidase. The enzymatic reaction was stopped after 90 seconds by diluting the vesicle dispersion to twice the original volume with 5M HCl. The resulting yellow product is stable for more than one hour, which allowed determining its absorbance at 450 nm using a Hewlett-Packard 8452A spectrophotometer.

The same procedure was applied to the AQP-0 containing vesicles made of ABC, ABA triblock copolymers and lipids. Control measurements with protein-free ABC, ABA and lipid vesicles indicated no unspecific binding between the triblock copolymer or lipid membranes and Anti-His HRP Conjugates.

To determine the total amount of AQP-0 in the vesicles we added the detergent octyl-POE up to a concentration of 3-wt % and treated the solution for approximately 2 minutes in an ultrasonic

bath. Dynamic light scattering clearly indicated that under these conditions the vesicles had been solubilized, i.e., only detergent micelles were present in the mixture. Afterwards the samples were incubated with the antibody as described above.

Immunofluorescence assay

Penta His Alexa Fluor 555 Conjugates (Qiagen) allow highly sensitive and specific direct detection of His tagged proteins. For the proteovesicles formed by the different amphiphiles we applied the same incubation procedure as described above. For that purpose the antibody Alexa Fluor 555 conjugate was diluted in PBS –IF buffer (100 mM Na₂HPO₄ 2H₂O; 1.4 M NaCl; pH 7.4) (diluted to 1/50 of the antibody stock solution).

The buffer for antibody dilution additionally contained 1% (w/v) BSA (Fluka) in PBS-IF buffer. It has to be noted that for these experiments we optimized again the concentration of the antibody stock solution, blocking reagent and the incubation times. The unattached antibodies were chromatographically removed using gel permeation chromatography on a Sepharose 4B column in presence of bovine serum albumin (BSA). The BSA blocks the unspecific sites of the antibodies; the number of unspecific interactions decreases.

Fluorescence experiments were carried out with a spectrofluorimeter Jasco F-P-773 in a 1x 0.4 cm cuvette. The excitation wavelengths had been set to 450 nm and slits were 5 nm for excitation and 10 nm for emission, respectively.

The fluorescence of the pure antibody commercial solution served as a standard.

Immunogold assay

The polymer, lipid proteovesicles and vesicles were incubated for 30 min with 5µl of a 5µg/mL primary anti-mouse anti-His antibody (Qiagen) in PBS/0.2% BSA solution directly on the microscopy grids. The presence of Bovine Serum Albumin (BSA) solution was necessary to prevent unspecific binding of the antibody to hydrophobic areas or domains with excessive positive charges based on multiple point interactions. The grids were rinsed with 0.2% BSA-PBS. Afterwards the grids were incubated for 60 min. with GAM IgG 6 nm secondary gold-labeled antibody (Aurion) solution, diluted to 1/50 with PBS/2%BSA. The grids were rinsed with PBS buffer (3 times for 5 minutes) and finally with distilled water. The samples were analyzed by Transmission Electron Microscopy (Philips EM 400). As a negative control we incubated protein-free vesicles using the same procedure as described above. A quantification of the amount of inserted protein turned out to be difficult since the stock solution of the gold-labeled antibody contained a considerable amount of non-labeled antibody.

REFERENCES

1. Tandford C., *Science*, 200, 1012-1018, 1978
2. Hamley I. W., *Angew. Chem. Int. Ed. Engl.*, 42, 1692, 2003
3. Menger F.M., Angelova M. I., *Acc. Chem. Res.*, 31, 789, 1998
4. Bangham A.D., *Chem. Phys. Lipids*, 64, 275, 1993
5. Sharma A., Sharma U.S., *Intern. J. Pharmaceutics*, 154, 123, 1997
6. Barenholz Y., *Curr. Opin. Colloid Interface Sci.*, 6, 66, 2001
7. Förster S., Antonietti M., *Adv. Mat.*, 3, 195, 1998
8. a. Nardin C., Hirt T., Leukel J., Meier W., *Langmuir*, 16, 1035, 2000; b. Zhang L., Eisenberg A., *Science* 268, 1728, 1995; c. Yu K. Eisenberg A., *Macromolecules* 31, 3509, 1998; d. Regenbrecht M., Akari S., Förster S., Möhwald H., *J. Phys. Chem. B*, 103, 6669, 1999; e. Moffit M., Khougaz K. Eisenberg A., *Acc. Chem. Res.*, 29, 95, 1996; f. Shen H., Eisenberg A., *J. Phys. Chem. B.*, 103, 9473, 1999; g. Maskos M., Harris J. R., *Macromol. Rapid Comm.*, 22, 271, 2001; h. Yu Y., Zhang L., Eisenberg A., *Macromolecules*, 31, 1144, 1998; i. Alexandris P., *Curr. Opin. Colloid Interface Sci.*, 1, 490, 1996
9. Won Y.Y., Ege D.S., Lee J.C.M, Bates F.S., Discher D.E, Hammer D.A., *Science*, 284, 1143, 1999
10. Discher B M., Hammer D. A., Bates F. S., Discher D. E., *Curr. Opin. Colloid Int. Sci*, 5, 125, 2000
11. Ko M.J., Kim S.H., Jo W.H., *Macromol. Theory Simul.*, 10, 381, 2001; Lee J., Bermudez H., Discher B., Sheehan M., Won Y.Y., F. Bates, D. Discher, *Biotechnol. Bioeng.*, 73, 135, 2001; Förster S., Plantenberg T., *Angew. Chem.*, 41, 688, 2001
12. Förster S., Antonietti M., *Adv. Mat.*, 15, 1323, 2003
13. Won Y.Y., Davis A. T, Bates F. S., *Science*, 283, 960, 2002; 8a.
14. a. Meier W., Nardin C., Winterhalter M., *Angew. Chem. Int Ed.*, 39, 4599, 2000; b. Nardin C., Widmer J., Winterhalter M. Meier W., *Eur. Phys. J. E.*, 4, 403, 2001; c. Nardin C., Thoeni S., Widmer J., Witerhalter M., Meier W., *Chem Comm.*, 1433, 2000
15. Rothman J., Lenard J., *Science*, 195, 743, 1977; Baumgärtner A., *J. Chem. Phys.*, 101, 9060, 1994
16. Bretscher M. S., *Nature New. Biol.*, 1972, 236, 11; Bretscher M. S., *Science*, 181, 622, 1972
17. Op den Kamp J.A.F., *A. Rev. Biochem.*, 48, 47, 1979

18. Stewart S., Liu G., *Chem. Mater.*, 11, 1048, 1999
19. Cassagrande C., Fabre P., Raphael E., Veyssié M., *Europhys. Lett.*, 1989, 9, 251
20. Patrickios C. S., C. Forder, S. P. Armes, N. C. Billingham, *J. Polym. Sci., Part A: Polym. Chem.*, 35, 1181, 1997
21. Whitesides G. M., Grzybowski B., *Science*, 295, 2418, 2002
22. Israelachvili J.N., *Intermolecular and Surface Forces*, 2nd edition, Academic Press, 1992
23. Gladyshev G.P., *J. Theor. Biol.*, 83, 17-42, 1980
24. Hamley I. W. *Introduction to Soft Matter, Polymer Colloids, Amphiphiles and Liquid Crystals*, J. Wiley & Sons, N.Y., 2000
25. Ikkala O., Brinke G., *Science*, 295, 2407, 2002
26. Förster S., Plantenberg T., *Angew. Chem. Int Ed.*, 41, 688-714, 2002
27. Hamley I. W., *Nanotechnology* 14, R39-R54, 2003
28. Benga Gh., Holmes R., *Prog. Biophys. Biol.*, 43, 257, 1984
29. Salditt T., *Science*, 5, 19-26, 2000
30. Mouritsen Ole G., Bloom M., *Biophys. J.*, 46, 141-153, 1984
31. Tanford C., *Biochemical Society Transactions*, vol. 15, 1S-7S, 1987
32. Soo Lim P., Eisenberg A., *J. of Polym. Sci., Part B: Polymer Physics*, 42, 923, 2004
33. Discher D., Eisenberg A., *Science*, 297, 2002
34. Choucair A., Eisenberg A., *Eur. Phys. J.*, E 10, 37, 2003
35. Bieringer R., Abetz V., Müller A.H. E., *Eur. Phys. J.*, E5, 5, 2001
36. Liu F., Eisenberg A., *J. Am. Chem. Soc.*, 125, 15059, 2003
37. Luo L., Eisenberg A., *J. Am. Chem. Soc.*, 123, 1012, 2001
38. Patrickios C., Lowe A., Armes S., Billingham N., *J. of Polym. Sci.: Part A: Polym. Chem.*, 36, 617, 1998
39. Gido S. P., Schwark D.W., Thomas E.L., Goncavales M. C., *Macromolecules*, 26, 2636, 1993
40. Anschra C., Stalder R., *Macromolecules*, 26, 2171, 1993; Stalder R., Anschra C., Beckmann J., Krappe U., Voigt-Martin, Leibler L., *Macromolecules*, 28, 3080, 1995
41. Krappe U., Stalder R., Voigt-Martin I., *Macromolecules*, 28, 4558, 1995
42. Zheng W., Wang Z.-G., *Macromolecules*, 28, 7215, 1995
43. Beginn U., Möller M., in *Supramolecular Materials and Technologies*, David N. Reinhoudt (Ed.), John Wiley Ltd., N. Y., 1999
44. Allen N., McGrath J. E., *Block Copolymers, Overview and Critical survey*, Academic Press, N.Y., 1977

45. Harris M. J., *Poly(ethylene glycol) Chemistry and Biological Applications*, in S. Zalipski (Ed.), ACS Symposium Series, San Francisco, 1997
46. Schmolka I.R., in “*Nonionic Surfactants*” (M. J. Schieck, ed.), Chapter 10, p.300, Dekker, New York, 1967
47. Jackson D. R., Lundsted L.G., *U.S. Patent 3,036,130* (Wyandotte Chemicals), 1962
48. Kray R.J., Stevenson R.W., *U.S. Patent 3,754,053* (Celanese Corp. of America), 1973
49. Finaz G., Rempp P., Parrod J., *J. Bull. Soc. Chim. Fr.*, 262, 1962
50. O'Malley J.J., Crystal R.G., Erhardt P.F., *Polym. Prepr. Am. Chem. Soc. Div. Polym. Chem.* 10(2), 796, 1969
51. Smidth J.J., Reichle W.T., *U.S. Patent 2,921,920* (Union Carbide Corporation) 1960
52. Bailey F.E., Jr. France H.G., *U.S. Patent 3,312,753* (Union Carbide Corporation), 1967
53. Yeon K. S., Lee Y. M., Shin H. J., Kang J., *Biomaterials*, 22, 2049-56, 2001
54. Boileau S, Sigwald P., *Makromol. Chem.*, 171, 11, 1973
55. Bronich T., Kabanov A., Kabanov V., Yu K., Eisenberg A., *Macromolecules*, 30, 3519-25, 1997
56. Lavasanifar A., Samuel J., Kwon G.S., *Advanced Drug Delivery Reviews*, 54, 169-90, 2002
57. Won Y. Y., Paso K., Davis T., Bates F., *J. Phys. Chem.*, 13, 105, 8302, 2001
58. Behraves E., Sheng A., Jo S., Mikos A., *Biomacromolecules*, 3, 153, 2002
59. Feng Y., Zhao J., Wang Q., Li M., Chen X., *J. Appl. Polym. Sci.*, 75, 475, 2000
60. Chang Y., Kwon C. Y., Lee S.C., Kim C., *Macromolecules*, 33, 4496-00, 2000
61. Budde H., Höring S., *Macromol. Chem. Phys.*, 199, 2541-46, 1998
62. Lunsted L.G., *U.S. Patent 2,674, 619* (WyandotteChem. Co.), 1954
63. Schmolka I.R, Bacon L.R., *J. Am. Oil Chem. Soc.*, 44(10), 559, 1967
64. Spronggs, J.S., *U.S. Patent 2,828, 345* (Dow Chemical Co), 1658
65. Teot A.S., *Canadian Patent 698,568* (Dow Chem. Co), 1964
66. Ishizu K., Ohta H., *J. Mat. Sci. Lett.*, 20, 1657, 2001
67. Kissel Th., Li Y., Unger F., *Adv. Drug Deliv. Rev.*, 54, 99-134, 2002
68. Lee S.-H, Kim S.H., Han Y.K., Kim Y.H., *J. Polym. Sci., Part A: Polym. Chem.*, 40, 2545, 2002
69. Kurian P., Zschoche J., Kennedy J., *J. Polym. Sci., Part A: Polym. Chem.*, 38, 3200, 2000
70. Mukae K., Bae Y. H., Okano T., Kim W.S., *Polym. J.*, 22, 206, 1990
71. Brooks T.W., Daffin C.L., *Polym. Prepr., Am. Chem. Soc., Div. Polym. Chem.*, 10(2), 1174, 1969

72. Kawai T., Shiozaki S., Sonoda S, Nakagawa H, Matsumoto T, Maeda H. *Makromol. Chem.*, 128,252, 1969
73. Furukawa J, Saegusa T., Mise N., *Makromol. Chem.*, 38,244,1960
74. Galin J.C., *Makromol. Chem.* 124,118, 1969
75. Perret R., Skoulios A., *C.R. Hebd. Sci. Acad., Ser C*, 268(3),230, 1969
76. Koleske J.V., Roberts R.M. J., DelGiudice F.P., *U.S.Patent*, 3,670,045 (Union Carbide Corporation), 1972
77. Coleman D., *J. Polym. Sci.*, 14, 15, 1954
78. Sangen O., Yamamoto Y., Imamura R., *Sen'i Gakkaishi* 29(11), T472, 1973
79. Riches K.M., Haward R.N., *Polymer* 9(2), 103, 1968
80. Riches K.M., *British Patent* 1,058,389 (Shell International), 1967
81. Galin M., Galin J.C., *Makromol.Chem.*, 160, 321, 1972
82. Feng X.-S., Pan C-Y., *Macromolecules* 2002, 35, 4888-4893
83. Lu Z., Chen S., Huang J., *Macromol. Rapid Commun.*, 20, 394-400, 1999
84. Huang X, Chen S., Huang J., *Journal of Polymer Science, Part A: Polymer Chemistry*, 37, 825-833, 1999
85. *French Patent* 1.598.865 (Frabenfabriken Bayer A.-G), 1970
86. Biggs S., Vincent B., *Colloid Polym. Sci.*, 270, 505-10, 1992
87. Massey J., Power N., Manners I., Winnik M., *J. Am. Chem. Soc.*, 120, 9533, 1998
88. Minoura Y., Mitoh M., Tabuse A., Yamada Y., *J. Polym. Sci, Part A-1*, 7(9), 2753, 1969
89. Saam J.C.,Gordon D.J., Lindsey S., *Macromolecules* 3, (1), 1, 1970
90. Minoura Y., Shundo M., Enomoto Y., *J. Polym. Sci., Part A-1*, 6(4), 979, 1968
91. Juliano P.C., *U.S.Patent* 3.663.650 (General Electric Co), 1972
92. *Nedherlands Patent Appl.* 6 408 970 (Union Carbide Corp.), 1965
93. Huang K., Bes L., Haddleton D., Khoshdel E., *J. of Polym. Sci., Part A: Polym. Chem.*, 39, 1833-42, 2001
94. Tang L., Shen M. S., Chu T., Huang Y. H., *Biomaterials*, 20, 1365-70, 1999
95. Maassen H. P., Yan J. L., Wegner G., *Makromol. Chem., Macromol. Symp.*, 39, 215-228, 1990
96. Fritsche A.K., Price F.P., *Polym. Prepr., Am. Chem. Soc., Div. Polym. Chem.*, 11(2), 462, 1970
97. Jones F.R., *Eur. Polym. J.*, 10, 249, 1974
98. Lee C.L., Johannson O.K., *Polym. Sci., Part A-1*, 4(12), 3013, 1966
99. Morton M., Rembaum A.A., Bostick E.E., *J.Appl. Polym. Sci.* 8(6), 2707,

100. Dean J.W., *U.S. Patent 3.673.272* (General Electric Co.), 1972
101. Owen M. J., Thompson J., *Br. Polym. J.*, 4(4), 297, 1972
102. Bostick E.E., Fessler W.A., *U.S. Patent 3.578.726* (General Electric Co.), 1971
103. Bostick E.E., Gaines G.L., LeGrand D.G., *U.S. Patent 3 640 943*, (General Electric Co.), 1972
104. Clark R.F., Krantz K.W., *U.S. Patent 3 696 137* (General Electric Co.). 1972
105. Saam J.C., Fearon F.W.G., *German Offen. 2.142.594* (Dow Corning Corp.), 1972
106. Nopshay A., Matzer M. Williams T.C., *Ind. Eng. Chem., Prod. Res. Dev.*, 12(4), 268, 1973
107. Matzer M., Noshay A., McGrath J.E., *Polym. Prepr., Am. Chem. Soc., Div. Polym. Chem.*, 14(1), 68, 1973
108. Matzer M., Noshay A., Schober D.L., McGrath J.E., *Ind. Chim. Belge*, 38, 1104, 1973
109. Chow S.W., Byck J.S., *U.S. Patent 3.562.353* (United States Dept. of Health, Education and Welfare), 1971
110. Nyilas E., *U.S. Patent 3.562.352*, (Avco Corp.), 1971
111. Greber G., *Angew. Makromol. Chem.*, 4/5, 212, 1968
112. Saegusa T., Kobayashi S., Kimura Y., *Macromolecules* 7(1), 139, 1974
113. Saegusa T., *Pur Appl. Chem.*, 39(1-2), 354, 1974
114. Saegusa T., Ikeda H., Fujii H., *Macromolecules* 5(4), 354, 1972
115. Morishima Y., Tanaka T., Nozakura P., *Polym. Bull.*, 5(1), 19, 1981
116. Percec V., *Polym. Prepr.*, 21(1), 301, 1982
117. Saegusa T., Ikeda H., *Macromolecules* 6(6), 805, 1973
118. Litt M., Swamikanni X., *Polym. Prepr.*, 25(1), 242, 1984
119. Yilgor I., Steckle W.P., Yilgor E., Freelin R.G., Riffle J.S., *Polym. Sci., Part A*, 27(11), 3673, 1989
120. Sinai-Zindge G., Verma A., Liu Q., Brink A., Bronk J.M., Marand H., McGrath J.E., Riffle J.S., *Makromol. Chem., Macromol. Symp.*, 42/43, 329, 1991
121. Seung S.N.L., Young R.N., *J. Polym. Sci., Polym. Lett. Ed.*, 18(2), 89, 1980
122. Schultz R.C., Schwarzenbach E., Zoeller J., *Polym. Prepr.*, 29(2), 44, 1988
123. Ikeda I., Kurushima Y., Susuki K., *Polym-Plast. Technol. Eng.*, 28(7-8), 877, 1989
124. Sinai-Zidge G., Verma A., Liu Q., Brink A., Bronk J., Allison D., Goforth A., Patel N., Marand H., McGrath J.E., Riffle J.S., *Polym. Prepr.*, 31(1), 63, 1990
125. Saegusa T., Ikeda H., Fujii H., *Polymer J.*, 3(1), 35, 1972

126. Tanaka R., Ueoka I., Takaki Y., Kataoka K., Saito M., *Macromolecules*, 16(6), 849, 1983
127. Clarson S.J., Semlyen J.A., *Polysiloxane Polymers*, PTR Prentice Hall, New York, 1993
128. Bostick E. E., *Ring-Opening Polymerization*, Frisch K.C., Reegen S.L. Eds., p 327, Dekker, N.Y., 1969
129. Wright P. V., *Ring Opening Polymerization*, Ivin K.J., and Saegusa T. Eds., Elsevier, London, New York, 1970
130. Noll W., *Chemistry and Technology of Silicones*, Academic press, New York, p 212, 1968
131. Chjnowski J., *Siloxane Polymers*, Clarson S. J., Semlyen J. A. Eds., PTR Prentice Hall, Englewood Cliffs, New Jersey, p 21, 1993
132. Wright P. V., Semley J.A., *Polymer*, 10, 543, 1969
133. McGrath J.E., Riffle J.S., Yilgor I., Banthia A.K., Sormani P, *Org. Coat. Appl. Polym. Sci*, 46, 693-700, 1981
134. Bryk M. T., *Vysokomol. Soedi*, A20, 147, 1978
135. Schindler S., Ruehlamn K., *Plaste Kautschuk*, 25, 384, 1978
136. Patnode W., Wilcock D.F., *J.Am. Chem. Soc.*, 68, 358, 1946
137. Kojima K., Tarumi N., Wakatuki S., *Nippon Kagaku Zasshi*, 76, 1205, 1975
138. Chojnowski J., Wilczek L., *Makromol. Chem.*, 180, 117, 1979
139. Chojnovski J., Mazurek M., *Makromol. Chem.*, 176, 1999, 1975
140. Boileau S., in J.E. McGrath, *Ring Opening Polymerization*, p 23, Am. Chem. Soc., Washington DC, 1985
141. Lee C. L., Johannson O.K., *J. Polym. Sci., Polym. Chem. Ed.*, 14, 729, 1976
142. Lee C.L., Marko O. W, Johannson O.K., *J. Polym. Sci., Polym. Chem. Ed.*, 14, 743, 1976
143. Lee C.L, Frye C. L., Johannson O. K., *Polym. Prepr.*, 100, 1361, 1969
144. Maschke U., Wagner T., *Makromol. Chem.*, 193, 2453, 1992
145. Bostick E.E., *Block Copolymers*, S.L. Aggarwal Ed., Plenum, N.Y., 1970
146. Richard G., Mingotaud E.-F., Cardinaud D., Soum A., *Polym. Bull.*, 39, 581, 1997
147. Mazurek M., 1987, in *Recent Advances in Anionic Polymerization*, Hogen-Esch 329
148. Gvodzdic N.V., Ibemesi J., Meier D.J., Proc. IUPAC, *Macromol. Symp.*, 69, 168, 1982
149. Dems A., Strobin G., *Macromol. Chem.*, 192, 2521, 1991

150. Rheingans O., Hugenberg N., Harris J. R., Fischer K., Maskos M., *Macromolecules*, 33, 4780, 2000
151. Saegusa T., Kobayashi S., *Encyclopedia of Polymer Science and Technology*, Wiley: New York, Suppl. Vol. 1, p 220, 1976
152. Kobayashi S., Saegusa T., *Ring Opening Polymerization*, Elsevier Essex, U.K., vol. 2, Chapter 11, 1984
153. Kobayashi S., *Prog. Polym. Sci.*, 15, 751, 1990
154. Oh Y. S., Yamazaki T., Goodma M., *Macromolecules* 25(23), 6322, 1992

155. Peihong Ni., Ximper C., Deyne Y., Jian H., Shoukan F., *Chin. Sci. Bull.*, 47, 280, 2002
156. Miyamoto M., Naka K., Tokumizu M., Saegusa T., *Macromolecules*, 22, 1604, 1989
157. Montaudo G., *Polym. Prep.*, 37, 290, 1996
158. Curtius T., *J. Prakt. Chem.*, 91, 1, 1915
159. Dust J. M., Fang Z., Harris J. M., *Macromolecules*, 23, 3742, 1990
160. Matzurek M., J. Chojnovski, *Makromol. Chem.*, 178, 1005, 1977
161. Bouveault H., Blanc A., *Compt. Rend.*, 1903, 137, 329; Carothers A., Hill A. , Kirby A., *J. Am. Chem. Soc.*, 1930, 52, 5287
162. Montaudo G., *Polym. Prep.*, 37, 290, 1996
163. Alonso B., Sanchez C., Maquet J., *J. Non-Cryst. Sol.*, 277, 58, 2000
164. Silva M.A., De Paoli M., Felisberti M. I., *Polymer*, 39, 2551, 1998
165. Curtius T., *J. Prakt. Chem.*, 91, 1, 1915
166. Ahmed F., Alexandris P., Neelamegham S., *Langmuir*, 17, 537-546, 2001
167. Xu H., Erhardt R., Abetz V., Müller A. H.E., Goedel W. A., *Langmuir*, 17, 6787, 2001
168. Hückstädt H., Göpfert A., Abetz V., *Macromol. Chem Phys.*, 201, 296, 2000
169. van Zanten J. H., Monbouquett H. G., *J. Colloid Interface Sci.*, 146, 330, 1991
170. D.D. Lasic, *Liposomes: From Physics to Applications*, Elsevier Science Publications B.V., Amsterdam, 1993
171. Nardin C., Meier W., *Chimia*, 55, 142, 2001
172. Langmuir I., *J. Am. Chem. Soc.*, 1917, 39, 1848; Blodgett K. B., *J. Am. Chem. Soc.*, 57, 1007, 1935
173. Graff A., Sauer M., van Gelder B., Meier W., *PNAS*, 99, 5064-5068, 2002
174. A. Taubert, E. Furrer, W. Meier, *Chem. Comm.*, submitted
175. van Gelder P., Dumas F., Winterhalter M., *BioPh. Chem.*, 85, 153, 2000

176. Wiese A., Reiners J. O., Brandenburg K., Kawahara K., U. Zahringer, U. Seydel, *BioPhys. J.*, 70, 321, 1996
177. Pautot S., Frisken B.J., Weitz D.A., *Proc. Natl. Acad. Sci. USA*, 100, 10718, 2003
178. Baumgärtner A., Skolnick J., *Phys. Rev. Lett*, 74, 2142, 1995
179. Borgnia M., Nielsen S., Engel A., Angre P, *Annu. Rev. Bioch.*, 68, 425, 1999
180. Scheuring S., Tittmann P., Stahlberg H., Ringler P., Borgnia M., Agre P., Gross H., A. Engel, *J. Mol. Biol.*, 299, 1271, 2000
181. Pohl P., Saparov S.M., M.J.Borgnia, P. Agre, *Proc. Natl. Acad. Sci. USA*, 98, 9624, 2001
182. Waltz T., Hirai T., Murate K., Hezmann J. B., Mitsuoka K., Fujizoshi Z., Smith B. L., Agre P., Engel A., *Nature*, 387, 624, 1997
183. G.B. Sigal, C. Bamdad, A. Barberis, J. Stroniger, G. M. Whitesides, *Anal. Chem.*, 68, 490, 1996
184. L. Hasler, T. Waltz, P. Tittmann, H. Gross, J. Kistler, A. Engel, *J. Mol. Biol.*, 279, 855, 1998
185. N. R. Kramarcy, R. Sealock, *J. Histochem. and Cytoschem.*, 39, 37, 1991
186. Sigma catalog references, *Product Information, Technical Bulletin* (TO 565 from JDS/ALC 02/02), 1998
187. Liljekvist P., Kronberg B., *J. Colloids and Int. Sci.*, 222, 159, 2000
188. Nardin C., Wintherhalter M., Meier W., *Angew. Chem., Int. Ed.*, 39, 4599, 2000
189. European Patent, *WO 99/00670*, 1998
190. Fotiadis D., Hasler L., Müller D. J., Stahlberg H., J. Kistler and A. Engel, *J. Mol. Biol.*, 300, 779, 2000
191. Lopez C. F., Nielsen S. O., Moore P. B., Klein L. M., *Proc. Natl. Acad. Sci. USA*, 101, 4431, 2004

Vitae

Personal

Name: Roxana Stoenescu
Date of Birth: February 10, 1975
Place of Birth: Ploiesti, Romania
Citizenship: Rumanian
Marital Status: single

Education

2001-2004 Ph. D. in Physical Chemistry at Basel University, Institute of Chemistry,
Switzerland. Supervisor: Prof. Dr. Wolfgang Meier
October, 2001 Degree in Chemical Engineering, Bucharest, Romania
September, 2001 Master degree in Chemistry, Institute National Polytechnique de
Toulouse, France
1997-2001 Studies in Polytechnic Institute, Department of Engineering Science,
Bucharest, Romania

Previous Research Experiences

Oct. 2001 –Sept. 2004 Ph. D. Thesis, Department of Physical Chemistry, University
of Basel, Switzerland
Supervisor: Prof. Dr. Wolfgang Meier
Jan. 2001 – July 2002 M.Sc. Thesis, National Polytechnic Institute, Laboratoire de
Chimie Agro-Industrielle, Toulouse, France
Supervisor: PD. Dr. J. P. Pontalier
Jan. 2001 – July 2002 M.Sc. Thesis, Polytechnic Engineering School, Department of
Engineering Science, French Option, Bucharest, Romania
Supervisors: Dr.Eng. Livia Butac and Dr. Eng. Gh. Nechifor
July 1999 Attendant - Summer School for Biochemistry “Biology &
Molecular Pathology. Biotechnology” Center of Molecular
Biology, Iasi, Romania
President: Sir Jean Maurice Montreuil (Lille)

Sept. 1997 Trainee laboratory student, CNRS Laboratories, Paul Sabatier University, Molecular Chemical & Photochemical Interactions Laboratory Toulouse, France,
Supervisors: Dr. E. Perez and Prof. Armand Lattes

Publications

Vesicles with asymmetric membranes from amphiphilic ABC triblock copolymers, R. Stoenescu, W. Meier, Chem. Comm., 2002, 3016-3017

Asymmetric ABC-Triblock Copolymer Membranes Induce a Directed Insertion of Membrane Proteins, R. Stoenescu, A. Graff, W. Meier, Macromolecular Bioscience, 2004, in press

Presentations

Matrixes for protein incorporation: mimicking the natural tendencies?, R. Stoenescu, W. Meier, World Polymer Congress, International Union of Pure and Applied Chemistry, Macromolecular Division, July 2004, Paris (France)

Asymmetric Membranes from Amphiphilic ABC Block Copolymers, R. Stoenescu, the 2nd Swiss Symposium, 2004, Zweisimmen (Switzerland)

Membranes and Nanocontainers from Amphiphilic Block Copolymers, R. Stoenescu and W. Meier, Gordon Research Conference, Chemistry of Supramolecular Assemblies, 2003, Boston, USA

Membranes from Asymmetric Amphiphilic ABC Block Copolymers, R. Stoenescu and W. Meier, the VIIth International Conference on "Frontiers of Polymers and Advanced Materials", NATO Advanced Research, 2003, Bucharest (Romania)

Asymmetric Membranes from Amphiphilic ABC Block Copolymers, R. Stoenescu and W. Meier, the VIIth Nachwuchstage der Kolloid- und Grenzflächenforschung, Ruprecht-Karls-Universität, 2003, Heidelberg (Deutschland)

Hybrid Polymer-Protein Materials based on ABA and ABC Amphiphilic Triblock Copolymers, R. Stoenescu, A. Graff and W. Meier, PGS (Polymer Gruppe der Schweiz), "Formulating Polymers for Product Design", 2003, Fribourg, Switzerland